

**POWER MANAGEMENT AND CONTROL OF HYBRID
AC/DC MICROGRIDS INTEGRATED WITH RENEWABLE
ENERGY SOURCES AND ELECTRIC VEHICLES**

by

Md Shamiur Rahman



MACQUARIE
University
SYDNEY · AUSTRALIA

Dissertation submitted in fulfilment of the requirements

for the degree of

DOCTOR OF PHILOSOPHY

School of Engineering
Faculty of Science and Engineering
Macquarie University
Sydney, Australia

April 2018

STATEMENT OF CANDIDATE

I certify that the work in this thesis entitled "Power Management and Control of Hybrid AC/DC Microgrids Integrated with Renewable Energy Sources and Electric Vehicles" has not previously been submitted for a degree nor has it been submitted as part of the requirements for a degree to any other university or institution other than Macquarie University.

I also certify that the thesis is an original piece of research and it has been written by me.

In addition, I certify that all information sources and literature used are indicated in the thesis.

.....

Name

Dedicated to my parents, my wife Anie, my brother

℘

all the people of Bangladesh

ACKNOWLEDGMENTS

*“All the praises and thanks be to
the one and the only Almighty Allah (sbw)”*

I owe my sincere gratitude to my principle supervisor Associate Professor Jahangir Hossain for his support and guidance throughout my years of Ph.D. It has been a great honor for me to work under his supervision. I am indebted to him for whatsoever research capabilities I have acquired so far. I would also like to take the opportunity to thank my associate and adjunct supervisors Professor Graham Town and Professor Junwei Lu respectively. Their encouraging words, constructive criticisms, valued wisdom and comprehensive approaches towards problem-solving contributed momentarily in writing this dissertation and to my intellectual growth. I would also like to thank the nominated thesis examiners who have given their consents to evaluate this dissertation despite their busy schedules.

My heartiest reverences are for my parents - my father, Md Amir Ali, being the first person to have faith in me in my pursuit of being an electrical engineer and my mother, Rokshana Sultana Urmi, to whom I owe my life. My cordial thanks are for my elder brother, Md Rizwanur Rahman, who has been always supportive to me and my endless love for my wife, Asia Sultana Anie, who has made my entire life beautiful. I dedicate this dissertation to all of them. Without their support and understanding, I would be nothing.

I would also like to thank my fellow colleagues - particularly Dr. Fida Rafi for

his insightful and innovative ideas related to my research and his unconditional friendship, Dr. Md Aminur Rahman Shah for teaching me to see the life through matured eyes and my friend, Dr. Nasif Mahmud, for our sparkling discussion regarding power systems over the phone. I am really fortunate to find large supportive Bangladeshi Communities in both Gold Coast and Sydney throughout my Ph.D. tenure and thankful to them for making my stay in Australia gratifying.

I appreciate the support of Dr. Keith Imrie, Honorary Associate at Macquarie University, for proofreading my publications including this thesis within a very short period.

Last but not the least, I would like to thank both Griffith University and Macquarie University for the transformative opportunity of pursuing Ph.D. in my preferred field with scholarships, without this opportunity my dream of higher study would not be possible.

ABSTRACT

Microgrids are the building blocks for the next generation power grid, the so-called '*Smart Grid*'. They facilitate the integration of various distributed-generation (DG) units such as electric vehicles (EV), diverse energy storage systems (ESS), and renewable energy resources (RER) utilizing intelligent forecasting, Information and Communication Technology (ICT) and control infrastructures to achieve active consumer participation, augmented network reliability, reduced expansion cost, and self-healing capabilities. Due to the binary nature of electricity i.e. alternating current (AC) and direct current (DC), microgrids are broadly classified as AC microgrids and DC microgrids. However, to comply with the legacy AC system and to interface with the growing DC technologies, lately, coupled AC and DC microgrids or hybrid AC/DC microgrid structures are gaining momentum. The benefit of this structure is that it can accommodate both AC and DC loads and generators instantaneously with minimum power-electronics-based losses. In addition, this structure is suitable for integrating distributed storages such as the emerging electric-vehicle energy-storage systems (EV-ESS) for vehicle-to-grid (V2G) applications. EV storages can effectively improve the overall performance of a hybrid microgrid in terms of voltage and frequency regulation, system stability, active and reactive power support and fault robustness. However, the optimized coordination of EV storages within microgrids is an intricate issue due to their different control and configuration structures along with inad-

equate standards regarding V2G applications. The centralized and distributed control structures are viable options to coordinate spatially dispersed EV storages within microgrids of different geographical sizes. Consequently, this Ph.D. thesis presents three contributions in the area of microgrid control techniques and V2G application within microgrids.

The first contribution of this research is the design and implementation of an improved three-layered centralized coordinated control strategy considering EV availability constraints for three-phase (3P) and DC type EV-ESSs to improve the operation of a hybrid AC/DC microgrid. The first layer of the algorithm ensures DC subgrid management, which includes DC bus voltage regulation and DC power management. The second and third layers are responsible for the AC subgrid management, which includes AC bus voltage and frequency regulation with active and reactive power management. The multi-layered coordination is embedded into the microgrid central controller (MGCC) which controls the interlinking controller in between the AC and DC subgrids as well as the interfacing controllers of the participating EVs and distributed RER.

The second contribution of this research is to develop a new need-based distributed coordination strategy (NDCS) for multiple EV storages in an islanded commercial hybrid AC/DC microgrid with extended geographical size. The control capacity of the interlinking converter is enhanced by incorporating combined power-droop and voltage-droop strategies to leverage the coupling of AC and DC voltages. Therefore, the AC bus voltage can be regulated simultaneously by regulating only the DC bus voltage without affecting the power-sharing capabilities of the converter. The NDCS is proposed to coordinate the EV storages to regulate the DC bus voltage. The main objective of the NDCS is to decide whether the coordination of the available EV storages is to be performed in a decentralized

or a distributed manner. The mathematical model and the algorithm to deploy NDCS are developed to realize its application to a real system.

The final contribution of this research is to establish an optimized distributed controller for coordinating EV storages within microgrids. An optimizer is incorporated with the previously developed distributed controller for EV storages. An economic dispatch problem is solved in real time with the optimizer to minimize the output power-generation cost. The optimizer adjusts the power setpoint for each EV, which ensures proper power management within the microgrid. As a result, a cost-effective distributed V2G operation can be ensured.

The hybrid AC/DC microgrid and its extended version are designed in a MATLAB/Simulink environment resembling the microgrid under construction at Griffith University, Australia. Extensive case studies are performed considering real-life solar irradiation, commercial load profiles, EV time delay, and EV plug-and-play and fault conditions etc. to validate each proposed control scheme. Additionally, the performance of the controllers is compared with the conventional controllers. The results of the case studies demonstrate the efficacy of the overall system in terms of improved transient response, fault-robustness, scalability, cost-effectiveness and reliability.

Contents

Table of Contents	xiii
List of Figures	xix
List of Tables	xxv
List of Publications	xxvii
1 Introduction	1
1.1 Background and Motivation	2
1.1.1 Renewable-Dominated Power Grids	2
1.1.2 Vehicle-to-Grid (V2G)	4
1.1.3 Microgrids and Their Control	5
1.1.4 Self-Sufficient Commercial Neighborhoods	7
1.2 Significance of the Research	9
1.3 Research Challenges and Objectives	10
1.4 Main Contributions	12
1.5 Thesis Outline	14
2 Literature Review	17
2.1 Introduction	17

2.2	Hybrid AC/DC Microgrid: a Future for Distribution Systems	18
2.3	Microgrid Control	20
2.3.1	Challenges	21
2.3.2	Expected Features	23
2.3.3	Controlled Variables	24
2.4	Overview on Hierarchical Microgrid Control Structure	26
2.5	Overview on Vehicle-to-Grid (V2G) and Vehicle-to-Microgrid (V2M)	29
2.5.1	Challenges of V2G/V2M Technology	29
2.5.2	Prospects of V2G/V2M Technology	30
2.5.3	Configurations and Control Strategies of Various EV Chargers	34
2.6	Interfacing Converter Control in Grid-Tied and Islanded Mode	38
2.6.1	Grid-Tied Control Structure	38
2.6.2	Islanded Control Structure	40
2.7	EV Storage Control in Grid-Tied and Islanded Mode	41
2.8	Overview on Distributed Control Techniques for Microgrids	42
2.8.1	Distributed Model Predictive Control	43
2.8.2	Consensus-Based Cooperative Techniques	44
2.8.3	Agent-Based Techniques	45
2.8.4	Decomposition-Based Techniques	47
2.9	Applications of Distributed Controller in Microgrid	47
2.9.1	Application in Voltage Regulation	48
2.9.2	Application in Economical Power Coordination	49
2.9.3	Application in Frequency Regulation	50
2.10	Relevant Standards	51
2.11	Chapter Summary	56

3	Centralized Coordinated Control of EVs for Improved Hybrid Microgrid Operations	57
3.1	Introduction	58
3.2	Hybrid AC/DC Microgrid	64
3.2.1	PV Module Modeling	66
3.2.2	EV Energy Storage Modelling	67
3.2.3	Interlinking/Interfacing Converter Control	68
3.2.4	DC/DC Converter Control	72
3.3	Coordinated Control Strategy	74
3.3.1	Coordinated Control Objectives	74
3.3.2	Coordinated Control Algorithm	76
3.4	Case Studies	82
3.4.1	Case A: Variable Irradiation and Loading Effects	83
3.4.2	Case B: Homogeneous Single-Phase EV Allocation	84
3.4.3	Case C: Heterogeneous Single-Phase EV Allocation	86
3.4.4	Case D: Grid Synchronization	92
3.5	Chapter Summary	92
4	A Need-Based Distributed Coordination Strategy for Multiple EVs in a Commercial Microgrid	95
4.1	Introduction	96
4.2	Proposed IC Control Topology	101
4.2.1	Power-Based Droop Control	101
4.2.2	Generation of P^* , Q^* and V^*	102
4.2.3	Voltage and Current Controllers	105
4.3	Need-Based Distributed Coordination Strategy	106
4.4	Case Studies	110

4.4.1	Case A: Step Load Change	111
4.4.2	Case B: Variable PV Generation and Commercial Loading	115
4.4.3	Case C: Effects of Time Delay	117
4.4.4	Case D: User-Preferred Disconnection	122
4.4.5	Case E: Performance Evaluation under Faults	122
4.5	Chapter Summary	125
5	V2M via Optimization-Incorporated Distributed EV Coordination Strategies	127
5.1	Introduction	128
5.2	Proposed V2M framework	133
5.2.1	EV Economic-Dispatch Problem Formulation	133
5.2.2	Optimization-Incorporated Distributed Control (ODC) for EV Storages	135
5.2.3	Power-Flow Control between Subgrids via IC	138
5.3	Case Studies	139
5.3.1	Case A: Variable Solar Insolation and Commercial Loading	141
5.3.2	Case B: Effects of Grid Reconnection	143
5.3.3	Case C: Effects of EV Disconnection and Time Delay	145
5.4	Conclusion	149
6	Conclusions and Future Work	151
6.1	Thesis Conclusions	151
6.2	Future Research Directions	155
A	Commercial Microgrid Testbed	157
B	List of Acronyms	159

C List of Symbols	161
D Reuse Permissions of Published Papers for Chapters 2, 3 and 4	163
References	169

List of Figures

1.1	Current status of commercial EV charging facilities in Australia (www.plugshare.com).	8
2.1	A conceptual hybrid AC/DC microgrid structure	20
2.2	Hierarchical microgrid control structure	26
a	Hierarchy of primary, secondary and tertiary control layers in a microgrid	26
b	Position of the inner control loops in the hierarchical structure	26
2.3	Typical EV DC fast chargers [1]	35
a	Configuration	35
b	Control strategy	35
2.4	Typical EV three-phase AC Fast Charger [1]	36
a	Configuration	36
b	Control strategy	36
2.5	Typical EV single-phase AC Fast Charger [1]	37
a	Configuration	37
b	Control strategy	37
2.6	Interfacing converter control in grid-tied mode	38
2.7	Interfacing converter control in islanded mode	39

2.8	EV storage controller in grid-tied mode [2]	41
2.9	EV storage controller in islanded mode	42
3.1	Hybrid AC/DC microgrid structure in Griffith University, Australia.	64
3.2	Modified local control structure for each interlinking/interfacing converters of the hybrid AC/DC microgrid	69
3.3	DC/DC converter controller	74
3.4	Proposed three-layered coordination algorithm	79
3.5	Input data for the hybrid AC/DC microgrid: (a) PV output power, (b) Solar irradiation and (c) Usual active and reactive power demand of the building for 24 hours	84
3.6	Control signals of the interlinking converter	85
3.7	DC bus voltage	86
3.8	AC bus RMS voltage (line to neutral)	87
3.9	Frequency	87
3.10	SOC of the single-phase EV-ESS	88
3.11	SOC of the DC type and 3P type EV-ESS	88
3.12	Active power profile of the system	89
3.13	Reactive power profile of the system	89
3.14	Charging power drawn by single-phase EV-ESS: (a) Single-phase power and (b) RMS value of the single -phase power	90
3.15	Voltage profile for case C: (a) DC bus voltage and (b) AC bus RMS voltage	90
3.16	Frequency for case C	91
3.17	Grid synchronization mode: (a) DC bus voltage, (b) AC bus RMS voltage and (c) Frequency	91
4.1	IC control structure with voltage-based droop.	100

4.2	EV converter controller with distributed cooperative control loop.	105
4.3	Need-based distributed coordination strategy of EV storages.	109
4.4	Single-line diagram of the test hybrid AC/DC microgrid.	111
4.5	Communication graph of EVs.	112
4.6	$v_{Batt}^1, v_{Batt}^2, v_{Batt}^3$ and v_{Batt}^4 for case A. At $t = 4$ s, a step load is applied at the DC bus for 2 s. At $t = 6$ s NDCS is activated to initiate the distributed operation.	113
4.7	Power supplied or consumed by the EVs for case A. Saturation constraints were applied to ensure that the EV powers do not exceed the maximum allowable limit of ± 20 kW for both decentralized and distributed operation.	113
4.8	%SOC for all EVs for case A during both decentralized and distributed operation.	114
4.9	Commercial AC and DC load profiles	115
4.10	Varying output power of all DG units. DC type DG units are shown in solid lines and the AC type DG units are shown in dotted lines.	116
4.11	$v_{Batt}^1, v_{Batt}^2, v_{Batt}^3$ and v_{Batt}^4 for case B.	117
4.12	AC-bus RMS voltage case B (red) and case C (blue).	118
4.13	$v_{Batt}^1, v_{Batt}^2, v_{Batt}^3$ and v_{Batt}^4 for case C.	118
4.14	Reference-tracking performance of the proposed controller.	119
4.15	$v_{Batt}^1, v_{Batt}^2, v_{Batt}^3$ and v_{Batt}^4 for case D.	119
4.16	AC-bus RMS voltage for case D.	120
4.17	Normalized DC bus voltage for cases B, C and D.	120
4.18	Output power of EV storages for case D.	121

4.19	Performance evaluation of the proposed scheme under the DC short circuit fault for case E. The fault was applied at $t = 3$ s for the duration of 40 ms. (a) Load current at the DC bus. (b) Load current at the AC bus. (c) Normalized DC bus voltage with the proposed distributed controller (solid black) and with the conventional decentralized controller (dotted blue). (d) AC bus RMS voltage in per unit (pu) with the proposed distributed controller (solid black) and with conventional decentralized controller (dotted blue).	123
4.20	Performance evaluation of the proposed scheme under three-phase AC symmetric fault for case E. The fault was applied at $t = 3$ s for the duration 60 ms (a) Load current at the DC bus. (b) Load current at the AC bus. (c) Normalized DC bus voltage with the proposed distributed controller (solid black) and with the conventional decentralized controller (dotted blue). (d) AC bus RMS voltage in per unit (pu) with the proposed distributed controller (solid black) and with conventional decentralized controller (dotted blue).	124
5.1	Proposed control topology. (a) ODC for individual EV storage.(b) Single-line circuit diagram of each IC. (c) IC control structure with voltage-based droop.	132
	a	132
	b	132
	c	132
5.2	Convergence of output powers with the distributed controller for various time delays. (a) Time delay, $T_d = 0$ s. (b) Time delay, $T_d = 0.3927$ s. (c) Time delay, $T_d = 1.5$ s. Dotted lines are the outputs measured from the distributed controller	136

5.3	Single-line circuit diagram of the test hybrid AC/DC microgrid.	140
5.4	Performance evaluation under variable solar insolation and commercial load profile. (a) Optimal incremental cost in ¢/kW . (b) AC bus voltage in per unit (p. u.). (c) Dynamic cost of all EV storages. (d) Normalized DC bus voltage. (e) Output power of all EV storages. (f) Frequency of the system.	144
	a	144
	b	144
	c	144
	d	144
	e	144
	f	144
5.5	Performance evaluation during and subsequent to grid reconnection. (a) Optimal incremental cost in ¢/kW . (b) AC bus voltage in per unit (p. u.). (c) Dynamic cost of all EV storages. (d) Normalized DC bus voltage. (e) Output power of all EV storages. (f) Frequency of the system.	146
	a	146
	b	146
	c	146
	d	146
	e	146
	f	146
5.6	Costs of all EV storages when EV-4 is intentionally disconnected at $t = 2$ s.	147
5.7	Output powers of all EV storages when EV-4 is intentionally disconnected at $t = 2$ s.	147

5.8	Effects of 30 ms time delay on the system power profile. (a) Output u_p^n of the distributed controllers for all EV storages with time delay (dotted) and without time delay (solid). (b) Discharged power of all EV storages with time delay (red) and without time delay (black)	148
a	148
b	148
A.1	Microrgrid components in N44 building of the Griffith University	158
A.2	Rooftop PV installation on N44 building of the Griffith University	158
D.1	164
D.2	165
D.3	166
D.4	167
D.5	168

List of Tables

2.1	State-of-the-Art Techniques for Hierarchical Microgrid Control [3–6]	28
2.2	Charging Power Level for Electric Vehicles	31
2.3	Default response for interconnection system during abnormal voltage variations	53
2.4	Default response for interconnection system during abnormal frequency variations	53
2.5	Maximum harmonic distortion of PCC voltage and current	54
2.6	NEM mainland frequency operating standards for islanded microgrids in the Australian distribution network [7]	54
2.7	Comparison of voltage requirements in Australia and New Zealand [8]	55
2.8	Islanding conditions for Australia	55
3.1	Salient features of the proposed approach in comparison with the contemporary literatures	61
3.2	Simulation parameters for the hybrid AC/DC microgrid	73
4.1	System parameters	112
5.1	Specifications of the Framework	142
A.1	N44 microgrid testing facility equipment	157

A.2 Installed solar PV specification 157

List of Publications

Refereed Journal Papers

1. **Md Shamiur Rahman**, M. J. Hossain, and J. Lu, “Coordinated control of three-phase AC and DC type EV–ESSs for efficient hybrid microgrid operations,” *Energy Conversion and Management*, vol. 122, pp. 488–503, 2016. [[Chapter 3](#)]
2. **Md Shamiur Rahman**, M. J. Hossain, J. Lu and H. R. Pota, “A Need-Based Distributed Coordination Strategy for EV Storages in a Commercial Hybrid AC/DC Microgrid with an Improved Interlinking Converter Control Topology,” *IEEE Transaction on Energy Conversion*, 2017 (early access online). [[Chapter 4](#)]
3. **Md Shamiur Rahman**, M. J. Hossain, F. H. M. Rafi and J. Lu, “A Vehicle-to-Microgrid (V2M) Framework with Optimization-Incorporated Distributed EV Coordination for a Commercial Neighborhood,” *IEEE Transaction on Sustainable Energy*, 2017 (under review), Manuscript ID: TSTE-00326-2018. [[Chapter 5](#)]

Scholarly Book Chapters

4. **Md Shamiur Rahman**, F. H. M. Rafi, M. J. Hossain, and J. Lu, “Power Control and Monitoring of the Smart Grid with EVs,” in *Vehicle-to-Grid: Linking Electric Vehicles to the Smart Grid*, IET publisher, 2015. [[Chapter 2](#)]

Refereed Conference Papers

5. **Md Shamiur Rahman**, M. J. Hossain, F. H. M. Rafi, and J. Lu, “EV charging in a commercial hybrid AC/DC microgrid: Configuration, control and impact analysis,” IEEE Australasian Universities Power Engineering Conference (AUPEC), 2016. [[Chapter 2](#)]
6. **Md Shamiur Rahman**, M. J. Hossain, F. H. M. Rafi, and J. Lu, “A multipurpose interlinking converter control for multiple hybrid AC/DC microgrid operations,” IEEE Innovative Smart Grid Technologies - Asia (ISGT-Asia), 2016. [[Chapter 2 and 3](#)]
7. **Md Shamiur Rahman**, M. J. Hossain, and J. Lu, “Utilization of Parked EV-ESS for Power Management in a Grid-Tied Hybrid AC/DC Microgrid,” in the 25th Australasian Universities Power Engineering Conference, 2015. [[Chapter 2](#)]

Other Co-authored Publications during PhD Candidature

8. J. Liu, **Md Shamiur Rahman**, J. Lu, and M. J. Hossain, “Performance investigation of hybrid AC/DC microgrids during mode transitions,” IEEE Australasian Universities Power Engineering Conference (AUPEC), 2016.
9. F. H. M. Rafi, M. J. Hossain, **Md Shamiur Rahman**, and J. Lu, “Implementation of independent improved neutral current controller using four leg PV-VSI,” IEEE Australasian Universities Power Engineering Conference (AUPEC), 2016.
10. F. H. M. Rafi, M. J. Hossain, **Md Shamiur Rahman**, and J. Lu, “Impact of controlling zero sequence current in a three-phase four-wire LV network with PV units,” IEEE Power and Energy Society General Meeting (PESGM), 2016.
11. N. Mahmud, A. Zahedi and **Md Shamiur Rahman**, “An event-triggered distributed coordinated voltage control strategy for large grid-tied PV system with battery energy

- storage,” IEEE Australasian Universities Power Engineering Conference (AUPEC), 2017.
12. N. Mahmud, A. Zahedi and **Md Shamiur Rahman**, Control of Renewable Energy Systems. In: Islam M., Roy N., Rahman S. (eds) Renewable Energy and the Environment. Renewable Energy Sources and Energy Storage. Springer, 2018.
13. Muhammad Kashif, M. J. Hossain, Yuba Raj Kafle and **Md Shamiur Rahman**, “A Comparative Study of Two Current-Control Techniques Applied to a Three-Phase Three-Level Active Power Filter,” IEEE International Communications Energy Conference (INTELEC), 2017.
14. F. H. M. Rafi, M. J. Hossain and **Md Shamiur Rahman**, “Trends in Unbalance Compensation Techniques using Power Electronic Converters for Three-Phase Four-Wire Distribution Systems: An Overview,” Applied Energy. (under review)

Chapter 1

Introduction

Microgrids have paved the path of the current electricity grid infrastructure towards the smart grid. They have emerged as enablers in integrating distributed-generation (DG) units, such as electric vehicles (EV), diverse energy storage systems (ESS), and renewable energy resources (RERs) utilizing intelligent forecasting, and Information and Communication Technology (ICT). Among various microgrid structures, hybrid alternating current (AC)/ direct current (DC) microgrids are becoming popular due to their compatibility with both AC and DC technologies. This structure is particularly suitable for the integration of electric-vehicle energy-storage systems (EV-ESS) for vehicle-to-grid (V2G) applications, as EV-ESS can operate as both AC and DC sources and loads. EV storages can improve the overall performance of hybrid microgrids in terms of voltage and frequency regulation, system stability, active and reactive power support and fault robustness. However, they need to be smartly controlled and coordinated in presence of RERs. The optimized coordination of EV storages within microgrids is a sophisticated issue due to their different control and configuration structures along with inadequate standards regarding V2G applications. The centralized and distributed control structures are viable options to coordinate spatially dispersed EV storages within microgrids of dif-

ferent geographical sizes. This dissertation focuses on the coordinated control and power management of EV storages in hybrid microgrids of different geographical sizes utilizing cost-effective centralized and distributed techniques to enhance the dynamic performance of hybrid microgrids with RERs.

1.1 Background and Motivation

1.1.1 Renewable-Dominated Power Grids

The existing power system infrastructure or unanimously called ‘*The Grid*’ was designed following a vertical structure that consists of generation, transmission, and distribution. Each step of the structure is supported by controllers and associated devices to ensure reliable, efficient and stable unidirectional operation. However, due to increased environmental concern, fuel price hiking and high penetration of RERs into the legacy system, operators are facing challenges which require technical and economical manifestation. As a result, the need for an updated ‘*smart*’ system with advanced monitoring, communication, control, coordination and decision-making capabilities is unarguably consistent. Consequently, a range of innovative research and developments are being carried out which is driving ‘*The Legacy Grid*’ towards a modernized version often termed as ‘*The Smart Grid*’ [9]. According to the definition of Standards Australia [10], the smart grid can be defined as:

“A ‘smart grid’ is an electricity system incorporating electricity and communications networks that can intelligently integrate the actions of parties connected to it.”

According to United States Department of Energy (US-DOE), the Smart Grid has to be: [11]

Intelligent: capable of sensing and decision making by supporting utilities, regulatory authorities, and consumers;

Efficient: capable of managing increased load without adding surplus expenditures;

Accommodating: competent in accepting any types of renewable, non-dispatchable and distributed resources;

Motivating: capable of communicating in real-time with consumers and associated utilities;

Opportunistic: capable of creating new opportunities in market to exploit plug-and-play facility irrespective of place and time;

Quality-focused: capable of delivering essential quality power to increase digital economy;

Resilient: resistant to natural disasters and cyber-attacks;

and

Green: environmental friendly.

Due to the proven technical, economic and environmental feasibility of renewable resources, various policies have been developed by many countries to promote green-energy technologies, such as solar, wind, geothermal, ocean energy, biofuels etc. These policies implicate feed-in tariffs, renewable portfolio standards, tradable green certificates, investment tax credits and capital aids etc. In Europe, the UK is targeting for 15% by the end of 2015/16 and Germany is directing towards 25–30% within 2020 and aiming for 50% by 2030 of their total electricity generation to be generated by distributed renewable resources. In Australia, renewable energy target (RET) is set for 20% by the end of 2020. A thorough and state-of-the-art condition regarding policies and targets with planned or installed projects regarding renewable energy throughout the world can be extracted from REN21 Global Status Report [12].

1.1.2 Vehicle-to-Grid (V2G)

Owing to increasing fuel cost and global concern regarding environmental issues, fuel-efficient automobiles along renewable resources are gaining market demand. EV or plug-in electric vehicles (PHEV) offer substantial advantages over even the most efficient internal combustion engine (ICE) vehicles [13]. EV owners can exploit benefits like curtailed fuel costs and accessibilities like workplace based charge station. Comprehensive communal benefits may involve low environmental impacts and low carbon footprint with reduced dependency on automotive oil. Considering these benefits many governments over the world offer incentives for the consumer to purchase EV. Consequently, the usage of EV and PHEV storages are increasing rapidly. One of the fascinating things about these vehicles is their dual dynamic characteristics as a load while in G2V (grid-to-vehicle) mode and as a generator while in V2G mode. With proper utilization of EV-ESS, the V2G concept can improve utility grid performance in the area of efficiency, stability, and reliability by offering reactive power management, active power control, tracking the intermittent renewable energy resources, load balancing and shifting via valley filling support, peak load shaving and filtering current harmonics in the output. However, extracting the optimum performance from EV-ESS requires the design of proper charging-discharging controllers. Sophisticated active and reactive power regulation, as well as the state-of-the-art monitoring system, is required to overcome the impacts and to implement successful interfacing. EV-ESS can significantly contribute to enhancing dynamic performance and stability of the microgrid under different operating and loading conditions if they can be implemented in a coordinated and controlled manner [14].

1.1.3 Microgrids and Their Control

Successful integration of distributed and renewable energy sources in presence of dynamic loads and storages like EV/PHEV has yet to overcome abundant technical challenges to ensure reliability and efficiency. These challenges include proper scheduling and dispatch of renewable sources, optimum demand side management, uncertain DG unit dynamics, load forecasting, EV charging pattern and their charging infrastructures, voltage and frequency control using power electronics interface in mostly low inertial DG units and unified plug-and-play features of corresponding DG units. The concept of microgrids could be an appealing solution in confronting these challenges.

The term “microgrid” actually refers to a localized and miniature version of existing grid that can support particular electrical vicinity during an outage. Both US-DOE and Electric Power Research Institute (EPRI) have adopted the following definition of microgrid [11]:

“A microgrid is a group of interconnected loads and distributed energy resources within clearly defined electrical boundaries that acts as a single controllable entity with respect to the grid and that connects and disconnects from such grid to enable it to operate in both grid-connected or “island” mode.”

These miniature and smart version of existing grid can support self-sustaining military base, hospitals, industrial plants, refineries, data centers or any institutions that cannot afford power outage not even for a minuscule period of time. But both utilities and customers are looking beyond the capability of microgrids just as a support rather as distributed generators that can generate power and contribute to overall demand management. A self-sustaining microgrid can not only help its corresponding neighborhood riding through disruptions but also can support grid during that time by exporting extra power. Actually these microgrids and its developed forms namely active distribution system (ADS), cognitive microgrid (CM) or virtual power plant (VPP) could be unavoidable

building blocks for the next generation smart grid if many of them can be properly planned and incorporated into a single point of interconnection with utilities and if they can be coordinated accordingly. Expected features that a microgrid should have are presented below:

Throughout grid-tied operation:

- Provision of integrating renewable, non-dispatchable and non-inertial distributed resources,
- Support for distributed resources market involvement,
- Optimized economical operation.

Throughout islanded operation:

- Durable, improved and economical islanded operation,
- Islanding detection, support, and operation,
- Smooth islanded operating condition with high penetration of distributed resources,
- Management of critical/non-critical loads with available resources.

Throughout both operations:

- Distributed, resilient and robust architecture,
- Secure cyber-physical network.

To achieve these expected features in microgrid during grid-connected, islanded and transient mode following technical challenges need to be addressed and surmounted [15]:

- Optimum power flow control within and outside of the microgrid,

- Robust voltage controller design to attain desired voltage level in corresponding nodes,
- Robust frequency controller design to attain stable frequency range within the system,
- Fault fortification,
- Dynamic load management by balancing generation-load-storage-loss balance,
- Power conditioner/filter design to ensure quality power,
- System parameters selection considering transients and post transients,
- Reserve margin by introducing energy storage systems,
- Adequate installed DG units within islanded microgrids to serve loads,
- Single and multiple point of common coupling (PCC) ensuring seamless integration of DG units and multi microgrid operation.

1.1.4 Self-Sufficient Commercial Neighborhoods

Modern commercial buildings are equipped with renewable and sustainable technologies such as smart EV parks; intelligent power electronic interfaced variable-speed drives (VSDs), four-quadrant inverters for rooftop photovoltaic (PV) units and smart high voltage air-conditioning (HVAC) system. These buildings can contribute to both electric power grids and electricity market by providing ancillary services by utilizing these technologies [16]. Particularly incorporation of EV storages along with smart energy management systems can ensure flexible, reliable, secure and profitable power delivery. Keeping track of the global trends, the number of commercially implemented EV charging stations are rapidly increasing in Australia. The current status of EV charging stations in



Figure 1.1: Current status of commercial EV charging facilities in Australia (www.plugshare.com).

commercial vicinities throughout Australia is illustrated in Fig. 1.1. By proper utilization of these chargers, commercial neighborhoods can operate as self-sufficient electrical entities or microgrids. Nevertheless, the coordination among multiple EV storages in a commercial vicinity is a difficult task, particularly when the neighborhood operates as an autonomous microgrid owing to a fault at the grid-side or just to utilize installed renewable resources. Considering prospects of smart autonomous commercial neighborhoods, research interests on vehicle-to-microgrid (V2M) application is increasing. Usually, the peak loads for commercial areas occurs during mid-daytime; therefore, parked EV storages in commercial neighborhoods can be utilized to provide ancillary services during office hours, which typically ranges between 9:00 am to 6:30 pm [17]– [18]. An attempt to quantify the economic benefits by using EV storages for commercial building microgrids

is presented in [19]. An energy management system (EMS) for a building with PV units and EV storages is presented in [20] to minimize the operating cost considering different charging and discharging profile. A real-time peak shaving model to reduce high peak demand combining demand response and load control is presented in [21]. A four-stage optimization algorithm is proposed in [22] for a PV-assisted EV charging station in a commercial building to minimize operation cost associated with customer satisfaction by the optimal scheduling of EV storages. However, above-mentioned methods have utilized hourly or daily forecasting to optimal coordination of EV storages for the commercial V2M operation. A combination of real-time optimization along with the coordination of renewable resources and EV storages will ensure techno-economic optimality.

1.2 Significance of the Research

The coordination of EV storages in commercial vicinities is important to envisage smart metropolitans. It is anticipated that in the near future, there will be a large number of EV storages parked in commercial parking lots during the day. With the smart coordination of these energy storages and with the aid of renewable sources, such as rooftop PV units, these commercial communities can operate as autonomous microgrids. Hybrid AC/DC microgrid structures are feasible options in this regards, as they are compatible with both AC and DC technologies. Moreover, these microgrids are likely to be interconnected with neighboring microgrids to form internet of energy (IoE) networks. As a result, this research intends to present new coordination schemes for EV storages in commercial hybrid microgrids to tackle challenges, such as simultaneous AC and DC bus voltage regulations, fault robustness, interconnection with multiple microgrids, coordinated power sharing among different DG units. This research also explores the technical and economic feasibilities of the proposed coordination strategies by employing distributed and

optimization-incorporated control topologies.

1.3 Research Challenges and Objectives

It is important to evaluate optimum microgrid structure to ensure better connectivity among different agents or nodes within a microgrid. The structure of a microgrid can vary based on various requirements. Microgrid structure may fall into three types namely AC microgrid, DC microgrid and hybrid AC/DC microgrid based on their outputs. As most of the renewable energy sources and energy storage devices have DC output and at the same time, due to increasing DC load demand, the concept of DC microgrid has recently been emerged and is getting acceptance. However, a majority of utility grids are still operating on AC system, DC microgrids are not expected to be deployed solely in near future. Nevertheless, both AC and DC microgrids would require multi-stage AC/DC or DC/AC conversion through the non-linear power electronics-based interface to serve DC and AC loads respectively. This results in a reduction of overall efficiency and at the same time making the system complex and vulnerable. As a result, the concept of a multi-bus hybrid AC/DC microgrid has been proposed in the literature. This structure of microgrid ensures better connectivity than individual AC or DC microgrid. However, the introduction of dynamic energy storages, such as EVs/PHEVs has challenged the feasibility of the structure. For seamless V2G operation and to extract the optimum benefit out of that operation, a modified microgrid structure with robust control strategies is required. The modified structure of microgrid should ensure viable connectivity of these dynamic storages and its control strategy should ensure proper power management and stability.

The main control variables of a microgrid are voltage, frequency, active and reactive power. As a result, the main target of microgrid controller is to maintain stable voltage

and frequency level throughout different operations of microgrid and at the same time achieving proper active and reactive power between energy nodes and loads. To achieve these objectives a hierarchical microgrid control structure emulating the existing power system control structure has been proposed recently. This structure includes primary, secondary and tertiary levels of controllers. Present literature is mostly based on designing primary controllers by adopting different approaches and most of the literature have concentrated on either AC or DC microgrid individually. Consequently, there are scopes for more research in developing other hierarchy of the control levels and for modified hybrid AC/DC microgrid structure integrated with renewable DG units and EV/PHEV storages.

Decentralization of microgrid control techniques can be considered as a major step towards smart grid vision. Both utility and consumers can get benefits by utilizing DG units and advanced ESSs. The challenge is the number of DG units and EV/PHEV units associated with a microgrid. Application of centralized controller in a microgrid with a huge number of energy nodes and loads is not a technically feasible and secure solution. Apart from the increasing complexity, the centralized controller is susceptible to catastrophic consequences which might occur due to single-point of failure, causing the whole system to shut down. As a result, researchers are looking for more control techniques with minimal communication infrastructures so that even shutting down of one node will not affect the whole system as much as it could have been done by the centralized controller. Moreover, emerging energy storages, such as EV units are spatially distributed. Coordinating these EV storages through centralized control structure is not a feasible solution. As a result, distributed control techniques can be considered viable resolutions. However, the need for communication structure cannot be avoided using distributed techniques. It is also important that the communication channels are not always burdened with sensor data. As a result, an algorithm is needed to administer the initiation and the duration

of distributed coordination. Furthermore, EV units may introduce undesirable network effects, such as voltage sagging, swelling unbalanced conditions, and power quality issues. These issues need to be tackled utilizing cost-effective and efficient methods.

Motivated by the issues relating to the design of microgrid controllers considering high penetration of DG units and EV/PHEV units the objectives of the current research is defined as follows:

- Evaluating an optimum microgrid structure for suitable connectivity of various energy nodes (i.e. DG units, loads etc.) with special attention to commercial vicinities.
- Developing a profound understanding of the characteristics of DG units particularly PV units that involve uncertainty, low inertia, and intermittency.
- Analyzing the aggregated impacts of loads, such as EV unit considering their indefinite charging pattern and existing charging station infrastructures.
- Quantifying the benefits of V2G and developing a better understanding regarding the characteristics of EV-ESS and their applicability into microgrid paradigm.
- Designing novel control methodologies to ensure primary voltage and frequency regulations in a multi-bus microgrid structure considering various operational modes.
- Applying communication-assisted centralized and distributed control techniques to ensure coordination among cooperating energy nodes.
- Providing cost-effective solution to the designed multipurpose microgrid controller.

1.4 Main Contributions

Based on the research challenges and objectives mentioned above, this dissertation provides three main contributions listed below:

- Design and implementation of a novel three-layered centralized coordinated control strategy for EV storages in a hybrid AC/DC microgrid with two commercial buildings. The algorithm takes EV availability constraints and power deviations in AC and DC subgrids into considerations and provide necessary reference power signals for primary controllers. It also ensures coordination among three-phase (3P) and DC type EV-ESSs to achieve this objective. The first layer of the algorithm ensures DC subgrid management, which includes DC bus voltage regulation and DC power management. The second and third layers are responsible for the AC subgrid management, which includes AC bus voltage and frequency regulation with active and reactive power management. The multi-layered coordination is embedded into the microgrid central controller (MGCC), also known as the secondary microgrid controller, which controls the interlinking controller in between the AC and DC subgrids as well as the interfacing controllers of the participating EVs and distributed RERs.
- Development of a new need-based distributed coordination strategy (NDCS) for multiple EV storages in an islanded commercial hybrid AC/DC microgrid with extended geographical size. The control capacity of the interlinking converter is enhanced by incorporating combined power-droop and voltage-droop strategies to leverage the coupling of AC and DC voltages. Therefore, the AC bus voltage can be regulated simultaneously by regulating only the DC bus voltage without affecting the power-sharing capabilities of the converter. The NDCS is proposed to coordinate the EV storages to regulate the DC bus voltage. The main objective of the NDCS is to decide whether the coordination of the available EV storages is to be performed in a decentralized or a distributed manner. The mathematical model and the algorithm to deploy NDCS are developed to realize its application to a real system.

- Establishment of an optimized and improved distributed control strategy to ensure cost-effective operations of hybrid microgrids. A hierarchical V2M framework is proposed which utilizes parked EV storages to ensure stable commercial hybrid microgrid operation. A centralized aggregator model is developed which optimizes EV economic dispatch problem in real time and generates references for the V2G-capable EV storages under its operational vicinity. The optimizer adjusts the power setpoint for each EV, which ensures proper power management within the microgrid. As a result, a cost-effective distributed V2G operation can be ensured.

The commercial hybrid AC/DC microgrid and its extended version are designed in a MATLAB/Simulink environment resembling the microgrid under construction at Griffith University, Australia. Extensive case studies are performed in order to assess the performance of each developed coordinated controllers, that include real-life solar irradiation, commercial load profiles, EV time delay, and EV plug-and-play and fault conditions etc. Additionally, the performance of the controllers is compared with the conventional controllers predominantly available in the literature to cement their individual performances in terms of transient response, fault-robustness, scalability, cost-effectiveness, and reliability.

1.5 Thesis Outline

Subject to the above research objectives and targeted contributions this dissertation is outlined as follows:

Chapter 1 is anticipated to provide the background and motivation of the current research including main contributions and significance of the research. Later, the thesis outline is presented at the end of this chapter.

Chapter 2 focuses on contemporary literature survey related to the structures and

controllers associated with microgrids and EV storages. This chapter also discusses existing relevant standards.

Chapter 3 presents a new and improved three-layered centralized coordinated control strategy considering EV availability constraints for 3P and DC type EV-ESSs to improve the operation of a hybrid AC/DC microgrid in terms of voltage and frequency regulations and power management.

Chapter 4 concentrates on distributed control techniques applicable to EV coordination. This chapter presents a novel NDCS for multiple EV storages in an islanded commercial hybrid AC/DC microgrid with extended geographical size.

Chapter 5 discusses the application optimization techniques to improve the performance of the designed distributed controller. An efficient optimization-incorporated distributed control technique for EV coordination in hybrid microgrids is presented to ensure a cost-effective solution for EV coordination in microgrid environment.

Chapter 6 provides the concluding remarks and future directives for this research.

Chapter 2

Literature Review

2.1 Introduction

Deployment of renewable-based distributed energy resources (DER) is increasing due to recent global concern about fuel price hiking and environmental pollution caused by conventional power sources. As a result, microgrid - a building block of future smart grid vision, is now an extensively accepted concept because of its flexible and bidirectional power flow strategy and superior connectivity with alternative sources and utility grids. Comparing to conventional bulk power system with centralized control operations, microgrid offer decentralized (local) control over power management and interconnection with the distribution system. According to The Consortium for Electric Reliability Technology Solutions (CERTS), the definition of microgrids is as follow,

“ A microgrid must be able to operate parallel with the grid, and also should have the ability to isolate itself from the utility seamlessly with little or no disruption to the loads within the microgrid during a disturbance [23] ”

As a result, by definition, microgrids are expected to be operated in both islanded and grid-connected mode with multiple distributed sources and prosumers. Islanded opera-

tion of microgrids particularly provides improved reliability. However, with the increased number of prosumers and the integration of large number of vehicle-to-grid (V2G) capable electric vehicles (EVs) in the distribution systems, the control of microgrids requires robust and improved solutions. Therefore, this chapter presents the state-of-the-art control topologies and techniques of microgrids for both islanded and grid-tied mode of operations. Firstly, hybrid alternating-current (AC)/direct-current (DC) microgrids are introduced. Challenges and prospects of V2G operation along with particular control strategies in a microgrid are discussed in the later sections. Finally, relevant national and international standards are summarized to understand the grid requirements.

2.2 Hybrid AC/DC Microgrid: a Future for Distribution Systems

Since most of the renewable energy sources have DC output power along with increasing DC load demand, the concept of DC microgrid has recently emerged with lots of potentials. Nevertheless, DC microgrids are not expected to be deployed solely in near future. It is due to the fact that majority of utility grids are still operating on legacy AC system and three-phase AC system is prevailing for more than hundred years. Moreover, DC sources are needed to be converted into the AC form to supply AC loads. As a result, AC microgrids are more common. However, AC microgrids again need conversion from the AC to DC for supplying DC loads. These multiple AC/DC/AC conversions through nonlinear power electronics based converters reduce overall efficiency and at the same time make the system complex and vulnerable. As a result, the concept of hybrid AC/DC microgrid has been proposed in literature [24,25]. The concept of hybrid AC/DC microgrid system is to combine both AC and DC renewable/non-renewable power sources along with corresponding AC and DC loads. A hybrid AC/DC microgrid is composed of individual

AC and DC buses. At the point of the AC bus, AC sources like wind turbines and utility grids along with AC loads like induction motors are connected. DC sources like PV, fuel cells, electric vehicle - energy storage systems (EV-ESS) etc. and loads like data centers, telecommunication base stations etc. are connected at the DC bus point. The AC and DC bus are interfaced with an interlinking converter which acts as a gateway for the power flow between AC and DC subgrids [24, 25]. A hybrid AC/DC microgrid structure has several advantages over conventional microgrid or distribution system structure. Some notable benefits include feasibility in integrating distributed generation (DG) units of both types with minimum conversion, minimum voltage and frequency synchronization efforts, and simple voltage transformation for both AC and DC bus using transformer and DC/DC converters respectively. Furthermore, due to fewer conversion efforts efficiency, reliability and economic operations can be ensured. As a result, this distinct microgrid structure can be considered as a viable solution to the future smart distribution system. A conceptual hybrid AC/DC microgrid structure is illustrated in Fig. 2.1. The hybrid AC/DC microgrid illustrated in Fig. 2.1 is comprised of AC and DC buses interfaced through multiple parallel interlinking converters. All DC-type DG units such as DC fast EV charging stations, PV units and community storages etc. along with DC loads are connected to the DC bus, whereas, AC-type DG units such as diesel generators, doubly-fed induction generator (DFIG) wind turbines, EV AC charging stations etc. and AC-type loads are connected to the AC bus. The utility grid is connected to the AC bus also known as the point of common coupling (PCC) through intelligent bypass switches (IBS). The main objective of IBS is to sense the island detection signal to disconnect the microgrid from the utility grid or to reconnect to the grid when necessary.

Power control and management techniques are a critical aspect of a hybrid microgrid operation. Main objectives of a microgrid controller are to ensure stable islanded and grid-tied operation by stabilizing and synchronizing voltage and frequency with propor-

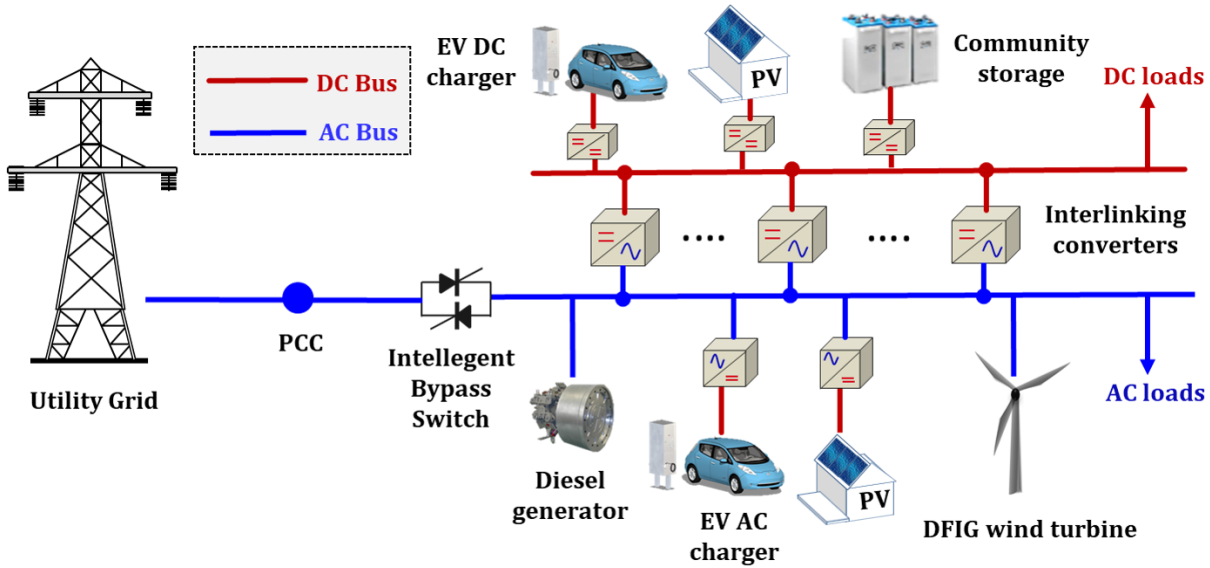


Figure 2.1: A conceptual hybrid AC/DC microgrid structure

tional active and reactive power sharing among multiple DG units. For grid integration, the DG units have to follow IEEE 1547 standard at their point of common coupling (PCC). However, after the publication of the standard, there have been lots of changes in the standard, like in IEEE 1547.4, they covered some missing point from the initial one regarding DG connection variable parameters like frequency, power quality, and the voltage impact [26]. Conventionally, utility grid operates as a slack bus to support the variation or change in real or reactive power. Therefore, microgrid control structures and relevant standards will be discussed in subsequent sections.

2.3 Microgrid Control

Integration of multiple numbers of intermittent renewable sources and emerging loads like EVs into the microgrid, introduce new technical and economic challenges. Appropriate control and proper coordination of microgrid are extremely important in order to address these challenges. This section will explore state-of-the-art literature on challenges,

features, structures, and techniques associated with microgrid control.

2.3.1 Challenges

The design of microgrid control and protection systems requires addressing functional challenges to ensure the contemporary level of reliability and to extract potential benefits of DER. Some of the challenges are derived from invalid assumptions which may lead to system instability. While considering the concept of emulating the power system control within microgrid, most of the challenges are derived from the conventional distribution and transmission system persistent in present power systems. Microgrid control challenges can be identified as below [3, 5]:

- *Bidirectional power flows:* Existing power system and its associated distribution feeders are designed for unidirectional power flow. It is expected that introduction of DG units in low voltage networks will require bidirectional power flow where consumers will act as prosumers. Complicities such as reverse power flow, unexpected power flow pattern, unbalanced voltage levels and fault current flow may arise if existing feeder systems persist in presence of DG units in low voltage networks.
- *Stability issues:* Local oscillation may appear due to the interaction among dissimilar control dynamics of DG units. Additionally, smooth transition between grid-tied and islanded mode of microgrid operation requires thorough a small signal and transient stability analysis.
- *System modeling:* Assumptions such as low X/R ratio, balanced three-phase condition and constant power loads can be considered valid in order to model a conventional power system at the transmission level. Nevertheless, these assumptions are invalid where a microgrid in low voltage distribution networks is considered. As a result, a revised modeling is required.

- *Low inertia:* Most of the renewable energy sources like solar modules, fuel cells etc. have no inertia and other renewable sources like wind turbines have low inertia. In contrast to large power systems with multitudes of synchronous generators ensuring high inertia, these power electronic-interfaced DG units in microgrids show low inertia characteristics. Even though power electronics based DG units show better dynamic performance, the low-inertia characteristics may lead to frequency deviations in the islanded mode of operation unless appropriate control mechanisms are not adopted.
- *Uncertainty:* Uncertainty, intermittency, non-linearity and unpredictability are associated characteristics of the most renewable DG units. Definite levels of coordination among different DG units are required to ensure efficient and consistent microgrid operation. Particularly during the islanded mode of microgrids where maintaining generation-consumption balance is more severe due to the consideration of the high rate of component failures and uncertainty associated with load profile and weather forecast. The unpredictability rate in a microgrid is actually higher than large power system due to the presence of highly correlated output variations of accessible energy sources which are known as the limited averaging effect.
- *Cyber-physical security:* Controllers need to communicate through communication networks due to the dispersed position of prosumers and DG units. Cyber networks are vulnerable to malware and data infringement. With the growing number of microgrids and their associated controllers, cyber-physical security is an important issue.

The primary focus of this dissertation is to focus on the stability of the system in presence of V2G-capable EV storages and PV units. Novel coordinated control approaches

are proposed to address challenges such as voltage and frequency stability, power management, system-modeling etc. Uncertainties associated with the PV output power and the load profile are considered while designing the controllers. The cyber-physical security and the economic aspects are not within the scope of this dissertation and could be future directives.

2.3.2 Expected Features

Control challenges mentioned in the previous section needs to be handled by the designed microgrid controllers. Expected features of the control system to ensure reliable, consistent and efficient operation of the microgrid involve:

- *Output control*: Output refers to the voltage and current generated by various DG units in a microgrid. Desired microgrid controllers should have the capability to control these outputs. They control the output voltage and current so that all associated DG units track their predefined or generated set points/reference values and oscillation is accurately damped.
- *Power balance*: Associated DG units in a microgrid should be able to meet load requirements even under extreme conditions like faults. It is expected that microgrid controllers will control both active and reactive power and initiate necessary steps of power-sharing and storage commands to balance overall power profile and at the same time keeping voltage/frequency deviations within acceptable levels.
- *Demand side management (DSM)*: Demand side management (DSM) is the mechanism to modify the consumer demand for energy by means of financial incentive and education. Generally, the objective of DSM is to motivate consumers to use less energy during peak hours or to shift the time of energy consumption to off-peak hours, for instance, night time and weekends. Economical DSM strategies should be

integrated within microgrid controllers in order to ensure load frequency control and active participation of prosumers. This will increase controllability over a portion of load [27, 28]. However, DSM has not been considered in this thesis and could be a future directive of this research.

- *Economic dispatch*: A proper and economical way to dispatch DG units particularly in islanded mode can contribute immensely to the reduction of the operational costs and maximization of the profit by taking reliability into consideration.
- *Durable operational mode transient*: An intelligent and reliable microgrid should operate in grid-tied, islanded and transition between these two modes. Various control techniques are applicable for grid-tied and islanded operation. To achieve seamless operation during the transition between these two modes require fast islanding detection and proper transient performance. As a result, microgrid controllers should be properly responsive to the islanding detection signal and have robust transient handling capability [29]. Moreover, the controllers need to be robust to cyber-physical anomalies and faults.

2.3.3 Controlled Variables

The controllable variables for microgrid controllers are rather straight forward, they are – voltage (V), frequency (f), active (P) and reactive power (Q).

In the grid-tied operation, the frequency of the microgrid and the voltage at the PCC are determined and regulated by the grid. Microgrid controller operates in grid-feeding or grid-supporting mode by handling and supplying the active and reactive power generated by DG units to supply load demand. Reactive power generated by individual DG units (i.e. wind turbine, diesel generators etc.) or by interfacing voltage source converters (VSC) for solar modules, fuel cells etc. can be injected to meet the reactive power demand.

VSCs can also take part in the operation of voltage regulation or power factor correction. According to the present IEEE standard 1547 for interconnecting distributed resources with electric power systems, DG units are not allowed to regulate or control the PCC voltage during grid-tied operation to avoid interaction with the similar feature provided by the grid [30]. However, with the recent modifications, VSCs can actively engage in voltage regulation by reactive power injection or absorption.

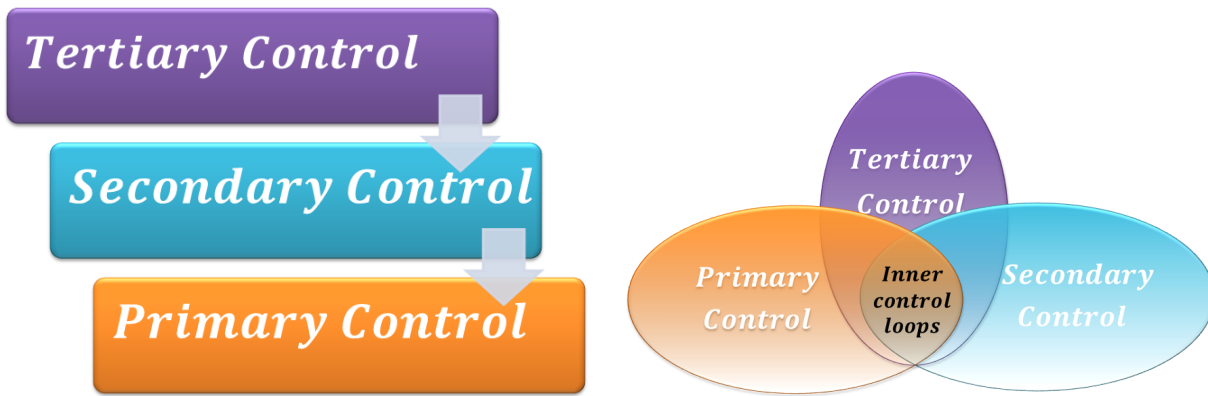
In the islanded mode of operation, the microgrid functions as a self-governing entity. This mode of operation is significantly more challenging than the grid-tied mode because it involves active power balancing and load sharing. Since voltages and frequency of the microgrid are no longer supported by the grid, thus separate voltage and frequency controller need to be activated. Active power is balanced either by the central controller or by the local controller. Local controllers of DG units use local measurements to generate reference on the other hand central controller generate reference values centrally and communicate these set points to DG units associated local controllers. The main objective of such a mechanism is to guarantee that all units contribute to supplying the load by tracking pre-specified set points [31].

Microgrid controllers can be classified from various perspectives. From the configuration point of view, there are controllers specific to AC, DC or hybrid AC/DC microgrids. Microgrid controllers can be classified as grid-forming, grid-supporting and grid-feeding types based on assigned objectives and the mode of operations. Mostly recognized microgrid control topology involves a hierarchy of controllers. All controllers within the hierarchy can be broadly classified into three major techniques that are centralized, decentralized and distributed methods. A brief depiction of the hierarchical microgrid structure are presented in the following section.

2.4 Overview on Hierarchical Microgrid Control Structure

Microgrid can operate in both grid connected and islanded mode. It is also expected that the microgrid will operate seamlessly during the transition between grid-tied to islanded mode or vice versa. Thus microgrid control is rather complicated topic to be addressed. The main objectives of microgrid controllers are [4]:

- Voltage and frequency regulation (in both operating mode)
- Proper load sharing and DER coordination (in both operating mode)
- Microgrid resynchronization with the main grid (transient mode)
- Power flow control between the microgrid and the main grid (grid connected mode)
- Optimizing the microgrid operational cost



(a) Hierarchy of primary, secondary and tertiary control layers in a microgrid (b) Position of the inner control loops in the hierarchical structure

Figure 2.2: Hierarchical microgrid control structure

It is important to standardize microgrid control structure to correlate with new grid codes. In order to do so the standardized structure for automated interface between

multiple enterprise and control systems given in ISA-95 is adopted [32]. According to [33] and [34] the microgrid control structure shown in Fig. 2.2 would be as follows:

1. **Level 3** (*Tertiary Control*): This level is responsible for importing and exporting power to/from the grid.
2. **Level 2** (*Secondary Control*): This level is responsible for the synchronization or restoration of microgrid with grid. It is also responsible for maintaining all electrical levels within acceptable region.
3. **Level 1** (*Primary Control*): This level is responsible for parallel power sharing between multiple DG units and stabilizing voltage and frequency using droop or similar methods
4. **Level 0** (*Inner Control Loops*): This level is responsible for handling voltage or current regulation issues associated with each module.

Within the hierarchical microgrid control structure, each layer of controllers follows a chain of commands. The higher layer has the supervisory authority over lower layer. Command and references signals from layer to layer should have a low impact on the system stability. As a result, the response time of the higher layers is slower as compared to the lower layers. Table 2.1 documents the objectives and some of cutting edge control techniques for different layers of the control structure predominantly utilized in the literature. The design of primary control loops are well researched. Primary control loops are mainly designed utilizing decentralized droop techniques due to the simplicity of mechanism and implementation. Conversely, secondary and tertiary control loops can be designed utilizing either distributed or centralized techniques. Several classical and modern control techniques are utilized to design and tune inner control loops. However, proportional-integral-derivative (PID) controllers are widely used in this loop due to the

Table 2.1: State-of-the-Art Techniques for Hierarchical Microgrid Control [3–6]

Control loop	Objectives	State-of-the-art techniques
Inner Loop Control	<ul style="list-style-type: none"> - Handling stability and regulation issues, - Maintaining performance parameters which includes rise time, settling time, steady-state error, damping etc. 	proportional-integral-derivative (PID) Control, proportional-resonant (PR) control, predictive control, dead-Beat (DB) control, hysteresis control, LQG/LQR control, sliding mode (SM) control, H_{inf} control, repetitive control, artificial neural networks (ANN) control, fuzzy logic (FL) control etc.
Primary control	<ul style="list-style-type: none"> - voltages and system frequency stabilization, - parallel power-sharing among multiple DG units, - avoiding circulating current during parallel operation 	conventional droop control (i.e. $P - f/Q - V$ or $P - V/Q - f$), P-D compensated droop control, adjustable load sharing control, VPD/FQB droop control, virtual frame transformation method, virtual output impedance method, adaptive voltage droop control, signal injection method, non-linear load sharing, centralized control, master-slave control, average load sharing control, circular chain control (3C) etc.
Secondary control	<ul style="list-style-type: none"> - microgrid energy management system (EMS), - compensating the voltage and frequency deviations caused by the primary control, - Synchronization or restoration of a microgrid with grid 	genetic algorithms (GA), particle swarm optimization (PSO), model predictive control (MPC), ant colony optimization (ACO), potential function-based control, voltage unbalance compensation technique, multi-agent (MAS) concept, gossip-based technique, distributed cooperative control etc.
Tertiary control	<ul style="list-style-type: none"> - sets ‘Optimal’ set points as per requirements of the host grid, - coordinates the operation of multiple microgrids, - control the power flow to/from the grid 	an equal marginal cost-based approach, the gossiping algorithm, game theory-based approach etc.

reasonable performance. As a result, PID controllers are used throughout this dissertation to design the inner control loops and decentralized droop techniques are adopted for the primary control loop within the microgrid controllers proposed throughout this dissertation.

2.5 Overview on Vehicle-to-Grid (V2G) and Vehicle-to-Microgrid (V2M)

It is expected that EV or plug-in hybrid electric vehicles (PHEV) will be significant parts of the connected load in the future smart grid. Decreasing battery costs, competitive markets and incentives from the governments are contributing to the quick growth of EVs. As of November 2017, the number of Hybrid electric vehicles (HEV), PHEV and battery electric vehicles (BEV) on the world's roads has passed the three million mark. EVs are suitable for demand response program and dynamical electrical storage resources due to their dual operations known as the V2G and grid-to-vehicle (G2V). These vehicles are generally equipped with large batteries in ranging 7.8kW h to 27.6kW h, which are to be connected to the grid to be fully charged. These batteries can be charged from the DG units, for example, wind and solar during the off-peak time in the microgrid and supply power back to the grid during peak time. In order to utilize EVs into microgrid paradigm robust coordinated controls are needed for charging and discharging. Advantages and challenges of EV penetration into microgrid are briefly quantified in the following subsections [35, 36].

2.5.1 Challenges of V2G/V2M Technology

Several research studies have been conducted for finding the optimum penetration level of EVs into the grid in dual mode. Power flow variation monitoring and designing plausible control methods have become a priority in recent years. Various literature has proposed different methods of controlling and monitoring power flow during V2G mode (i.e. EV discharging mode) and G2V mode (i.e. EV charging mode) and tried to quantify the effects making realistic assumptions. Considerable efforts have been focused on the investigation of the impacts of a huge number of EVs in distribution grids. In several pieces

of literature, the impacts of EV penetrations have been analyzed either by simulation or by doing realistic case studies. In V2G concept both grid operators and car owners share benefits among themselves which is a reason behind recent rapid EV development. EV can behave either as a load or as a generator. Their behavior pattern depends on several factors like type of charger connections (unidirectional/bidirectional), the number of EVs being charged in given vicinity, voltage and current levels, battery status and capacity, charging duration, geographical locations etc. [35]. Fast charging of these EVs can have a huge impact on the distribution grid as typical EV load is almost double of an average household load. Adding up harmonics resulting low power factor can be serious problems if the charger does not utilize state-of-the-art conversion. The challenges associated with the V2G operations can be summarized as follows:

- Stochastic charging pattern
- Voltage and frequency fluctuation
- Storage life-cycle degradation
- Harmonic distortion
- Fast charging
- Peak demand management
- Smart coordinated charging
- Additional infrastructure requirements

The primary focus of this research is to evaluate the feasibility of utilizing EV storages of different configurations and to design coordinated controllers to improve and stabilize the technical parameters such as voltage and frequency by maintaining robust power management among participating DG units. Different types of EV chargers and their corresponding charging time, maximum power consumption, maximum current drawing capability and standard voltage levels are presented in Table 2.2.

2.5.2 Prospects of V2G/V2M Technology

EVs, with an adequate intelligent connection to the grid, interactive hardwires and software control, can serve as direct resources or as a spinning reserve during a power outage.

Table 2.2: Charging Power Level for EVs [1]

Charging time	Type	Power	Voltage	Max. current
6~8 hours	Single-phase	3.3 kW	230 V	16 A
3~4 hours	Single-phase	7.4 kW	230 V	32 A
2~3 hours	Three-phase	10 kW	400 V	16 A
1~2 hours	Three-phase	22 kW	400 V	32 A
20~30 minutes	Three-phase	43 kW	400 V	63 A
20~30 minutes	Direct current	50 kW	400~500 V	100~125 A
10 minutes	Direct current	120 kW	300~500 V	300~350 A

The V2G concept with appropriated control can improve the utility grid's performance in the area of efficiency, stability, and reliability by offering reactive power support and active power regulation, tracking and supporting the efficient integration of variable intermittent renewable energy sources, load balancing and shifting via valley filling, peak load shaving, and current harmonic filtering. According to Yilmaz et al. [14] to maintain grid reliability, balancing supply and demand V2G concept can provide higher quality ancillary services: quick frequency and voltage regulation, load leveling, and peak power management and effective spinning reserve.

In order to facilitate proper function of the grid, it is required to unremittingly balance production and consumption of both active and reactive power, so that the frequency and voltage amplitude can be closer to their nominal values. Active power can be controlled by controlling frequency and reactive power control relies on voltage control of the system. Thus, frequency and voltage are important factors in determining the power quality of utility grids. Implementing V2G in overall voltage and frequency regulation will pave a path towards active and reactive power quality improvement. Currently, frequency regulation is achieved by the expensive process of cycling large generators. EV can be used in this case as they can act as a medium sized generator. An aggregator based revenue model has been proposed in the literature which is able to provide the regulation up to certain desired level by organizing EVs. An Energy Management System (EMS)

will be placed at grid side which will dispatch appropriate regulation signal within the contracted boundary of the aggregator. Idle EVs will respond to the regulation signal based on the developed algorithm. A proper logic of charging and discharging of EVs can be implanted in the battery charger with a voltage control to compensate reactive power, which will select the current phase angle to operate in the inductive or capacitive mode of charging. Despite large penetration of EVs for charging batteries from grid could be a reason of line overloading and voltage instability at a low voltage network, it can regulate reactive power within local vicinity. According to the Union for the Coordination of Transmission of Electricity (UCTE) the control of frequency stability in the distribution system can be categorized into three types: primary, secondary and tertiary [35].

Due to global awareness regarding energy security, fuel diversity and climate change, the usage of renewable energy resources for power generation are increasing rapidly. Integration of renewable energy sources into the grid has become a necessity. But the unpredictability of the availability of sources has become a prime concern on integration. Presently the most prevalent renewable energy resources are wind power and solar energy, particularly in Australia. Solar irradiation is not constant throughout the day and not available to generate solar power at night. On the other hand, wind power is more complex due to the unpredictable variations in the wind speed, which makes it strongly intermittent and can lead to overall system instability. A number of studies have been carried out to combine EVs with renewable energy sources to serve different purposes, such as battery storage, reactive power system and active power control. In [37] an investigation on the possibility of V2G concept to overcome intermittency in wind power is conducted. Guille and Gross et al. [38] proposed a structure using model predicated control to analyze the positive effect of EVs on the wind generator. In [39] an autonomous distributed V2G control has been proposed for providing distributed spinning reserve during intermittency. Different strategies for integrating EVs into wind thermal power plant

have been investigated in other literature [35]. A combination of demand response with wind integration to balance the power is also analyzed. The V2G concept can provide flexibility in power saving. In a renewable-dominated smart grid if the power generated by renewable sources is high then without curtailment this energy can be stored in EV batteries with designed charging model. This energy can be further used in residential areas or industrial areas; if not can be supplied to the grid later on thus a flexible power supply can be managed.

It has been mention previously that PHEVs or EVs can be used as a dynamic storage and they can act as both as a generator and load. V2G can contribute to even out peak energy load by discharging during peak time and charging during low demand (i.e. overnight or off-peak hours). Several pieces of literature proposed different methods for smart vehicle charging systems using various algorithms to level the curve. An algorithm that can be utilized for load leveling purpose by using dynamic electricity pricing curve has been proposed. This curve can optimize an ideal minimum charge when EV users derogate their electric bill. EV should be charged late night due to low demand level during that time. In a case study of California grid with 4 million EVs showed that charging load can be met by the present power system without requiring additional power sources. Mets et al. [40] showed that smart charging/discharging can reduce peak load and level the load curve and described different local/global smart charging/discharging and their coordinated control strategies. Chakraborty et al. [41] observed that for New York City where 100,000 vehicles were simulated using Level 2 charging a benefit of \$110 million per year can be achieved considering 50% simultaneous EV penetration level and contribute approximately 10% of peaking capacity safely where up to 87.5% penetration of EV charging does not pose any protection issue. For high penetration load shifting of EV, fleets can reduce the overall impact on the grid. This can be achieved by coordinated charging of EVs. The target of a controlled battery charger is to scale down peak load

by shifting energy demand. This also gives opportunities for smart charging. A study in 13 U.S. regions without smart charging considering high penetration of EVs showed that additional 160 power plants will be required if every EVs are charged in the early evening. In some literature like [42, 43] it is shown that there is little financial incentive with increased PEV penetration when V2G is used for peak load reduction. According to [44], peak power control has been proven economically feasible solution in Japan. Overall, the advantages of the V2G operation can be quantified in following grounds:

- Active power regulation
- Reactive power support
- Load balancing
- Load shifting via valley filling
- Smoothing the output powers of the DG units
- Peak load shaving
- Current harmonics filtering
- Voltage regulation
- Frequency regulation
- Congestion management

2.5.3 Configurations and Control Strategies of Various EV Chargers

An overview of the configurations and the control strategies used in this dissertation for DC type, three-phase AC and single-phase AC type EV chargers are briefly presented in subsequent sections.

DC Fast Charger

The configuration and the control strategy for the DC fast charger used in this dissertation, particularly while utilizing them in islanded microgrids, are shown in Figs. 2.3a and 2.3b respectively. It includes a DC/DC bidirectional converter as the interfacing converter for EV-ESSs. The control strategy for the converter involves a voltage-control loop (VCL) and a current-control loop (CCL). PI controllers are used to control individual

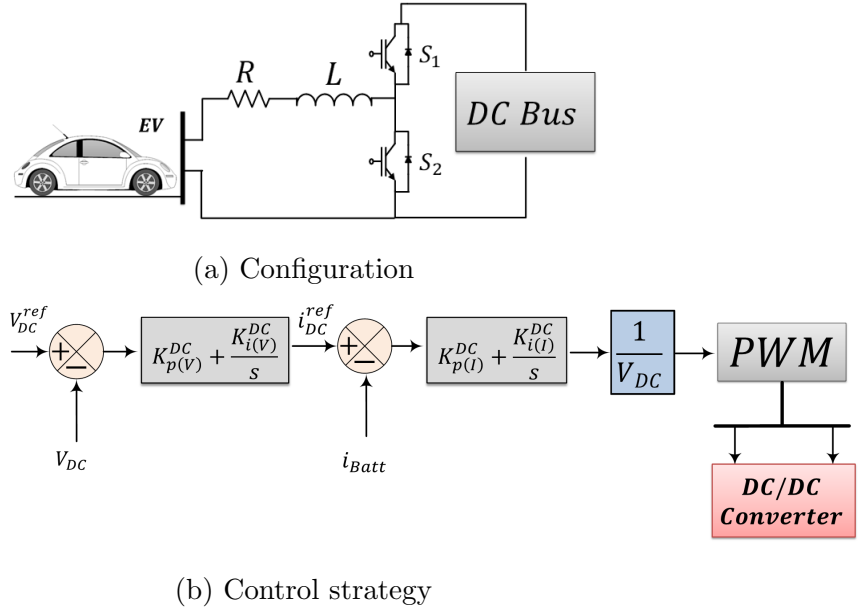
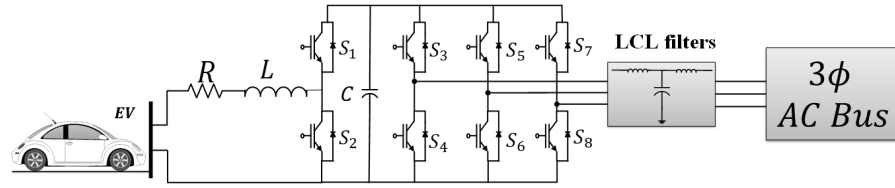


Figure 2.3: Typical EV DC fast chargers [1]

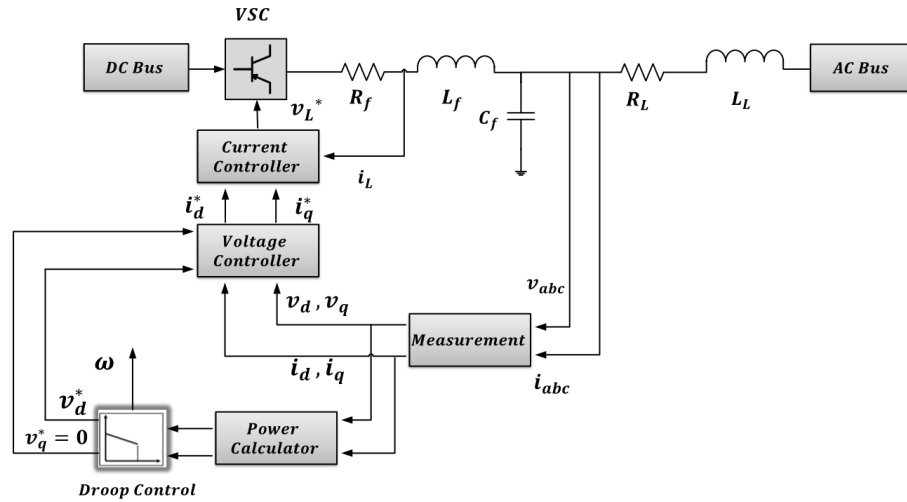
loop parameters. The VCL stabilizes the DC link voltage by tracking V_{DC}^{ref} . Therefore, the output DC voltage of the converter is regulated. Later, the VCL generates reference current signals for the CCL, which in turns generate necessary duty cycles for the interfacing EV-ESS converters.

Three-phase AC Fast Charger

Typical configuration and associated control strategies of a bidirectional three-phase EV charger are shown in Figs. 2.4a and 2.4b. It consists of a DC/DC converter interfaced with a three-phase inverter. In practical cases, there is a galvanic isolation in between the converter and the inverter. The three-phase AC fast charger requires distinct control strategy to achieve the V2G capability. The control strategy is developed utilizing decoupled $d - q$ control of three-phase inverters using pulse-width modulation (PWM). It consists of three inner control loops *i.e.* power-control loop (PCL), VCL and CCL. The PCL is basically a droop control that ensures effective bidirectional active and reactive



(a) Configuration



(b) Control strategy

Figure 2.4: Typical EV three-phase AC Fast Charger [1]

power allocation among several EV units. The designed droop controller generates references for the voltage controller which are later fed to the current controller. The current controller generates the necessary modulation signal for the inverter of the charger. Usually, LCL filters are used after the inverter in order to achieve smooth voltage and current wave shapes. An elaborate description of the control strategy for the three-phase AC fast charger used in this section can be obtained from [17]. Though the primary focus of this dissertation is conventional charging, currently three-phase AC faster-charging system has been introduced under the umbrella of onboard charging systems which utilizes the internal bi-directional DC (Battery source) /AC (Motor drive) inverter. The AC Motor drive can be connected to a three-phase AC side of 50/60 Hz only.

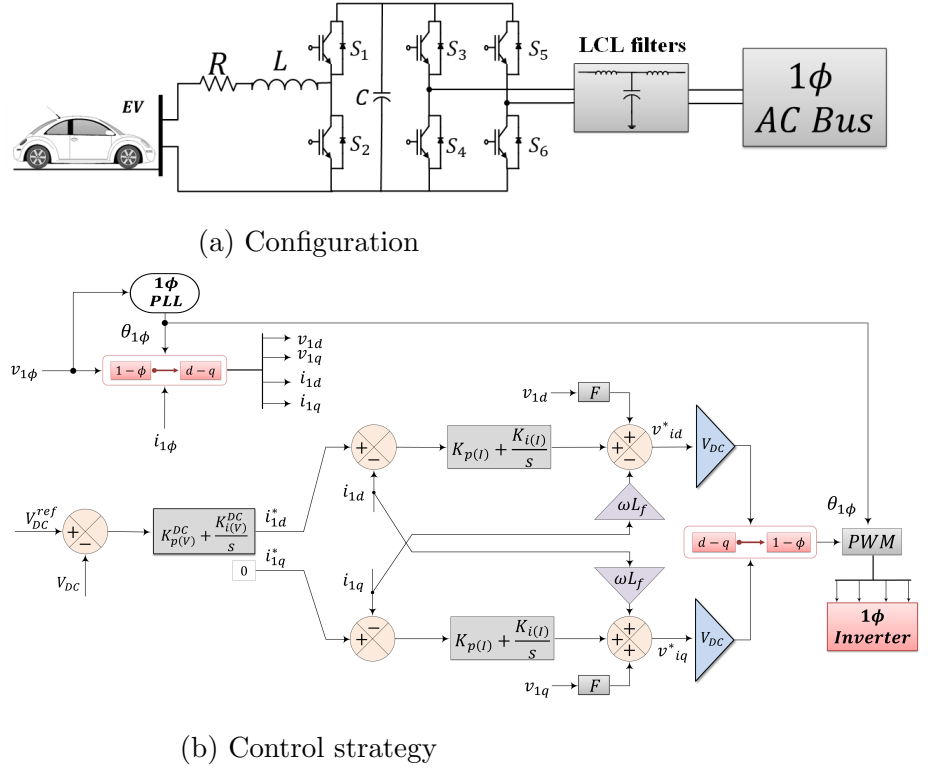


Figure 2.5: Typical EV single-phase AC Fast Charger [1]

Single-phase AC Domestic Charger

Single-phase AC domestic charger configuration and control strategies are shown in Figs. 2.5a and 2.5b respectively. Single-phase EV chargers are designed to operate as active loads. The operation of EVs is designed with single-phase phase-locked-loop (PLL) and associated controllers as proposed in [45]. Single-phase PLL includes one orthogonal signal generator which generates β components of the single-phase input voltage and current signals. Later the virtual $\alpha - \beta$ components of the voltage and current are converted into $d - q$ components. The generated $d - q$ components are used in the decoupled $d - q$ synchronous reference frame (SRF) controller for single-phase inverters as presented in [46]. The terminal voltage magnitude of the single-phase AC chargers is reasonably constant due to their active load operating control strategy.

2.6 Interfacing Converter Control in Grid-Tied and Islanded Mode

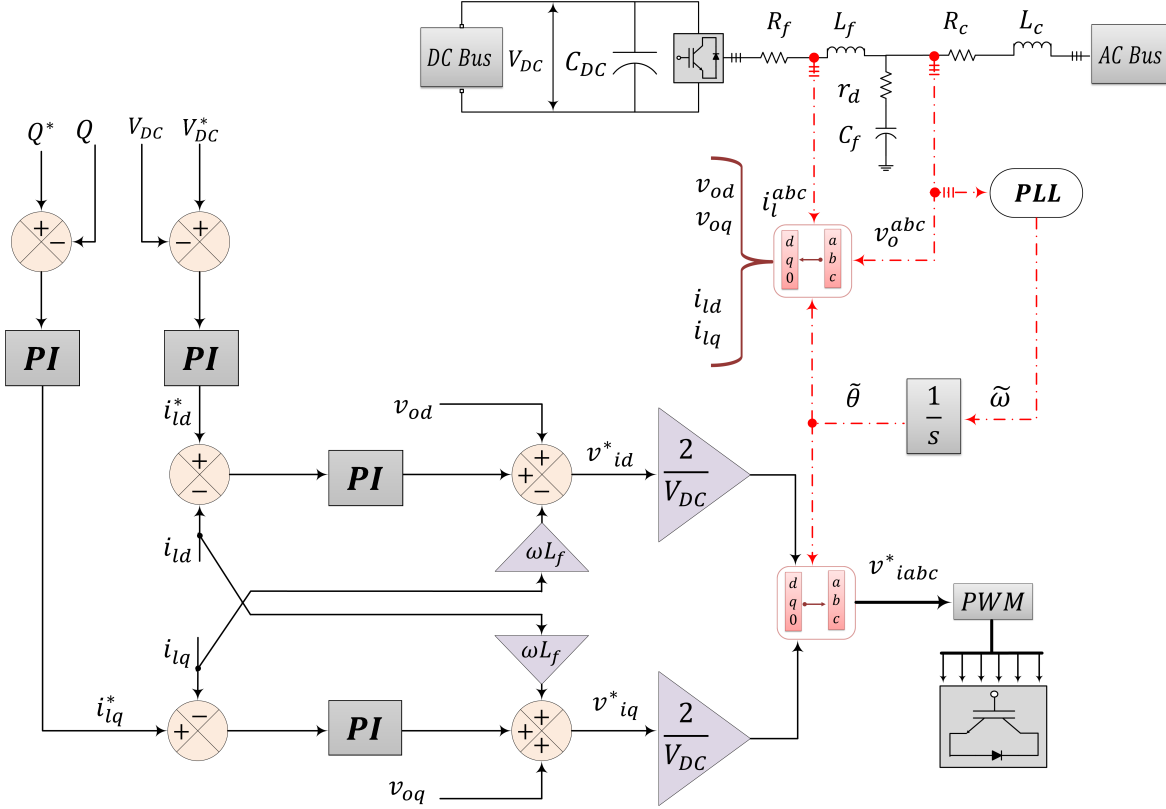


Figure 2.6: Interfacing converter control in grid-tied mode

In this section, the conventional control structures of a grid-tied and islanded interfacing converter are depicted. Detailed description of each control structures and their design guidelines can be obtained from [2, 17, 47, 48].

2.6.1 Grid-Tied Control Structure

A grid-tied interfacing converter controller as shown in Fig. 2.6 is consists of two control loops i.e. direct-quadrature reference current (i_{id}^* and i_{iq}^*) generator loop and current-control loop. Initially, grid side voltage (v_o^{abc}) is fed to a PLL to get instantaneous angle

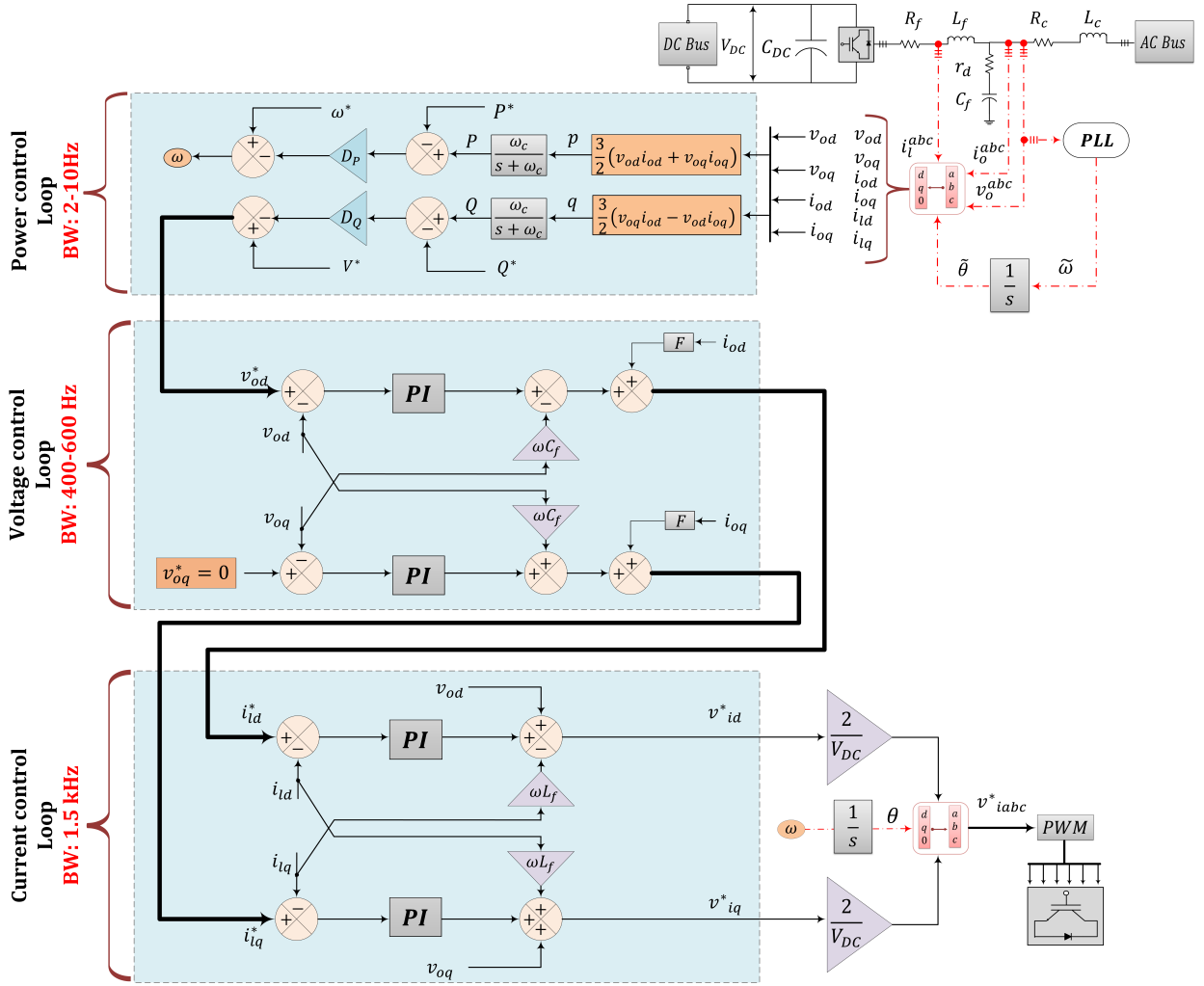


Figure 2.7: Interfacing converter control in islanded mode

measurement which is later fed into $abc - dq0$ converter. Later, v_o^{abc} and inverter output current (i_l^{abc}) are passed through $abc - dq0$ converter to get corresponding d and q axis components i.e. v_{od} , v_{oq} , i_{ld} and i_{lq} .

Active and reactive power of the interfacing controller during grid-tied mode can be controlled by i_{ld} and i_{lq} respectively [49]. Both i_{ld} and i_{lq} need to follow their corresponding references to achieve desired control objectives. The voltage deviation across the DC-link capacitor indicates the active power deviations at the output of the inverter. As a result, measured DC-link voltage is compared with its reference voltage and the error signal

are passed through a proportional-integral (PI) controller to generate control input i_{ld}^* . Similarly, load reactive power (Q) is compared with the inverter reactive power reference (Q^*) and the error is minimized using a PI controller by generating i_{lq}^* .

The main task of the current-control loops is to compare i_{ld} and i_{lq} with their associated references i_{ld}^* and i_{lq}^* and decouple active and reactive power control from each other. As a result, the controller performance becomes independent of system dynamics. Finally, inverter voltage reference v_{id}^* and v_{iq} are passed through a $dq0/abc$ converter to generate modulation signal (v_{iabc}^*) for to produce pulse width modulation (PWM) signal of the inverter.

2.6.2 Islanded Control Structure

The islanded control structure as shown in Fig. 2.7 is consists of three control loops i.e. power-control loop, voltage-control loop and current-control loop. During islanded condition, a microgrid needs to work as self-governing entity. The additional power and voltage-control loops ensure the frequency and the voltage stability and regulation during islanded operation. Generally, droop control schemes are adopted in the power-control loop. Power-control loop generates angular frequency reference (ω) to drive $abc - dq0$ and $dq0 - abc$ converters. Power-control loop also generates reference value v_{od}^* . Assuming the d-axis to be aligned with the line voltage measured by the PLL, the value of v_{oq}^* can be assumed 0. The bandwidth (BW) for the power-control loop is 2–10 Hz. The generated voltage reference values are fed to the voltage-control loop (BW: 400–600 Hz) and later fed to the current-control loop (BW: 1.5 kHz) to generate necessary modulation signals. More discussion on the improvement of the islanded microgrid control structure is presented in subsequent chapters.

2.7 EV Storage Control in Grid-Tied and Islanded Mode

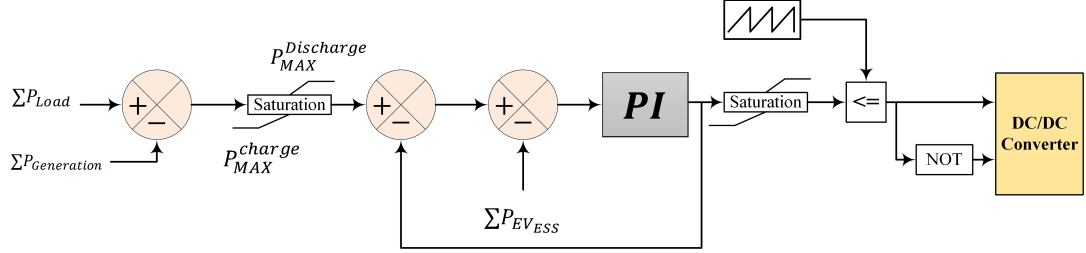


Figure 2.8: EV storage controller in grid-tied mode [2]

In grid-connected mode it is expected that grid will provide necessary load requirement at the same time it will contribute to the active and reactive power regulation [50]. However, in case of overloading due to variable loading or variable irradiation effects, parked EV-ESS can contribute to line voltage regulation and power management. For a hybrid AC/DC microgrid, generation and load demand can be calculated as below:

$$P_{Generation} = \sum P_{AC(DGs)} + \sum P_{DC(DGs)} + P_{grid} \quad (2.1)$$

Where P_{grid} = power supplied by the grid,

$P_{DC(DGs)}$ = power generated by DC DGs,

$P_{AC(DGs)}$ = power generated by AC DGs, so overall load demand is

$$P_{Load} = \sum P_{AC(Loads)} + \sum P_{DC(Loads)} + P_{Loss} \quad (2.2)$$

In normal condition it is expected that

$$P_{Generation} \geq P_{Load};$$

During that time EV-ESS will be charged via buck/boost converter or maintain halt mode based on battery SOC requirement. But if there is any generation-consumption

mismatch occurs at the PCC point then there might be condition when the following situation will occur

$$P_{Generation} < P_{Load};$$

For this case EV-ESS will measure the power difference $\delta P = P_{Load} - P_{Generation}$ and compare δP with maximum allowable power range of EV-ESS battery packs. The error signal is passed through a PI controller to generate duty cycles for the DC/DC converters of EV-ESS. The illustration of the EV storage controller in grid-tied mode is given in Fig. 2.8.

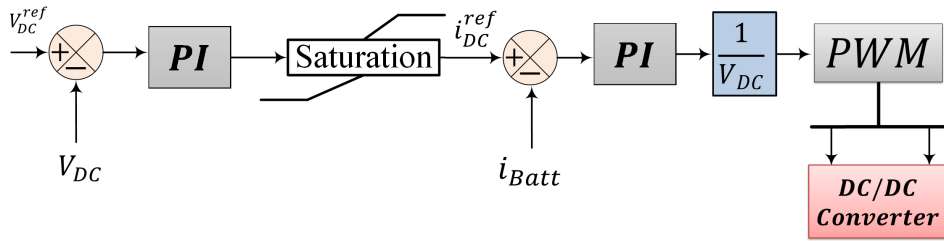


Figure 2.9: EV storage controller in islanded mode

During islanded mode, EV storages have to regulate the DC bus voltages before power dispatch. As a result, EV storage controllers have two control loops to control both voltage and current as shown in Fig. 2.9. More discussion on EV storage controller in the islanded mode is presented in subsequent chapters.

2.8 Overview on Distributed Control Techniques for Microgrids

As mentioned before, all the layers of the hierarchical microgrid control structure can be designed in decentralized, distributed or centralized manner. The secondary and the tertiary layer of the controllers requires communication among multiple DG units and the grid. As a result, for these two layers, the decentralized structure is not an option.

Moreover, the centralized structure has multiple shortcomings. It cannot operate securely and reliably due to several reasons, such as the absence of dedicated demand management unit, higher computational burden due to the presence of a bulk number of resources and loads, a high number of communication links, single point of failure and unavailability of DG units plug-and-play feature. Distributed control structure requires sparse communication, thus, it is less prone to communication failure. Hence, distributed controllers are a better choice to achieve required functionalities. Some distributed control techniques those are predominant in existing literature are presented below, later on, the application of these distributed controllers in the different layers of the microgrid control hierarchy is presented. Detailed review of various distributed control techniques and their application in the areas of power systems can be obtained in [51–53].

2.8.1 Distributed Model Predictive Control

Distributed model predictive control (DMPC) is a preferred control scheme in large industrial applications because of their distinct features like multiple control variable handling, simple tuning methods and plant constraints handling capabilities. DMPC is a discrete-time control strategy where system control sequence is determined by minimizing the cost function associated with the system performance over a finite number of future time steps considering the system mode. The cost function is defined as mathematical functions of variables responsible for the minimization of the deviation of system states from predefined set points. Each time step of DMPC includes calculation of the control sequence for N future time steps, where N is the prediction horizon. Initially, the first input is applied and the rest are updated in the next time step to minimize the weighted sum of errors. The same procedure is repeated at each consecutive time step [54, 55].

An MPC based method of reactive power control in an unbalanced microgrid has been proposed in [56]. A linearized voltage control model is derived in the method which is

integrated into MPC that predicts voltage profile for next step and set reactive power reference value. In [57] a decomposition based MPC strategy for coordinated energy management of DG units associated in a microgrid is proposed. In this method, the control optimization problem is decomposed into steady state and transient sub-problems. Decomposed steady state sub-problem requires slower time frame thus reducing overall computation weight.

2.8.2 Consensus-Based Cooperative Techniques

Pioneering work of [58] proposes distributed computation that concentrates on decentralized optimization where a defined global objective function is known to every associated unit in the system. Recently this problem is studied under newly introduced term ‘consensus’. The consensus is a method of solving distributed optimization problem by converging the associated units parameter to a single parametric value like fish school or bird flocks. This value could be voltage or frequency if microgrid is concerned. A consensus-based method attains global optimality using partial, time-varying communication between neighboring units, without the need of a dedicated unit for communication purpose. In [59] and [60] the unconstrained consensus algorithms in a distributed environment is discussed and the constrained situation is studied in [61–65]. A novel distributed multiagent-based load restoration algorithm is presented in [66] where each agent communicates with its neighbors to determine global information based on the average consensus theorem.

The distributed cooperative control method is actually a concept that ensures cooperation among multiple agents. This method is inspired by natural phenomena like swarming in insects, thermodynamics law, flocking in birds and synchronization in a physical system. In this system, each agent communicates with another agent by exchanging limited information through restricted communication protocols and cooperates with each other

to achieve a global or local objective [67]. This control and coordination can be achieved in various ways like using a un-directed graph, by solving average consensus problem or rendezvous problem or by flocking. In [68] a cooperative control technique is proposed where agents can communicate and exchange data regarding active and reactive power with their neighbors only. This exchange is done at a low rate and to facilitate the method node to node distance need to be known. In [69–72] a distributed cooperative secondary voltage control using input-output feedback linearization is proposed for islanded AC microgrid. In [73, 74] a distributed cooperative secondary control for voltage and frequency is presented. In this method, communication links are modeled using unidirectional digraph. A multi-objective distributed control for islanded AC microgrid is proposed in [75, 76]. The method includes two layers of communication where the first layer deals with voltage-controlled voltage source inverter (VCVSI) and regulates voltage and frequency of the system whereas the second layer deals with current-controlled voltage source inverter (CCVSI) and manages active and reactive power. Each DG units in the communication network graph require unidirectional communication with its neighbor. In [77], a consensus-based distributed cooperative control is proposed for voltage regulation and reactive power management. In [78] distributed cooperative control method has been extended to DC microgrid for voltage regulation and in [79, 80] distributed cooperative method has been used to coordinate distributed storages using the graph theory. Apart from that, the efficiency of the distributed cooperative controllers in conditions such as communication link failure and time delay are analyzed in [81, 82].

2.8.3 Agent-Based Techniques

In multi-agent system (MAS), agents are defined as specific entities that have communication skills, restricted goal oriented autonomy and a partial knowledge of the environment [83]. An intelligent agent has to be responsive to the change of the environment,

opportunity seekers and communicative. State estimation in power system can be employed to address the limited knowledge of agent [84]. Although agents can communicate, a large part of the control is achieved locally based on the autonomy and limited knowledge of the agent. Agents can be categorized as follows.

1. Centralized agent architecture that consists of a single agent,
2. Decentralized agent architecture consists of several agents without communication,
3. Hierarchical agent consists of different layers of agents.

The information flows from lower to higher layers, while the demand flows from higher layers to lower layers. Besides information flow in layers, different agents in one layer may also be able to communicate with each other [85]. MAS is appropriate for a large complex system like power systems where the humongous amount of dissimilar agents exist and interact with each other. MAS can be implemented to monitor, control, model, simulate and manage microgrids as they can be considered as a single entity in the islanded mode. An extensive review of MAS concepts and challenges related to it are presented in [86] and [87]. Agent programming in power systems is usually carried out in Java agent development framework (JADE). Simulation of agent-based power systems requires combining a power system simulator like PSCAD/EMTDC or MATLAB/SIMULINK with a communication backbone simulator by proper interfacing. The interfacing issues and partial resolutions are presented in [88]. In order to manage power sharing and to maintain voltage levels in a microgrid reference, [89] proposes a neighbor-to-neighbor three-step communication scheme to device MAS architecture within the microgrid. Reference [90] develops a MAS based hierarchical control to address the need for hierarchical control and hybrid dynamic behavior of the microgrid altogether in order maintain voltage levels and maximum economic benefits out of the microgrid. More detailed information on MAS-based control in microgrid applications can be obtained from [91].

2.8.4 Decomposition-Based Techniques

Decomposition refers to breaking a problem into multiple subproblems where solving those subproblems individually leads to a global solution. Several decomposition techniques have been proposed in literatures such as auxiliary problem principle (APP), predictor-corrector proximal multiplier method (PCPM), and alternating direction method (ADM) [61, 62, 92–96]. These methods are based on decomposing the original optimization problem into multiple subproblems/areas. Those subproblems are then solved iteratively until convergence. There are various methods for defining areas for example areas can be defined based on their sensitivity factors and controllability of associated buses. In microgrid this segmentation are done based on the available information which is alike physical adjacency [51].

2.9 Applications of Distributed Controller in Microgrid

The decentralized control techniques provide a scalable solution, whereas, the centralized controllers provide enhanced monitoring and control capabilities. However, the centralized control techniques require intense communication and processing power. Conversely, distributed control techniques provide alike control capability as the centralized structure with sparse communication. As a result, nowadays, the application of these control techniques in the microgrid vicinity is increasing. In the following section, some of these applications are presented.

2.9.1 Application in Voltage Regulation

The main objective of the microgrid voltage controller is to provide a flat voltage profile in the microgrid by maintaining the voltage level in different nodes within an acceptable range. Insignificant line impedance in transmission and distribution lines causes large current flow even under minuscule voltage differences across buses. To prevent this proper voltage regulation strategy is mandatory. Voltage controller can be designed either centrally or locally. Local voltage controller performs voltage regulation directly utilizing droop method through inner control loop (i.e. PI, PR, LQG etc.). A centralized or distributed clustered controller will update reactive power set point and communicate these references with local controllers of DG units. For low voltage (LV) and medium voltage (MV) grids voltage control requires determination of active power set points in addition to reactive power set points due to their resistive network behaviors. Earlier works like in [97] proposes secondary voltage regulation in bulk power systems by reactive power injection which has limited applicability only in transmission level. In [55] a communication-based DMPC is proposed for multi-area power systems to achieve voltage regulation. In this method, a simplified neighbor area is defined and designed DMPC works with the information obtained from neighboring controllers. In [98] a distributed controller based on droop strategy is proposed for low voltage DC microgrids to achieve voltage regulation and active power sharing. In [99] a two-stage voltage regulation strategy based on reactive power injection is proposed. In the first stage, DG units inject reactive power into the system to mitigate voltage deviation. The second stage is only activated when the first stage cannot fulfill required regulation. In the second stage, necessary amount of reactive power to regulate voltage deviation is exported from neighboring units. A secondary voltage control method is proposed in [100] which regulate sensitive load bus (SLB) voltage into the acceptable region by rejecting harmonics under hierarchical microgrid control structure. A decentralized non-hierarchical voltage controller based on smart and coopera-

tive entities is proposed in [101]. The distributed voltage controllers use local bus variables and mutually coupled oscillators to determine the main variables that characterize the global operation of the smart grid. These variables are then processed by distributed optimizers to estimate appropriate control actions. The global aim of the control actions is to minimize the objective function that describes voltage regulation objective. Recently a distributed cooperative control strategy has been proposed in AC microgrid which applies feedback linearization to convert secondary voltage control problem into tracking synchronization problem. All the associated agents communicate with their corresponding neighbors to address the voltage regulation problem and act cooperatively towards the common synchronization goal which is voltage regulation. References [102] and [103] propose a distributed secondary voltage control scheme for islanded operation of microgrids.

2.9.2 Application in Economical Power Coordination

Economical power coordination and optimal power flow (OPF) are important operational concerns. Conventionally distributed optimization schemes usually do not take into consideration issues like time variability of communication links as they may lead to a high computational burden. This may hamper OPF for microgrid application. In [104] distributed OPF is presented for large power system considering discrete variables. The algorithm can solve continuous distributed optimal power flow as the main scheme under ordinal optimization technique which leads to the selection of discrete control variables. In [96] a fast distributed OPF namely coarse-grained OPF is implemented. A comparison of three decomposition-based methods namely the Auxiliary Problem Principle (APP), the Predictor-Corrector Proximal Multiplier Method (PCPM) and the Alternating Direction Method (ADM) is provided in [95]. In [105] DMPC strategy has been implemented in a DC microgrid and in the [106] decentralized protocol for EV charging has been pro-

posed. A consensus-based algorithm for the economic dispatch of DG units is studied in [107]. The algorithm adjusts active power and frequency set points for each DG units using aggregate power imbalance in the network by minimizing area control error (ACE). A decentralized multi-agent system is proposed in [108] for the economic dispatch of DG units in microgrids considering all the agents being identical and self-governing. The centralized economic dispatch problem (CEDP) is solved in a distributed method in [109] by using incremental cost consensus (ICC) algorithm.

2.9.3 Application in Frequency Regulation

The main objective of microgrid frequency control is to have all associated DG units converge to a global frequency set point. Frequency control is applicable when DG units are electronically interfaced and have independent controllability on the frequency and the microgrid is in an islanded mode. During frequency control operation at least one unit has to act as the master unit with fixed frequency set point and other DG units should follow that unit as slave units. Every unit may have its own minimum and maximum allowable power and terminal voltage values. In the conventional power system, there exists precise coupling between rotor angular speed and electrical frequency to aid frequency regulation. As previously mentioned in microgrid control challenges majority of renewable energy sources do not have inertia, as a result emulating a virtual inertia for these DG units are required to imitate the operation of synchronous generators. In [110] a term proportional to the time derivative of the frequency is introduced in the power control loop which actually a measurement based derivative feedback term, as a result, is dependent on bandwidth limits. Besides, this method does not address the complexity of the existing power systems and their multi-input-multi-output (MIMO) natures [111]. Lots of literature explore the possibility of implementing frequency regulation of microgrid via droop characteristics. But conventional droop control strategy has certain limita-

tions discussed earlier. A DMPC strategy and a consensus-based control are applied for optimal coordination of frequency in multi-terminal high voltage DC (HVDC) in reference [54] and [112] respectively. Additionally distributed secondary microgrid control can be applied to regulate frequency to the normal operating condition during stand-alone operation. In a conventional bulk power system, a central controller namely load-frequency controller (LFC) in Europe or automatic gain controller (AGC) in North America, are used to operate for frequency restoration. The secondary microgrid controller uses the similar concept by using energy storage units to restore frequency of the microgrid within nominal values.

In this thesis, a novel consensus-based distributed cooperative controller has been designed to coordinate multiple EV storages within a microgrid to improve power-sharing, simultaneous regulation of the AC and the DC bus voltages and the frequency regulation. Consensus-based cooperative distributed techniques are simple to use and have the faster convergence property considering broad-range of time delays. Suitabilities and advantages of this techniques are elaborately discussed in consecutive chapters.

2.10 Relevant Standards

For optimum DG penetration into the grid or to form a microgrid, a set of rules, guidelines or standards are needed. In order to standardize the procedure, IEEE published a series of standards, numbered as 1547, on DG integration to electrical power system (EPS). These standards present uniform rules and regulations related to testing, maintenance operation, performance and safety of the interconnected EPS. Until now there are ten versions of IEEE standard-1547 are available. These are:

1. **IEEE 1547**, published in 2003, the first standard was prepared for ruling out governing conditions of connecting DG units to the electric power system [113].

2. **IEEE 1547.1**, published in 2005, further describes about conformance testings for DG units which determine their connection capability to electrical power systems [114].
3. **IEEE 1547.2**, published in 2008, provides a technical background on the standard [115].
4. **IEEE 1547.3**, published in 2007, details techniques for monitoring and communication of distributed systems [116].
5. **IEEE 1547.4**, published in 2011, is a guide for the design, operation, and integration of conforming systems. It focuses on the integration of islanded system with the utility [117].
6. **IEEE 1547.5**, is designed for distributed sources larger than 10 MVA. This standard has been withdrawn recently.
7. **IEEE 1547.6**, published in 2011, describes practices for secondary network interconnections [118].
8. **IEEE 1547.7**, published in 2013, provides distribution impact studies for distributed resource interconnection [119].
9. **IEEE 1547a (Amendment -1)**, published in 2014, in this version, the acceptable ranges of voltage and frequency have been modified for fault case [120].
10. **IEEE 1547.1a (Amendment -1)**, published in 2015, some modifications have been done in conformance testing [121].

In the latest amendment of the 1547 standard [120], operational voltage and frequency range for interconnection system during abnormal operations have been changed. The acceptable voltage range is documented in Table 2.3 and the acceptable frequency range with

fault clearing time during islanding or fault condition are presented in Table 2.4. In order to sustain power quality, the total harmonic distortion (THD) of the PCC voltage and current waveform needs to be within 5%. The maximum allowable harmonic distortion in the PCC for both voltage and current waveforms are presented Table 2.5.

Table 2.3: Default response for interconnection system during abnormal voltage variations

Default settings		
Voltage range (% of base voltage)	Clearing time (s)	Clearing time: adjustable up to and including (s)
$V < 45\%$	0.16	0.16
$45\% \leq V < 60\%$	1	11
$60\% \leq V < 80\%$	2	21
$110\% < V < 120\%$	1	13
$V \geq 120\%$	0.16	0.16

Table 2.4: Default response for interconnection system during abnormal frequency variations

Function	Default settings		Adjustability range	
	Frequency (Hz)	Clearing time (s)	Frequency (Hz)	Clearing time (s) adjustable up to and including
Under Frequency -1	< 57	0.16	56 – 60	10
Under Frequency -2	< 59.5	2	56 – 60	300
Over Frequency -1	> 60.5	2	60 – 64	300
Over Frequency -2	62	0.16	60 – 64	10

In Australia, the nominal frequency is required to be 50 Hz according to National Electricity Market (NEM). However, for an islanded microgrid condition, the frequency range can vary between 49.5 Hz to 50.5 Hz. For contingency conditions, frequency regulation goes through three phases namely containment, stabilization and recovery. NEM approved mainland frequency operating standards is documented in Table 2.6 for islanded microgrids in the Australian distribution networks during normal and emergency condi-

Table 2.5: Maximum harmonic distortion of PCC voltage and current

Individual harmonic order h (odd harmonics)	$h < 11$	$11 \leq h < 17$	$17 \leq h < 23$	$23 \leq h < 35$	$35 \leq h$	THD
Percent (%)	4.0	2.0	1.5	0.6	0.3	5.0

Table 2.6: NEM mainland frequency operating standards for islanded microgrids in the Australian distribution network [7]

Nominal frequency : 50 Hz

Condition	Containment	Stabilization	Recovery
No contingency event, or load event	49.5–50.5 Hz		
Generation event, load event or network event	49–51 Hz		49.5–50.5 Hz within 5 minutes
The separation event that formed the island	49–51 Hz or a wider band notified to AEMO by a relevant Jurisdictional Coordinator	49.0–51.0 Hz within 2 minutes	49.5–50.5 Hz within 10 minutes
Protected event	47–52 Hz	49.0–51.0 Hz within 2 minutes	49.5–50.5 Hz within 10 minutes
Multiple contingency event including a further separation event	47 to 52 Hz	49.0–51.0 Hz within 2 minutes	49.5–50.5 Hz within 10 minutes

tions. The operating phase-to-neutral voltage level of all states in Australia and New Zealand by various power companies are shown in Table 2.7. Surprisingly, the range and the levels of voltages are inconsistent mainly in Australia due to various codes and regulations¹. Based on the above-mentioned requirements, the islanding conditions selected in this dissertation for Australia are presented in Table 2.8.

¹The Voltage limits in Queensland will change from 240 volts +/-6% to 230 volts +10/-6% according to the Australian Standard (AS) 60038 (Standard voltages) from 27 October 2018.

Table 2.7: Comparison of voltage requirements in Australia and New Zealand [8]

State	Power company	Nominal phase-neutral voltage (V)	Range		Regulation/Codes
			Upper	Lower	
QLD	Energex Ergon Energy	240	+6%	-6%	Electricity Regulation 2006 (QLD)
NSW	Country Energy	230	+10%	-2%	NSW Dept. of Water and Energy's Code of Practice - electricity distributors require detailing their standards.
	Energy Australia	240	+6%	-6%	
	Integral Energy	230	+10%	-2%	
ACT	ACTEWAGL	240	+6%	-6%	ACTEWAGL Service and Installation Rules
VIC	Citipower Jemena Powercor SPAusNet	230	+10%	-6%	Electricity Distribution Code (VIC)
TAS	Aurora Energy	230	+10%	-6%	Electricity Code (TAS)
SA	SA Power Networks	230	+10%	-6%	Electricity (General) Regulations 1997 (SA) specifies AS2926. ETSA Utilities Service and Installation Rules
WA	Horizon Power	240	+6%	-6%	WA Connections Manual and Technical Code
	Western Power	240	+6%	-6%	
NT	PowerWater	230	+10%	-10%	Nominal voltage set by Electricity Reform (Safety and Technical) Regulation PowerWater: Power Network Connection Technical Code
New Zealand	All	230	+6%	-6%	Electrical Safety Regulations 2010 (NZ)

Table 2.8: Islanding conditions for Australia

Parameter	Tripping condition
Voltage (V)	Operating Range 216V – 253V
	$V > 255$ (phase- neutral)
	$V < 210$ (phase - neutral)
Frequency (f)	$49 \leq f \leq 51$
	$f > 51$ Hz
	$f < 49$ Hz

2.11 Chapter Summary

A thorough literature survey on microgrid control structure and techniques, V2G technologies, distributed control techniques and relevant electricity connection standards are presented in this chapter. Based on the analysis presented in this chapter, a hybrid microgrid has been designed with PV and multiple EV-ESS complying with the design structure of a university-based microgrid in the Griffith University, Australia. A centralized coordinated control is developed in Chapter 3 for multiple three-phase AC and DC EV-ESS to improve the control capability of the designed hybrid microgrid. The efficacy of the system is further improved utilizing distributed control techniques and enhanced interfacing converter controller as presented in Chapter 3 by adopting sparse communication networks and augmented stability. In Chapter 4, the developed distributed controller is optimized using a real-time optimization technique to attain economic benefits.

The next chapter provides the design and modeling of the hybrid microgrid along with the proposed centralized coordinated controller for multiple EVs with different configurations to attain simultaneous AC and DC bus voltages and frequency regulation during the islanded mode.

Chapter 3

Centralized Coordinated Control of EVs for Improved Hybrid Microgrid Operations

The progressive deployment of electric vehicles (EV) and the increased penetration of alternating current (AC) and direct current (DC) type renewable resources paves the path towards hybrid AC/DC microgrid operation. Considering the potentials of EVs in the realm of the microgrids, this chapter presents a three layered coordinated control strategy considering EV availability constraints for three-phase (3P) and DC type EV energy storage systems (EV-ESS) to improve the hybrid AC/DC microgrid operation. The first layer of the algorithm ensures DC subgrid management, which includes DC bus voltage regulation and DC power management. The second and third layer are responsible for the AC subgrid management, which include AC bus voltage and frequency regulation with active and reactive energy management. The multi-layered coordination is embedded into the microgrid central controller (MGCC) which controls the interlinking controller in between AC and DC microgrid as well as the interfacing controllers of the participat-

ing EVs and distributed renewable resources (DER). The hybrid AC/DC microgrid has been designed in MATLAB/SIMULINK[®] environment resembling the under construction microgrid at Griffith University, Australia. Extensive case studies have been performed considering real life irradiation data and commercial loads of the campus building. Impacts of homogeneous and heterogeneous single-phase EV charging are investigated to observe the unbalanced scenario. Synchronization state while switching from islanded to grid connected mode has also been tested considering contingency situation. From the comparative simulation results it is evident that the proposed controller exhibits effective and robust performance for all the cases.

3.1 Introduction

The accelerated depletion rate of fossil fuels and the raising environmental concerns associated with the fossil-fired power generations are driving the global electricity generation systems towards distributed generation (DG) units. Microgrids have the capability of clustering DG units such as renewable/sustainable resources and energy storage systems (ESS) through intelligent and coordinated control. As a result, the microgrid concept has been widely adopted in different countries including Australia. It can provide several ancillary services such as grid voltage and frequency regulation, active and reactive power control, uninterruptable power supply (UPS) and fault ride through service during any grid fault. It can also contribute to enhance power quality and system reliability in an economic manner [122]. Based on the outputs of the participating DG units and loads, microgrids can be classified into AC, DC and hybrid AC/DC types. Each type of microgrid has its own characteristics, benefits and challenges associated with it. Currently, AC microgrid is predominant because of the AC nature of the existing grid. DC microgrid concept has recently been emerged in the distribution arena due to increased

penetration of DC types DG units such as photovoltaic (PV), electric vehicles (EV) and so on. On the hand, hybrid AC/DC microgrid has been proposed in some recent literatures [24, 25, 123] to combine the advantages of both AC and DC nature of the electric system. A hybrid AC/DC microgrid has several potential advantages over conventional AC and DC type microgrids, for instance the feasible integration of both AC and DC type DG units and loads with minimal AC/DC conversion, reduced requirement of synchronization due to the direct coupling of sources and loads to alike type common buses, simple voltage transformation using transformer for the AC side and DC/DC converters for DC sides, increased efficiency and reliability with improved economical operation due to less conversion loss [124]. Conceptual European super grid or so called mega-grid is the high level version of the hybrid AC/DC microgrid which includes high voltage AC and DC transmission links to connect offshore wind turbines and desert based solar farms to serve the load consumption of the entire continent. Furthermore, commercial buildings consume approximately 32% of the worldwide energy usage. They hold accountable for about 30% of the total end-use energy-related CO_2 emissions. As a result, commercial building can be operated with hybrid DG units such as PV and electric vehicle-energy storage systems (EV-ESS) by forming commercial hybrid AC/DC microgrids which can provide pivotal role in constructing green energy metropolitans [19, 125, 126].

However, hybrid AC/DC microgrid requires complex protection and control structures to ensure reliable operation, especially when the participating DG units are intermittent like PV and wind turbines. Even though the advantages of predominant renewable sources like PV and wind turbines are widely acknowledged, their fluctuating outputs raises the problem of maintaining balance between electricity generation and demand. This issue can severely affect the system operation when the system operates in islanded mode. Tackling this issue with regulated AC and DC bus voltage and frequency requires the utilization of energy storages, such as battery energy storages (BESS) and EV-ESS.

The progressive deployment of electric vehicles in recent years has driven the Distribution System Operators (DSOs) to consider the implications and the advantages of using EV-ESS in low voltage (LV) networks. With proper utilization of EV-ESS, vehicle-to-grid (V2G) concept can improve the performance of the utility grids or microgrids in terms of efficiency, stability and reliability by offering ancillary services such as reactive power management, active power control, tracking the intermittent renewable energy resources, load balancing and shifting via valley filling support, peak load shaving and filtering current harmonics in the output. Although electric vehicle owners may obtain some benefit by individually providing ancillary services to the DSOs, V2G operation makes sense only when there is reasonably large number of EVs can take part into the operation. Aggregators or aggregation agents are intermediary authorities or computational entities that unify and coordinate distributed EV-ESS to provide medium to large-scale ancillary services [127–129]. However, due to various types of charging configurations such as DC and three-phase AC fast charging and single-phase AC slow charging make the aggregation of EVs a challenging task. Furthermore, increased penetration of single-phase or residential EV chargers introduce unbalanced phase voltage and current which may go beyond acceptable tolerance limit of the microgrid system.

Intensive ongoing research has been being performed in order to tackle the aforementioned issues. In [24] coordinated control of an islanded hybrid AC/DC microgrid with BESS, PV and wind turbine is presented. In [25] an autonomous control of the interlinking controller is presented by using normalized droop control. Both [24] and [25] have emphasised on active power management even though during islanded condition reactive power management is equally necessary. Furthermore, the unbalanced condition has not been explored. Power management and control of a islanded and grid-connected hybrid AC/DC microgrid is presented in [50]. Robust power management with DC bus voltage regulation by exploiting ESS is explored in [130]. However, the grid synchronization has

Table 3.1: Salient features of the proposed approach in comparison with the contemporary literatures

Considered issues	[24], [25]	[50], [130]	[133]	[134]	[135]	[136]	[137]	[138]	This chapter
Concurrent AC/DC voltage regulation	✓	✓							✓
Frequency regulation	✓	✓		✓	✓	✓		✓	✓
Single-phase EV charging					✓	✓	✓		✓
Four quadrant V2G operaiton			✓			✓		✓	✓
Grid synchronization	✓				✓				✓

not been considered and more focus is given on the active power management. The feasibility of reactive power support through V2G operation is explored for single-phase and three-phase off-board chargers in [131, 132] respectively and the concept of Smartpark is introduced in [133], which has the capability of four quadrant V2G operation. However, a microgrid environment requires both active and reactive power sharing among multiple DG units. These requirements cannot be achieved by the aforementioned control strategies. A coordinated control is presented in [134] for frequency regulation only by incorporating large scale EVs through monitoring and controlling of the area control signal (ACS). The role of EVs in microgrid service restoration by black starting is explored in [135]. This paper [135] has also explored the active power sharing capability using conventional droop control. However, the conventional droop control mechanism is not able to provide enough damping to stabilize the voltage and frequency in islanded microgrids. Stability analysis has been performed in [136] for asymmetrical virtual inertia caused by the single-phase EV charges in a droop based weak grid or microgrid. The paper [136] has also shown that the conventional droop control is unable to provide accurate frequency regulation. Tackling the unbalanced distribution grid using coupled PV inverter and EV chargers is presented in [137]. The primary focus is given to explore the potential of EVs of balancing phase voltages which in turns reduce the unbalanced condition.

Motivated by the ongoing research and the aforementioned scopes of improvements,

this chapter presents a unified approach which include the design of an interlinking/interfacing controller with four quadrant operational capability and a three-layered coordinated control strategy for three-phase and DC type EV-ESS taking EV availability constraints into account to improve the performance of an islanded commercial hybrid AC/DC microgrid. The first layer of the proposed algorithm manages the DC subgrid. The main responsibility of this layer is to ensure DC bus voltage regulation and the power management within the DC subgrid. The second and third layers are accountable for the management of the AC subgrid. Both layers simultaneously operate to ensure AC bus voltage and frequency regulation within the AC subgrid. The designed coordination algorithm is embedded into the microgrid central controller (MGCC) as a single entity. The MGCC is responsible to generate necessary power management commands for the local controllers (LC). LCs such as interlinking/interfacing controllers receive these commands and perform required actions on smart inverters. The hybrid AC/DC microgrid and the controllers are designed and tested in MATLAB/SIMULINK[®] environment. The hybrid AC/DC microgrid is designed considering the under construction microgrid structure at Griffith University, Australia. In order to validate the robust performance of the coordinated control various case studies have been performed. These case studies include the performance and the impact analysis of the designed controllers under heterogeneous and homogeneous charging of single-phase EVs with variable commercial loads and solar irradiation. Furthermore, considering the contingency condition, the controller has been tested from islanded to grid connected mode as well. Table 3.1 shows the comparison of the proposed approach with the contemporary literatures regarding microgrids and V2G. The main contributions of this research can be summarized as follows,

- Concurrent variable PV output due to intermittent irradiation and variable real commercial load profile has been considered.

- A four-quadrant alike structured interlinking and interfacing LCs has been designed. The designed LCs can regulate both active and reactive power by exploiting the four-quadrant operational capability of the V2G operation.
- A multi-layered coordination algorithm has been proposed for the MGCC in order to coordinate three-phase (3P) and DC type EV-ESS considering their availability constraints. The layered coordination ensures optimum energy management by prioritizing autonomous DC and AC microgrid operation without unnecessary power flow caused by the hybrid operation.
- Simultaneous AC and DC bus voltage and system frequency regulation has been ensured in order to obtain improved hybrid AC/DC operation. Unlike the previous literatures [24, 25, 130] unbalanced condition has also been considered caused by single-phase EV chargers.

The rest of the chapter is organized as follows. Section 3.2 gives a brief introduction of the under construction hybrid AC/DC microgrid in Griffith University, Australia. Later, dynamic model of the PV, EV-ESS, the developed interlinking/interfacing controller and DC/DC converter controller are presented sequentially under the umbrella of Section 3.2. Coordinated control structure with its objectives and step-by-step algorithm is presented in Section 3.3. The proposed control scheme is verified by simulation with real-time data. The case studies of the simulation results are presented and elaborately discussed in Section 3.4. Section 3.5 draws the conclusion for the chapter. Table 3.2 presents the simulation parameters for the designed hybrid AC/DC microgrid and its controllers. Appendix A shows illustrations with description tables for the testing facility equipments.

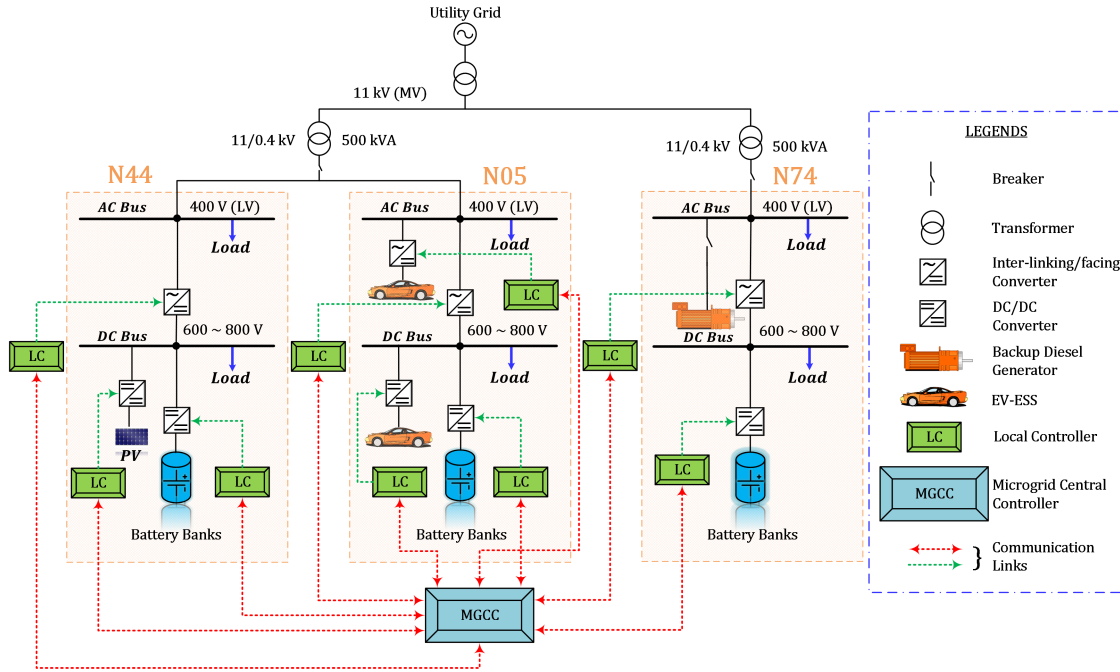


Figure 3.1: Hybrid AC/DC microgrid structure in Griffith University, Australia.

3.2 Hybrid AC/DC Microgrid

The test hybrid AC/DC microgrid system has been designed based on the under developed microgrid at the Griffith University, Australia. The microgrid includes three buildings, namely N44, N05 and N74 as shown in Fig. 3.1 [2]. Each building operates as an individual smart hybrid AC/DC microgrid with separate AC and DC buses. Each AC and DC bus of these buildings accommodate separate AC and DC sources and loads. Every pair of AC and DC buses are interfaced with the bidirectional interlinking distribution static synchronous compensators (D-STATCOM) or smart voltage source inverters (VSI) [139].

N44 building contains PV panels of 16 kilowatt-peak (kWp) with 60 kilowatt-hour (kWh) Lithium-ion polymer (Li-ion) BESS [140]. The BESS are connected to the corresponding DC bus through an intelligent DC/DC converter. The benefits of having BESS attached to the PV system are twofold. Primarily, the BESS will tightly regulate the output voltage of the PV system and secondarily, it will buffer the intermittent PV out-

put power [2]. The combined DG units (PV and BESS) are presently used for the peak demand management purpose. The capacity of these DG units will be increased in the future based on the total load demand to utilize them in microgrid operation within one or multiple buildings.

N05 building is allocated for smart EV/plug-in hybrid electric vehicle (PHEV) charging station, which will facilitate V2G operation. EV-ESSs will be charged using bidirectional DC fast chargers when they are connected to the DC bus. AC charging is planned to be installed at the AC bus of the N05 building. The bidirectional AC charging will include off-board three-phase fast charging and single-phase slow charging. N74 building contains sensitive loads attached to both buses. This building requires an uninterruptible power supply (UPS) operation due to the presence of critical loads like laboratory equipment and testing samples. The building is presently served by backup diesel generator and battery energy storages during outage. The diesel generators are inherently slower compared to the micro-turbines due to the high inertia. As a result, the backup diesel generators will be replaced in the future with micro-turbines for their fast starting capability.

In order to monitor and analyse data sensor-based smart power meter (Power Meter PM5350A) has been installed in each of the buildings. Sensor-based data have been collected using OSI PI software using a centralized communication structure in order to monitor and control the microgrid operation. Modbus TCP/IP (Transmission Control Protocol/Internet Protocol) has been used as the communication protocol for supervisory control and data acquisition (SCADA) systems. Hypertext Transfer Protocol (HTTP) TCP/IP communication protocol has been used as the backup protocol when the Modbus TCP/IP is not available [141]. Microgrid central controller (MGCC) is responsible for generating command signals for the LCs. These command signals are transmitted through Modbus TCP/IP communication protocol to the remote terminal units (RTU) such as

LCs of D-STATCOMs, DC/DC converters etc.

In this chapter the primary concern is directed towards the microgrid operation of N44 and N05. As a result, the simulation model has been designed comprising only N44 and N05 microgrid system. The model of N74 is not included for the case studies in this chapter. Both islanded and grid connected operation of the buildings have been taken into consideration. The capacity of the DG units has been adjusted comparing with the real load profile of the buildings. For the simulation purpose 250 kW PV with 60 kWh high capacity energy storage systems are used. PV module comprises of PV panels and maximum power point tracking (MPPT) system integrated boost converter. Perturb and observe (P and O) algorithm has been chosen for the MPPT system [142]. BESS are attached nearby through separate DC/DC converter which is controlled by charge/discharge algorithm. Intelligent DC fast charging has been designed in N05 building with EV-ESS and DC/DC converter and connected to the DC bus. Single-phase AC and three-phase AC charging has been modeled with EV-ESS and associated bidirectional single-phase and three-phase inverters respectively. Both DC buses of N44 and N05 buildings are inter-linked with corresponding AC buses through interlinking VSIs and LCL filters. A concise modeling of the DG units and the control strategies used in the design are presented in consequent subsections. Necessary parameters related to the model and controller are provided in 3.2.

3.2.1 PV Module Modeling

Using the physical property of the $p - n$ semiconductor, the model of PV module can be obtained based on the PV array current-voltage relationship presented in (3.1)

$$i_{pvi} = N_{pi}I_{Li} - N_{pi}I_{si} \left[\exp \left\{ \alpha_{pi} \left(\frac{V_{pvi}}{N_{si}} + \frac{R_{si}i_{pvi}}{N_{pi}} \right) \right\} - 1 \right] - \frac{N_{pi}}{R_{shi}} \left(\frac{V_{pvi}}{N_{si}} + \frac{R_{si}i_{pvi}}{N_{pi}} \right) \quad (3.1)$$

Where, I_{Li} = current corresponding to light

I_{si} = reverse saturation current chosen as $9 \times 10^{-11} A$

N_{si} = the number of cells in series

N_{pi} = the number of modules in parallel

R_{si} and R_{shi} = series and shunt resistances of the array

i_{pvi} = the current flowing through the array

V_{pvi} = the output voltage of the array

The constant $\alpha_{pi} = \frac{q_i}{A_i k_i T_{ri}}$

Where, $k_i = 1.3807 \times 10^{-23} JK^{-1}$ is the Boltzmann constant

$q_i = 1.6022 \times 10^{-19} C$ is the charge of an electron

A_i = the $p - n$ junction ideality factor with a value between 1 and 5,

and T_{ri} = the cell reference temperature

To extract the maximum power from the PV module different MPPT systems, for instance perturb and observe (P & O), incremental conductance (IC), hill climbing etc. are usually used. For this chapter perturb and observe method has been chosen due to ease in implementation and reasonably satisfactory performance [143–145].

3.2.2 EV Energy Storage Modelling

Li-ion based battery energy storage has been used to design both battery banks and EV-ESS battery packs in the hybrid AC/DC microgrid. Generic third order Thevenin equivalent circuit model presented in [146] has been used to model the battery. The only difference in designing the battery banks and the EV-ESS battery pack is that the EV-ESS battery pack possess the higher kWh capacity than ordinary battery banks. Both types of energy storage systems are interfaced with DC/DC converter. The DC/DC converter executes the charge and discharge command generated by LC or MGCC. Both battery banks and DC type EV-ESS are directly connected to the DC bus through individual

DC/DC converters. For three-phase or single-phase AC charging the EV-ESS battery packs coupled with associated DC/DC converters are later connected to the three-phase or single-phase inverters respectively. The dynamic charging and discharging of Li-Ion battery model is designed based on (3.2) and (3.3) respectively [147, 148].

For $i^* > 0$ the battery will act as in discharge mode which can be represented as:

$$f_1(it, i^*, i) = E_0 - K \frac{Q}{Q - it} i^* - K \frac{Q}{Q - it} it + A e^{-B \times it} \tag{3.2}$$

For $i^* < 0$ the battery will act as in charge mode which can be represented as:

$$f_1(it, i^*, i) = E_0 - K \frac{Q}{it + 0.1Q} i^* - K \frac{Q}{Q - it} it + A e^{-B \times it} \tag{3.3}$$

Where, E_0 = Constant voltage (V)

K = Polarization constant $(Ah)^{-1}$ or Polarization resistance (Ω)

i^* = Low frequency current dynamics (A)

i = Battery current (A)

it = Extracted capacity (Ah)

Q = Maximum battery capacity (Ah)

A = Exponential voltage (V)

B = Exponential capacity $(Ah)^{-1}$

3.2.3 Interlinking/Interfacing Converter Control

From the controlling point of view, the most important part of a hybrid AC/DC microgrid is the interlinking converter controller which links the DC bus with the AC bus. The interlinking converter controller consists of three inner loop controllers for both islanded

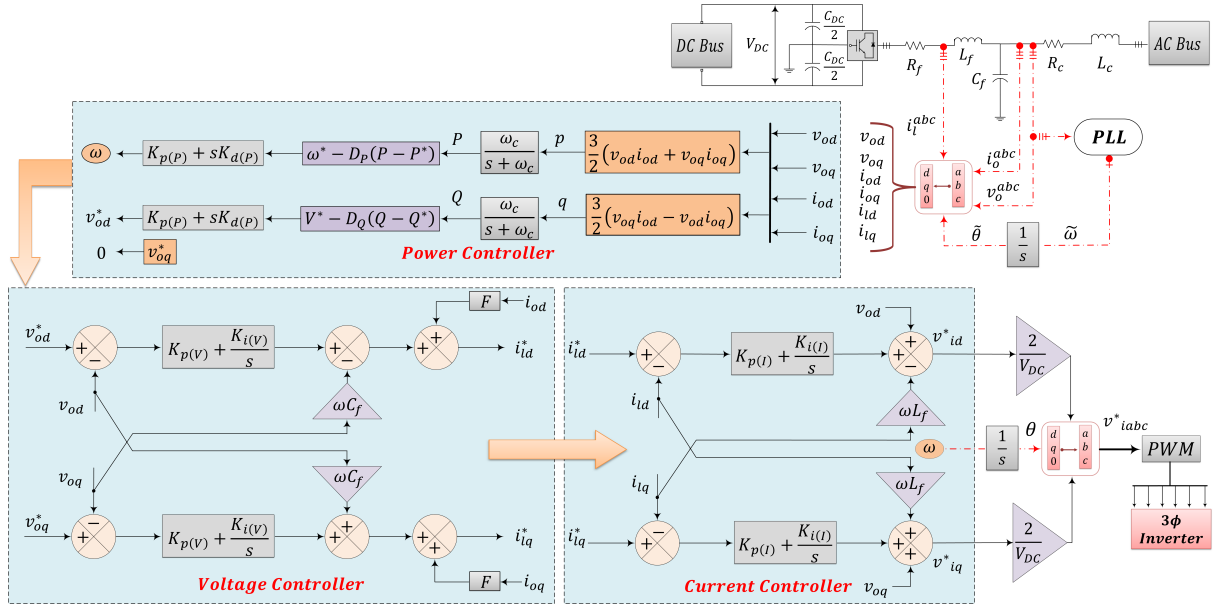


Figure 3.2: Modified local control structure for each interlinking/interfacing converters of the hybrid AC/DC microgrid

and grid connected operation of the microgrid. These inner control loops are power controller, voltage controller and current controller. The dynamic modeling for each of the control loops are derived and presented in the succeeding subsections.

Power Controller

The power controller is shown in Fig. 3.2. Instantaneous voltage (v_o^{abc}) and current (i_o^{abc}) after the LC filter and the inverter output current (i_l^{abc}) are measured and transformed into their corresponding $d - q$ components (denoted by separate subscripts in d and q). The real and reactive power can be calculated from the measured line voltage and current components as [149]:

$$\begin{cases} p = \frac{3}{2} (v_{od}i_{od} + v_{oq}i_{oq}) \\ q = \frac{3}{2} (v_{oq}i_{od} - v_{od}i_{oq}) \end{cases} \quad (3.4)$$

Fundamental components of the calculated real and reactive power are extracted using a low pass filter (LPF) with cutoff frequency ω_c . The outputs of the LPF are the inputs for the droop control which are given by:

$$\begin{cases} P = \frac{\omega_c}{s + \omega_c} p \\ Q = \frac{\omega_c}{s + \omega_c} q \end{cases} \quad (3.5)$$

Voltage and frequency regulation during islanded microgrid operation requires specific control actions. These requirements can be achieved through an embedded droop control mechanism within VSI LCs. The main concept of the droop mechanism is to mimic the characteristics of synchronous generators which include reduced angular velocity with increased load demand. Generally the X/R ratio of a microgrid is very high due to the high value of the inductors present in LC filters. As a result of this inductive nature of a microgrid, well known P/ω and Q/V droop control can be applied to regulate the frequency and the voltage. The conventional droop control schemes can be presented as [150]:

$$\begin{cases} \omega = \omega^* - D_P(P - P^*) \\ V = V^* - D_Q(Q - Q^*) \end{cases} \quad (3.6)$$

where, D_P and D_Q are the droop coefficients for P/ω and Q/V droop controller respectively. "*" represents the reference signals of the corresponding variables. The $d - q$ reference frame is rotating synchronously with the frequency of the line voltage measured by the phase-locked-loop (PLL). As a result, v_{oq}^* is taken 0. The conventional droop mechanism possesses inherent trade-off between active and reactive power sharing accuracy and frequency and amplitude regulation. Considering this issue a modified proportional-derivative (PD) compensated droop control has been utilized in this research according

to [33]. The PD compensated droop control ensures proper damping and desirable power sharing accuracy with adequate frequency and voltage regulation. The droop coefficients can be calculated using the following equations,

$$\begin{cases} D_P = \frac{2\pi(f_{max} - f_{min})}{P_{max}} \\ D_Q = \frac{V_{max} - V_{min}}{Q_{max}} \end{cases} \quad (3.7)$$

Considering that the three-phase inverter interfaced EV chargers are V2G capable and can absorb or supply both real and reactive power. Then the above droop coefficients for the three-phase inverter interfaced EV-ESS would be [80]:

$$\begin{cases} D_P = \frac{2\pi(f_{max} - f_{min})}{2P_{max}} \\ D_Q = \frac{V_{max} - V_{min}}{2Q_{max}} \end{cases} \quad (3.8)$$

According to the Australian Energy Market Operator (AEMO) specification, the acceptable frequency range for islanded microgrid operation in Australia is in between 49.5Hz and 50.5Hz [151, 152] and the voltage magnitude limit lies within -6% to +10% [153]. So the f_{max} , f_{min} , V_{max} and V_{min} have been taken as specified standard. By observing the load profile maximum KVA ratings for both interlinking converters have been chosen.

Voltage Controller

The differential algebraic equations (DAE) for the voltage controller have been derived and given as [80, 154–156]:

$$\begin{cases} \dot{\phi}_{od} = v_{od}^* - v_{od} \\ \dot{\phi}_{oq} = v_{oq}^* - v_{oq} \end{cases} \quad (3.9)$$

$$\begin{cases} i_{ld}^* = F i_{od} - \omega C_f v_{oq} + K_{p(V)} \dot{\phi}_{od} + K_{i(V)} \phi_{od} \\ i_{lq}^* = F i_{oq} - \omega C_f v_{od} + K_{p(V)} \dot{\phi}_{oq} + K_{i(V)} \phi_{oq} \end{cases} \quad (3.10)$$

where $\dot{\phi}_{od}$ and $\dot{\phi}_{oq}$ are state variables corresponding to the proportional-integral (PI) controller of the voltage controller. "*" represents reference signal of corresponding d and q components of voltage and current. ω is the angular frequency generated by the droop control. $K_{p(V)}$ and $K_{i(V)}$ are respectively proportional and integral gain. F is the feed-forward gain also known as the virtual impedance. F can be calculated from the line and filter resistances.

Current Controller

The DAEs for the voltage controller are given as [80, 154–156]:

$$\begin{cases} \dot{\lambda}_{ld} = i_{ld}^* - i_{ld} \\ \dot{\lambda}_{lq} = i_{lq}^* - i_{lq} \end{cases} \quad (3.11)$$

$$\begin{cases} v_{id}^* = v_{od} - \omega L_f i_{lq} + K_{p(I)} \dot{\lambda}_{ld} + K_{i(I)} \lambda_{ld} \\ v_{iq}^* = v_{oq} + \omega L_f i_{ld} + K_{p(I)} \dot{\lambda}_{lq} + K_{i(I)} \lambda_{lq} \end{cases} \quad (3.12)$$

where $\dot{\lambda}_{ld}$ and $\dot{\lambda}_{lq}$ are state variables corresponding to the proportional-integral (PI) controller of the current controller. "*" represents reference signal of corresponding d and q components of voltage and current. $K_{p(I)}$ and $K_{i(I)}$ are respectively proportional and integral gain. The conventional current controller has been modified by feed-forwarding the line voltage components to get improved performance.

3.2.4 DC/DC Converter Control

The DC/DC converter is the interfacing converter for battery banks and EV-ESS battery packs as illustrated in Fig. 3.3. The DC/DC converter includes a voltage control loop cascaded with a current control loop. The voltage control loop keeps the DC link voltage of the energy storage between VSI or DC bus at V_{DC}^{ref} and generate reference current

Table 3.2: Simulation parameters for the hybrid AC/DC microgrid

Energy nodes							
Solar PV	250 kW						
PV BESS	60 kWh						
3P BESS	48 kWh						
EV-ESS							
DC EV-ESS	48 kWh						
3P EV-ESS	48 kWh						
Single-phase EV-ESS	19.2 kWh						
Line parameters							
Nominal AC bus RMS voltage (line to neutral)	230 ~ 240 V						
Nominal DC bus voltage	600 ~ 800 V						
Frequency	50 Hz						
C_{DC}	$100 \times 10^{-3} F$						
R_f	$2 \times 10^{-3} \Omega$						
L_f	$250 \times 10^{-6} H$						
C_f	$16.9 \times 10^{-3} F$						
R_c	$2 \times 10^{-3} \Omega$						
L_c	$500 \times 10^{-6} H$						
Damping resistor	$20 \times 10^{-2} \Omega$						
Control parameters							
Power controller		Voltage controller		Current controller		DC/DC converter	
ω_c	31.42 rad/s	$K_{p(V)}$	4.1497	$K_{p(I)}$	0.7390	$K_{p(V)}^{DC}$	7
V^*	340 V	$K_{i(V)}$	3.90×10^3	$K_{i(I)}$	3.17×10^4	$K_{i(V)}^{DC}$	800
ω^*	314.16 rad/s	F	0.75			$K_{p(I)}^{DC}$	0.3
D_P	3.14×10^{-5}					$K_{i(I)}^{DC}$	20
D_Q	1.36×10^{-4}						
$K_{p(P)}$	2.5×10^{-4}						
$K_{d(P)}$	3×10^{-3}						

signals for the battery. DAEs for the voltage and current control loop of the DC/DC converter controller are given as [157]:

$$\begin{cases} i_{DC}^{ref} = (V_{DC}^{ref} - V_{DC}) \left(K_{p(V)}^{DC} + \frac{K_{i(V)}^{DC}}{s} \right) \\ D_{Batt} = \frac{(i_{DC}^{ref} - i_{Batt}) \left(K_{p(I)}^{DC} + \frac{K_{i(I)}^{DC}}{s} \right)}{V_{DC}} \end{cases} \quad (3.13)$$

where $K_{p(V)}^{DC}$ and $K_{i(V)}^{DC}$ are the proportional and integral gains for the voltage control loop respectively and $K_{p(I)}^{DC}$ and $K_{i(I)}^{DC}$ are the proportional and integral gains for the current

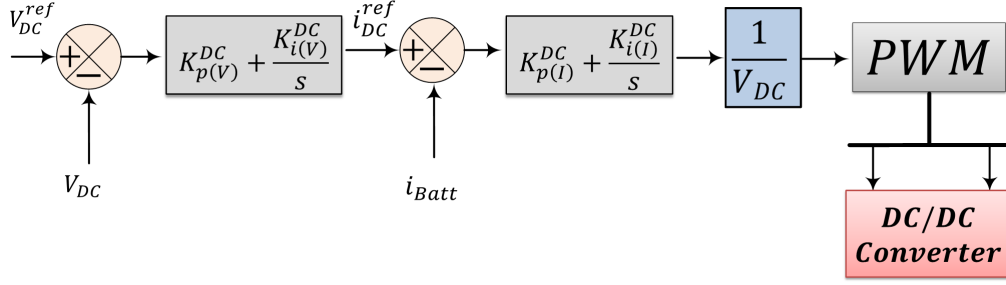


Figure 3.3: DC/DC converter controller

control loop respectively. D_{Batt} is the generated duty ratio for the pulse width modulation (PWM) of the DC/DC converter.

3.3 Coordinated Control Strategy

3.3.1 Coordinated Control Objectives

The coordinated control of the three-phase and the DC type EV-ESS is designed considering the following objectives:

- *Bus voltage regulation:* Hybrid AC/DC microgrids are composed of single or multiple AC and DC buses. It is essential to maintain both AC and DC bus voltage levels within an acceptable range to maintain a stable hybrid AC/DC microgrid operation. Usually, during islanded condition the amplitude and frequency of the AC bus voltage are regulated by the bidirectional interlinking converter and the DC bus voltage is controlled by the DC/DC converter connected to energy storage devices. According to [158] the input DC bus voltage and the output AC bus RMS voltage of the interconnecting VSI maintains a linear relationship as given by:

$$V_{DC} = 2 \times \underbrace{\left(\frac{\Lambda}{m}\right) \times \left(\frac{\sqrt{2}}{\sqrt{3}}\right)}_{\text{}} \times V_{L-L} \quad (3.14)$$

Where, V_{DC} = DC bus voltage;

V_{L-L} = Peak-to-peak magnitude of the phase-to-phase voltage;

Λ = voltage compensating factor for the VSI interconnection loss and

m = modulation index.

Considering the loss less interconnection of the VSI (*i.e.* $\Lambda = 1$) and the maximum value of the modulation index (*i.e.* $m = 1$) then the (3.14) can be rewritten as follows

$$V_{DC} \approx 2 \times \underbrace{\left(\frac{\sqrt{2}}{\sqrt{3}} \right)}_{V_{L-N}^{RMS}} \times V_{L-L} \quad (3.15)$$

It can be observed from (3.15) that the DC bus voltage needs to be double in magnitude of the phase-to-neutral RMS voltage (*i.e.* V_{L-N}^{RMS}). As mentioned previously that based on AEMO standard the AC bus RMS voltage should be in between -6% to +10%. Due to the linear relation between DC bus voltage and AC bus RMS voltage, the acceptable deviation for DC bus voltage should be within -3% to +5%. This defined relation has been utilized for the medium voltage (MV) DC microgrid in [159], however, this relationship can be applied to the low voltage (LV) distribution networks as well.

- *Frequency regulation:* During grid connected operation the frequency of the AC subgrid is regulated by the utility grid itself. However, islanded operation requires the frequency of the output voltage of each VSI or interlinking converter to be adjusted through the embedded droop control of the associated VSIs.
- *Power sharing:* During grid-tied mode, DG sources generate pre-specified active/reactive power and the main utility grid act as slack bus. Throughout this operation, the main objective of the utility grid is to provide or absorb power to balance the frequency by managing loads. The challenging condition arises when microgrids

operate in islanded operation as during islanded operation microgrids are solely responsible for managing the total load demand by proportional sharing of real and reactive power.

- *Reduction of phase unbalance:* The introduction of single-phase or residential charger for the EVs can generate unbalanced phase voltage and current. With increased penetration of EVs this unbalanced condition might go beyond acceptable range, which require optimal coordination among EV-ESS aggregators of various configurations. This research considers the generation of separate sinusoidal modulation indexes for each phase to partially tackle this issue. However, proper load planning from the DSOs is required to distribute the single-phase loads among phases in order to avoid the higher unbalanced condition.

3.3.2 Coordinated Control Algorithm

During normal operation of the microgrid it is expected that the overall demand of active and reactive power is balanced with the respective generation. Any mismatch in total generation and load demand requires regulation services. Usually DC bus voltage magnitude and the frequency of the AC bus voltage are closely related to the balance of active power generation and load demand. If the active power generation is higher than the load demand, then the excess active power will increase the value of the frequency and the DC bus voltage. As a result a regulation down service is required for both DC bus voltage and frequency of the system. Regulation down service involves routing the energy to the grid or charge the energy storage system which are not taking part in the microgrid operation. Regulation-up service are required when there is a shortage of generating active power than load. Then additional active power demand will decrease the DC bus voltage and at the same time the frequency of the system. Regulation-up service involves importing

additional power from the grid (grid connected mode) or from the participating ESS (in islanded condition) which results in the discharging mode of the ESS.

On the contrary, for a converter dominated microgrid with relatively high value of the inductors in the LC or LCL filters, the magnitude of the AC bus RMS voltage is regulated by matching the reactive power generation and demand. Similar to the DC bus voltage and frequency regulation, if the reactive power generation is higher than the total reactive load, it will increase the magnitude of the AC bus RMS voltage, as a result regulation-down service is required. On the other hand, if the reactive power generation is less than the total reactive load, then the magnitude of the AC bus RMS voltage will decrease which requires regulation-up service. Regulation-up or down of the AC bus voltage magnitude can be obtained by absorbing or supplying the reactive power from or to the grid or from/to the four quadrant STATCOM attached to DG units or distributed energy storages like EV-ESS.

Synchronous generators/alternators run by natural gas and coal units can provide regulation-up or regulation-down for all essential parameters, by reducing their production or by supplying additional power to the grid, respectively, to match the load. Due to their slower dynamics and environmental impacts the fast responding converter based DG units and ESS are preferred in this research. Due to comparative higher expenses of ESS they require smart coordination to be utilized. As a result, this chapter introduces a smart coordination algorithm that can effectively provide satisfactory performance for the hybrid AC/DC microgrid for both grid connected and islanded operation even in the presence of single-phase EV-ESS charging station.

The proposed coordination algorithm is illustrated in Fig. 3.4. The smart coordination algorithm has considered the operation of the discharging mode of the DC fast charging station and the four quadrant operation of the three-phase charging station in the presence of single-phase AC charging for the electric vehicles. The coordination algorithm

has three layers. It should be noted that all three layers can operate concurrently and autonomously without any overlapping factors in order to improve hybrid AC/DC microgrid operation. The advantages of simultaneously operating multi-layered coordination are, for instances, it will avoid excessive power transport due to hybrid operation, which results in lower power electronic based loss and it will also ensure the highest possible autonomy to the individual AC and DC microgrid. The notations presented in the Fig. 3.4 have following meanings,

- $P_{DC}^{MG} \rightarrow P_{AC}^{MG}$: Active power is flowing through the interlinking converter from the DC microgrid to the AC microgrid
- $P_{DC}^{MG} \leftarrow P_{AC}^{MG}$: Active power is flowing through the interlinking converter from the AC microgrid to the DC microgrid
- $Q_{DC}^{MG} \rightarrow Q_{AC}^{MG}$: Reactive power is flowing through the interlinking converter from the DC microgrid to the AC microgrid
- $Q_{DC}^{MG} \leftarrow Q_{AC}^{MG}$: Reactive power is flowing through the interlinking converter from the AC microgrid to the DC microgrid

ΔV_{DC} and ΔV_{AC} denote the deviation of the DC and AC bus voltages from their corresponding nominal values.

Layer 01: The first layer is responsible for the DC subgrid management and the DC bus voltage regulation. This layer prioritized the DC side load management by coordinating the DC EV-ESS. Initially this control layer will check whether the DC bus voltage requires regulation-up or regulation-down service by instantaneously checking the DC bus voltage magnitude and comparing that value with the allowable range. If the DC bus voltage is within acceptable range, then it will check whether AC subgrid requires additional active power. If the required power by the AC subgrid is within the acceptable KVA rating of the interlinking converter then it will export power to the AC subgrid. On the other hand, if the DC bus voltage requires regulation down service, then it will

charge the DC EV-ESS battery based on the requirement or no control action will be taken as shown in the illustration. For the regulation-up service this control initiates the EV-ESS discharging operation. The layer will prioritize the initiation of DC EV-ESS over 3P EV-ESS based on the availability. Later, if necessary it can import/export additional power to/from the AC subgrid through the interlinking converter by initiating 3P EV-ESS operation based on their availability. For contingency purpose if even with the simultaneous DC and 3P EV-ESS operation the DC bus voltage cannot be regulated within the limit, DC load curtailment for the islanded condition or switching back to the grid has been suggested.

Layer 02: The second and third layer are dedicated to AC subgrid management. The second layer is closely resembled to the first layer as both parameters *i.e.* DC bus voltage and the frequency are closely related to the active power regulation. The exemption between Layer 01 and Layer 02 is the prioritized choice of operating 3P EV-ESS over DC EV-ESS due to their close proximity and configuration in the AC subgrid.

Layer 03: The third layer manages the reactive power of the AC subgrid to regulate the AC bus RMS voltage. This layer changes the reactive power references of the control system of the interlinking converters or the 3P EV-ESS interfacing converter. This layer will initially look for reactive power support (either source or sink of reactive power) from the 3P EV-ESS. However, if no reactive power support can be obtained from the 3P EV-ESS then it will send the required reactive power signal to the interlinking converter droop controller to supply or absorb additional reactive power.

It is not expected that EVs are allowed to be available all the time compared to any other static ESS such as BESS. Moreover, economical aspects of the application of large scale EV-ESS in distribution level is still a major research topic. Apart from these issues, optimum utilization of V2G operation requires a rigorous market framework. As the primary focus of this chapter is inclined to the design of the coordination and control

strategy of various types of EV-ESS, the details about the possible market framework for V2G operation are not discussed here. However, EV availability constraints which are relevant to the design process of the proposed controller are presented in the next section.

EV Availability Constraints

- *EV-ESS capacity constraints:* Overcharging or discharging has adverse effect on EV battery lifetime. As a result, charging/discharging of both DC or 3P EV-ESS need to satisfy energy constraints mentioned below:

$$(SOC_i^{max} - SOC_i^0)Q_i^{Rated} \leq \Delta Q_i^{\Delta T_i} \leq (SOC_i^0 - SOC_i^{min})Q_i^{Rated} \quad (3.16)$$

where,

$$\begin{cases} \Delta Q_i^{\Delta T_i} = \Delta T_i P_i \\ \Delta T_i = T_{i(final)} - T_{i(initial)} \end{cases} \quad (3.17)$$

In the above equations,

SOC_i^{max} and SOC_i^{min} are the maximum and minimum allowable SOC for the i th EV;

SOC_i^0 is the initial SOC of the i th EV before participation;

Q_i^{Rated} is the rated battery capacity in ampere-hour (Ah) of the i th EV;

ΔT_i is the charging/discharging duration of the i th EV;

$\Delta Q_i^{\Delta T_i}$ is the change in battery capacity within ΔT_i duration of the i th EV

- *EV user requirements:* In order to ensure flexible user experiences, the EV user should be able to pre-set the available time and minimum required SOC value for their EVs:

$$\begin{aligned} T_i &\in \{T_{i(initial)}, T_{i(final)}\} \\ SOC_i^{final} &\geq SOC_i^{pre-set} \end{aligned} \quad (3.18)$$

where,

T_i is the available or controllable time of i th EV, during the period that EV can be involved in V2G service;

$T_{i(initial)}$ and $T_{i(stop)}$ are the allowable start and stop time (charging or discharging) of i th EV respectively. The start and stop time of charging and discharging are dependent on several factors such as time of use pricing, driving patterns of EV owners etc.

SOC_i^{final} and $SOC_i^{pre-set}$ are the battery SOC value after its participation for V2G service the minimum SOC required value of i th EV pre-set by the user respectively.

- *Active and reactive power constraint:* When EV-ESSs respond to the control signals, their V2G capability of supplying or absorbing active and reactive power through their corresponding interfacing converters must be within the allowable range:

$$\begin{cases} -P_i^{max} \leq P_i^* \leq P_i^{max} \\ -Q_i^{max} \leq Q_i^* \leq Q_i^{max} \end{cases} \quad (3.19)$$

where, P_i^{max} and Q_i^{max} are the maximum allowable active and reactive power respectively for i th EV. P_i^* and Q_i^* are the active and reactive power reference for the power controller illustrated in Fig. 3.2. The negative (–) sign represents the absorption of active or reactive power by the EV-ESS.

3.4 Case Studies

In this section, simulations have been carried out to demonstrate the performance of the coordinated control strategy for three-phase (3P) and DC EV-ESS in a hybrid AC/DC microgrid with developed interlinking/interfacing controller. The hybrid AC/DC microgrid is composed of 250 kW PV and 60 kWh BESS at the DC side and 48 kWh BESS at the AC side. EV-ESS for both DC and three-phase AC configurations are 48 kWh, whereas

for single-phase configuration they are 19.2 kWh. All the necessary parameters have been provided in the 3.2. The hybrid AC/DC microgrid and the control structure have been designed in MATLAB/SIMULINK[®] environment using SimPowerSystems[™] toolbox. The simulations are run on Intel(R) Core(TM)i5-4570 CPU 3.20 GHz with 8.00 GB RAM. Four case studies have been carried out in this chapter. In case A, the performance of the interlinking/interfacing converter controller has been demonstrated for islanded hybrid AC/DC microgrid operation considering simultaneous variable irradiation of the PV system and the commercial load profile for one day (24 hours) of N44 building without any participation of EVs. In Case B, single-phase EV charging has been introduced considering that all the single-phase EV chargers are allocated homogeneously among the three phases. Case C considers the heterogeneous allocation of single-phase EV chargers. In the last case study, which is case D, demonstrates the capability of the designed controller to synchronize with the grid when the grid is available.

3.4.1 Case A: Variable Irradiation and Loading Effects

In this case study, the performance of hybrid AC/DC microgrid operation has been observed without any EV participation. The main purpose of this case study is to demonstrate the performance of the interlinking converter during the islanded operation of the microgrid. The solar irradiation data, PV output power and the load real and reactive power for the N44 building is collected using OSI PI data acquisition software. This software collects data from the building smart power meters. The solar irradiation, PV output power and the building load profile are shown in Fig. 3.5. The main control parameters for the interlinking/interfacing converter controller are v_d and v_q . The references for v_d and v_q are generated by the combined action of the power controller/droop controller and the coordinated control algorithm. Later, references for i_d and i_q are generated to control the interlinking/interfacing converter. In Fig. 3.6 the interlinking converter

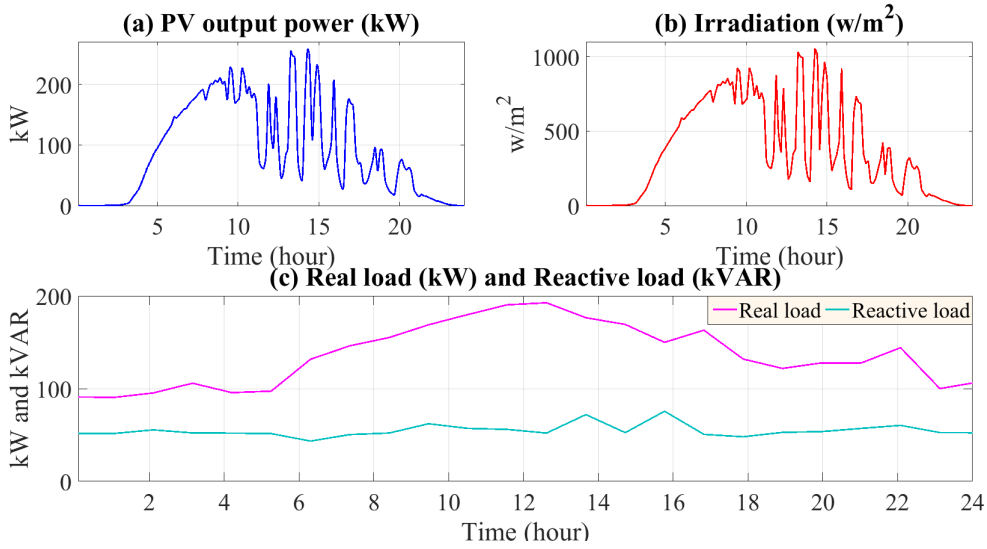


Figure 3.5: Input data for the hybrid AC/DC microgrid: (a) PV output power, (b) Solar irradiation and (c) Usual active and reactive power demand of the building for 24 hours

control signals have been presented for normal operating condition.

3.4.2 Case B: Homogeneous Single-Phase EV Allocation

In this case study, single-phase EV charging has been introduced. Initially homogeneous allocation of single-phase EV chargers have been considered. Homogeneous allocation of single-phase EV charging station means each phase (i.e. a, b and c) of the three-phase system is equally loaded with EV chargers. Usually for residential single-phase charging the overnight charging is suggested when the peak demand is less and EV owners are at home. Unlike residential EV charging the commercial EV owners need to charge their EVs during day time while they are working in office or for this case in the university campus. So the charging period has been taken for this simulation is form 9:30 AM till 5:30 PM, which is usual office hours. Results obtained from this simulation for DC bus voltage, AC bus RMS voltage and frequency are presented in Figs. 3.7, 3.8 and 3.9 respectively. Both AC and DC bus voltages are measured in per unit (p.u.). It can be observed from the

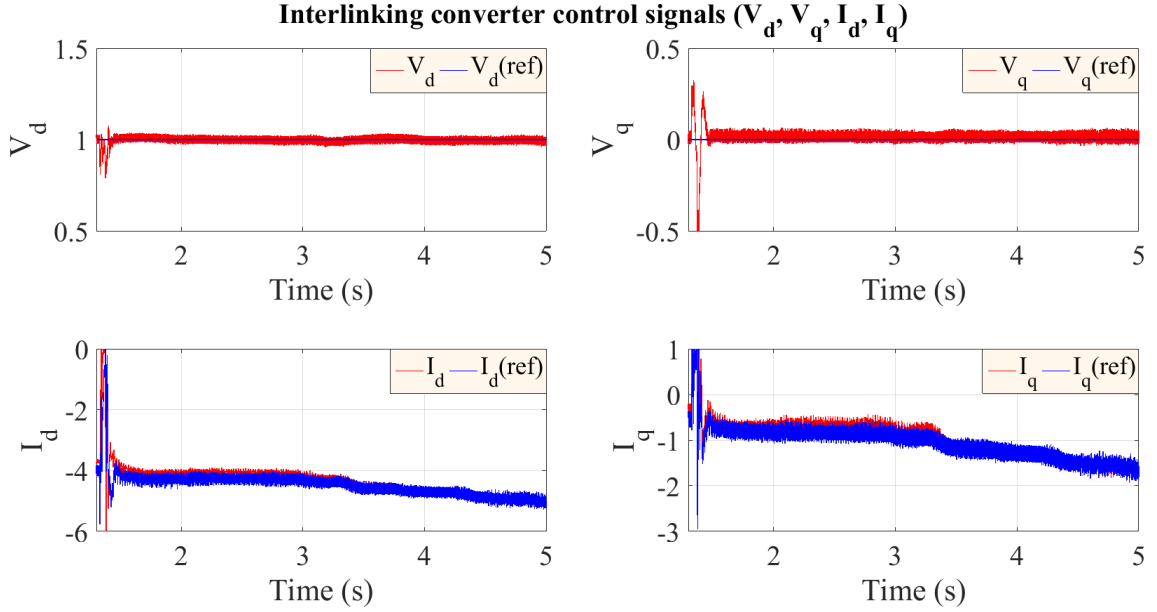


Figure 3.6: Control signals of the interlinking converter

figures that the DC and AC bus voltages and system frequency are within acceptable limit during the islanded operation when there is no EVs are participating for charging. With the introduction of EV charging in each phase, there is a drop in both DC bus voltage and AC bus RMS voltage while the frequency is not severely affected due to the droop control mechanism. In order to keep the AC and DC bus voltage within acceptable limit three coordination methods have been utilized. These methods include, participation of only DC EV-ESS, participation of only 3P EV-ESS and for the worst case scenario, simultaneous participation of DC and 3P type EV-ESS operation has been considered. It can be observed that only 3P EV-ESS support is not enough to ensure DC bus voltage regulation, though it can ensure regulated AC bus RMS voltage. It is evident that simultaneous DC and 3P EV-ESS operation (which is referred as aggregated operation) improves both AC and DC bus voltage effectively. However, aggregated operation may not be economical for long time operation. Comparative simulation results for DC bus voltage, AC bus RMS voltage and frequency considering without EVs, with EVs, only DC EV-ESS support,

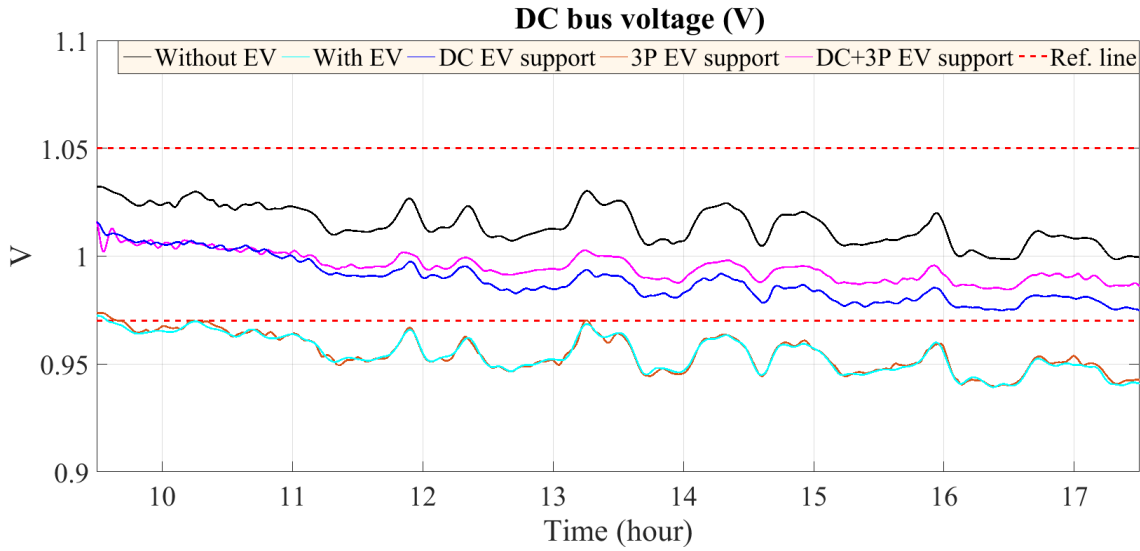


Figure 3.7: DC bus voltage

only 3P EV-ESS support and aggregated operation are shown in Figs. 3.7, 3.8 and 3.9 respectively. Meanwhile, the state-of-charge (SOC) for charging and discharging EV-ESS considering all these modes are shown in Figs. 3.10 and 3.11. Active and reactive power profiles for the aggregated operation are shown in Figs. 3.12 and 3.13 to show the effectiveness of the designed droop controller.

3.4.3 Case C: Heterogeneous Single-Phase EV Allocation

Heterogeneous allocation EV-ESS has been considered for this case study. It refers that each phase is loaded whimsically as presented in Fig. 3.14. It should be noted that each single-phase EV charger has been designed to act as active load operation. The active load operation of EV is designed with single-phase PLL and corresponding controllers as presented in [45]. It can be observed from Figs. 3.15 and 3.16 that even with the unbalanced loading condition the controller effectively regulates DC and AC bus voltages and frequency.

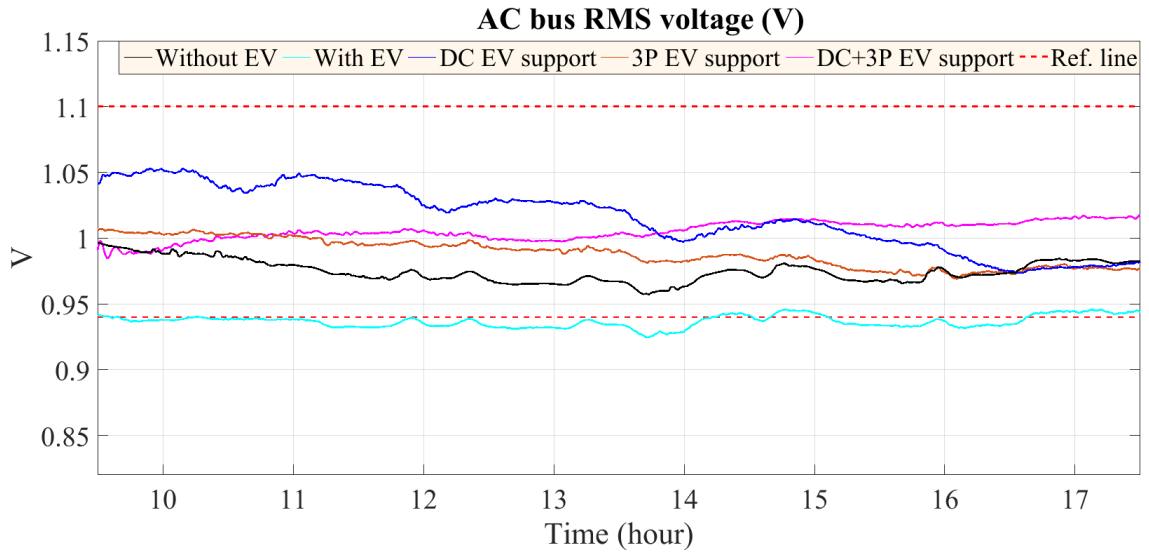


Figure 3.8: AC bus RMS voltage (line to neutral)

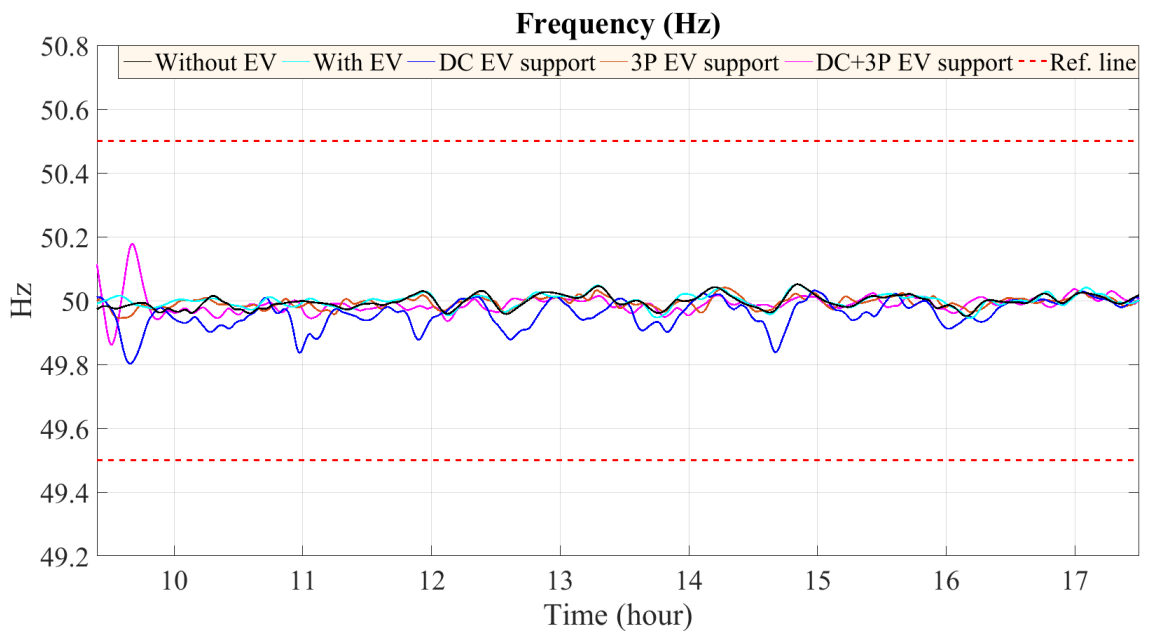


Figure 3.9: Frequency

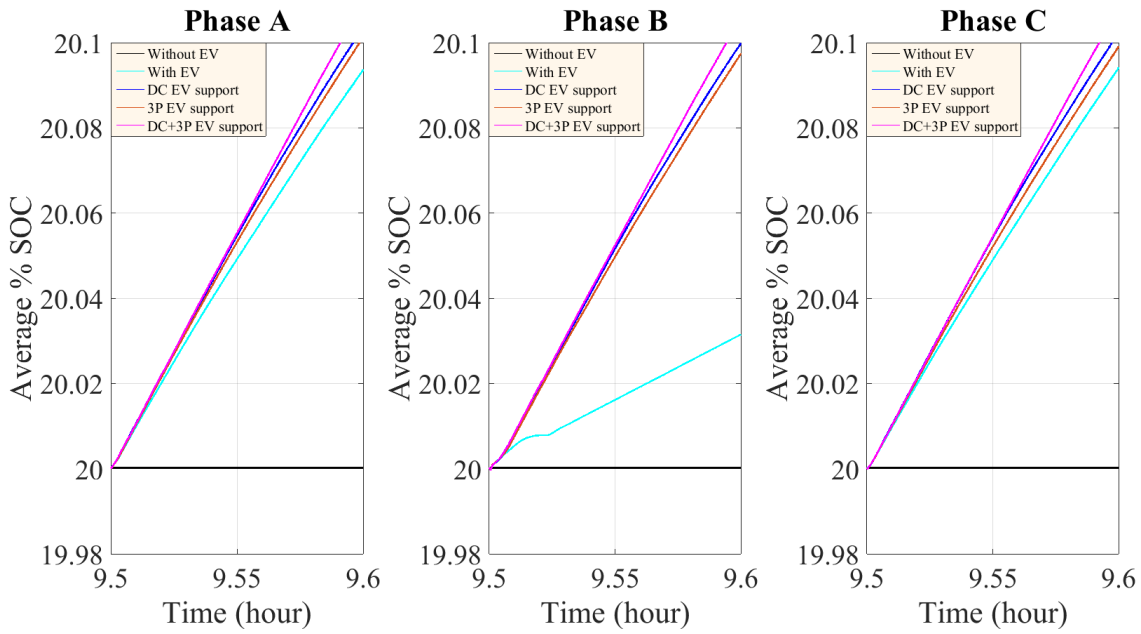


Figure 3.10: SOC of the single-phase EV-ESS

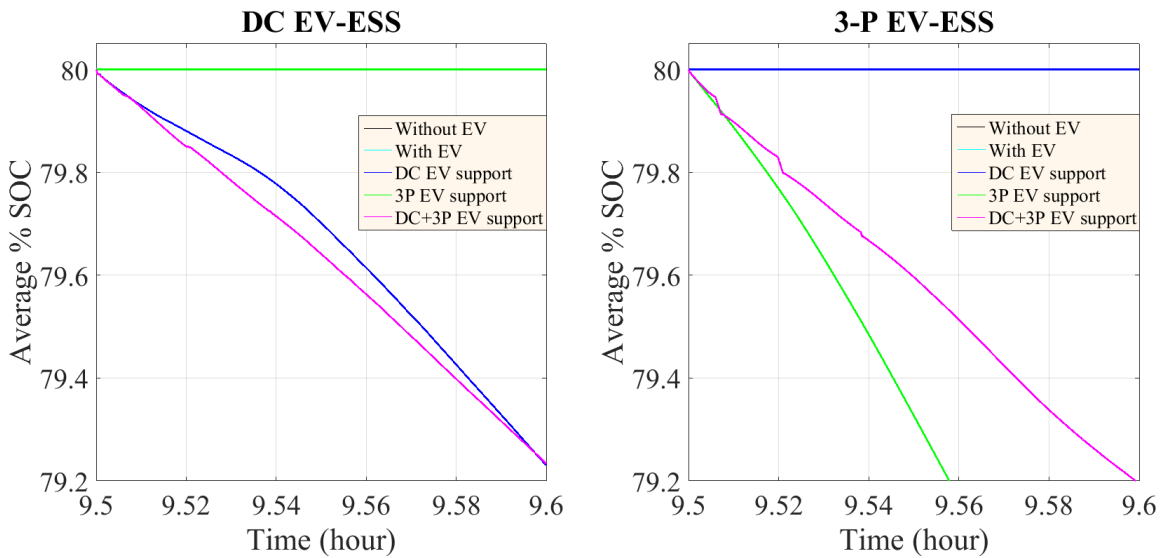


Figure 3.11: SOC of the DC type and 3P type EV-ESS

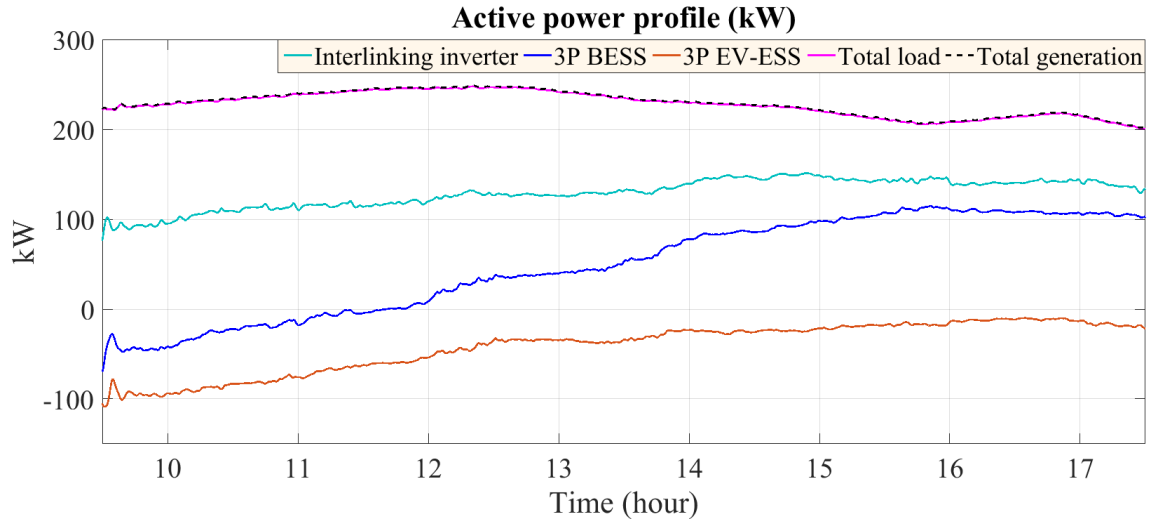


Figure 3.12: Active power profile of the system

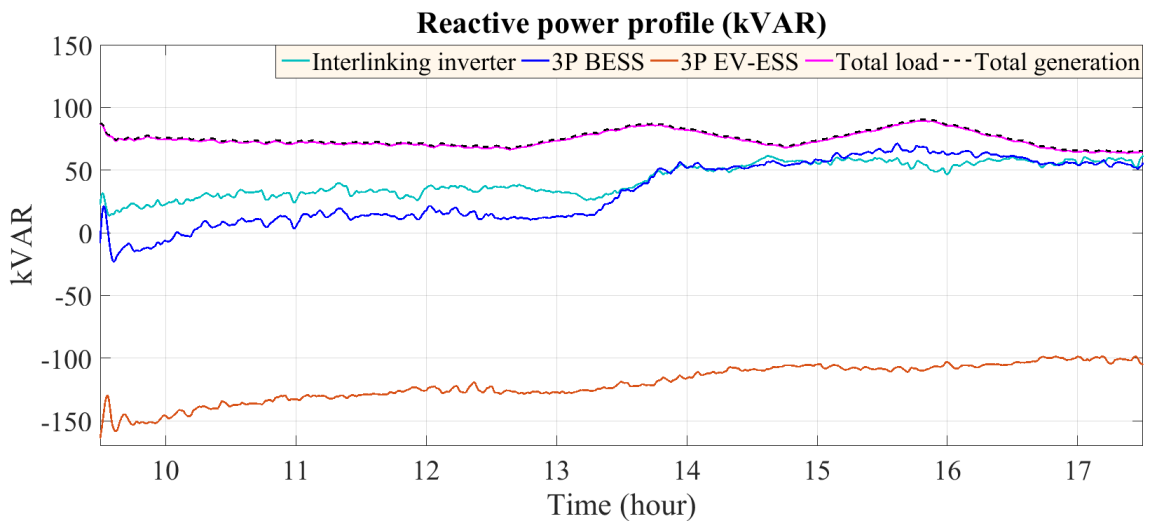


Figure 3.13: Reactive power profile of the system

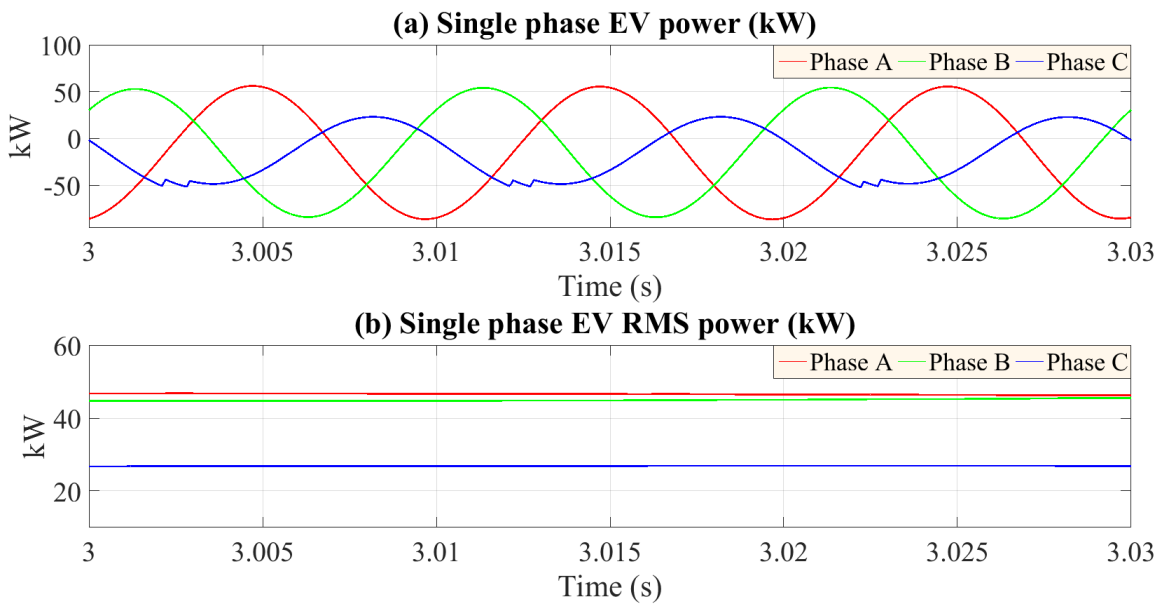


Figure 3.14: Charging power drawn by single-phase EV-ESS: (a) Single-phase power and (b) RMS value of the single -phase power

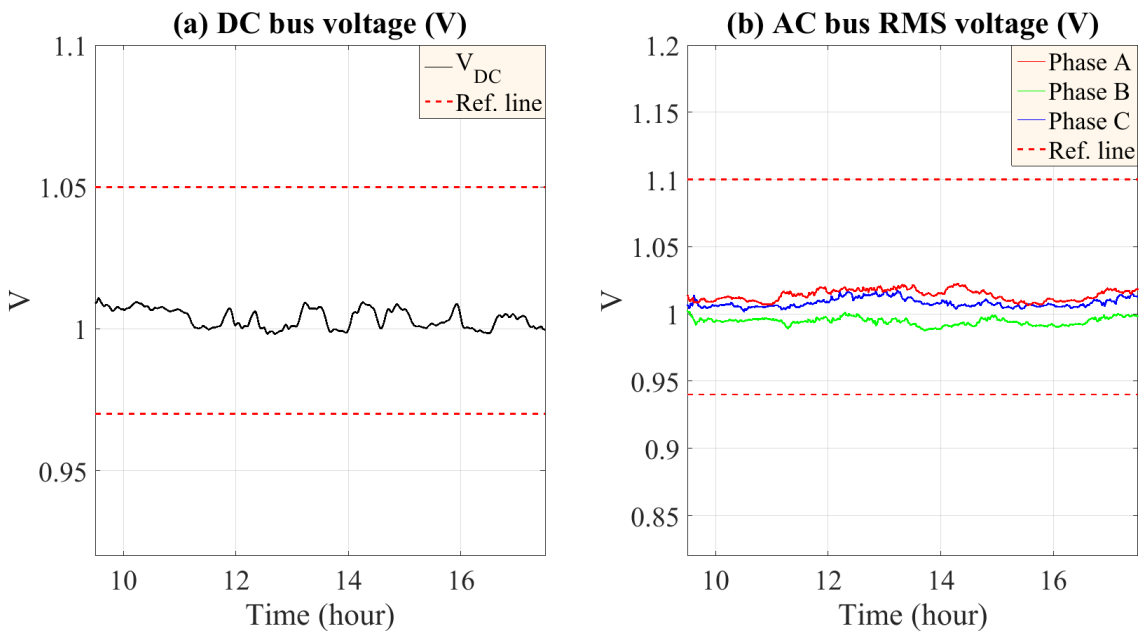


Figure 3.15: Voltage profile for case C: (a) DC bus voltage and (b) AC bus RMS voltage

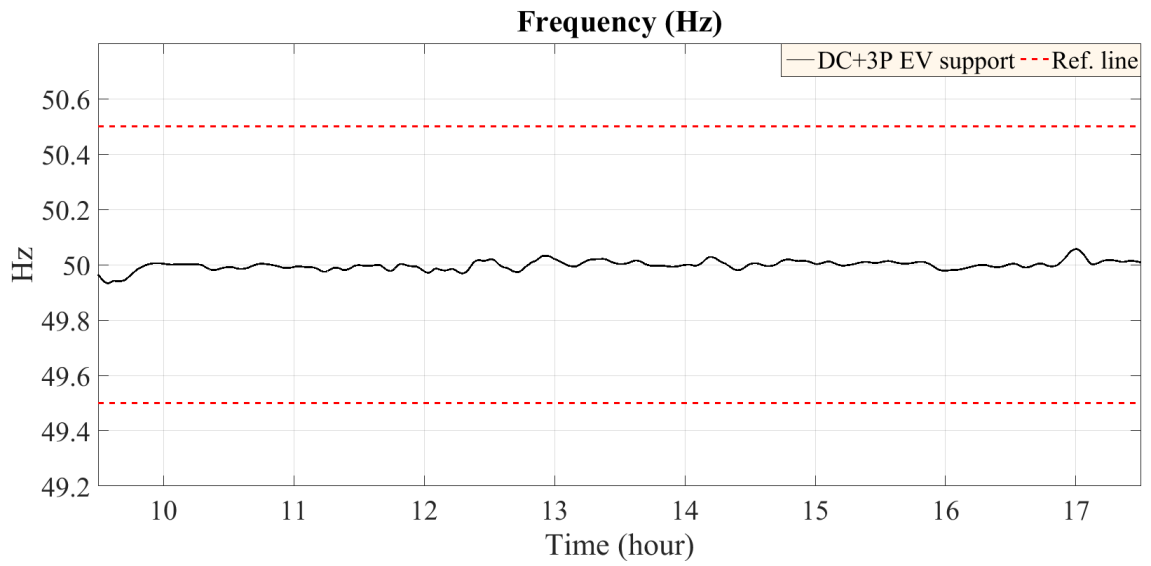


Figure 3.16: Frequency for case C

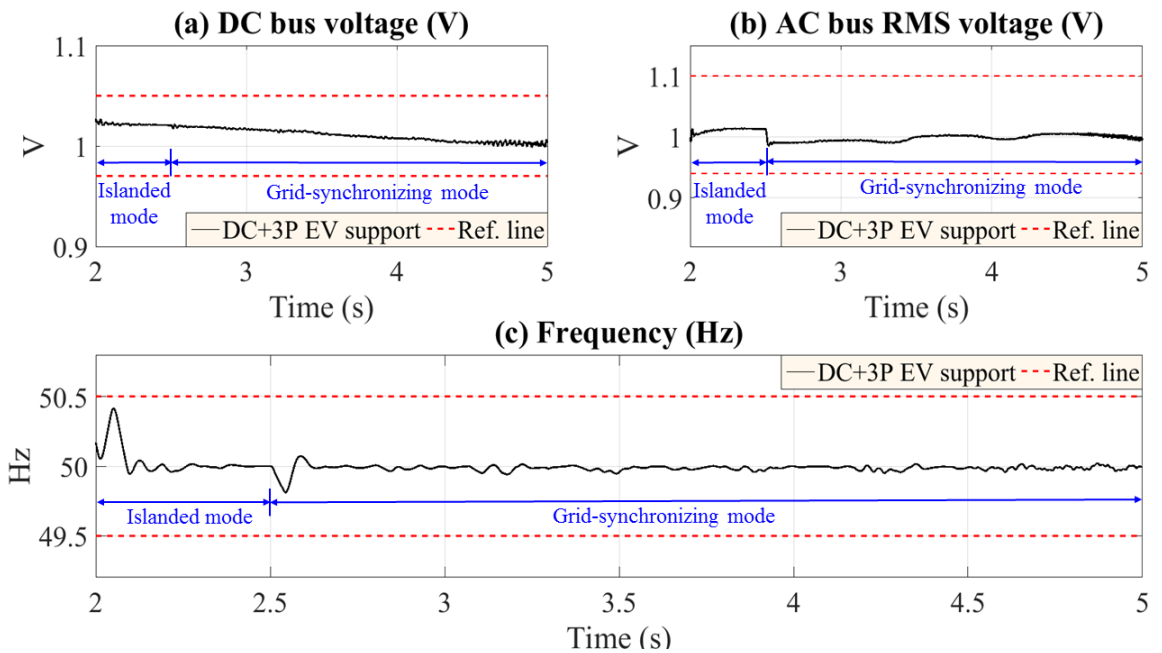


Figure 3.17: Grid synchronization mode: (a) DC bus voltage, (b) AC bus RMS voltage and (c) Frequency

3.4.4 Case D: Grid Synchronization

Meanwhile, microgrid may need to switch from islanded to grid connected condition during contingency. During the switching period from islanded mode to grid connected mode, the designed controller ensures smooth operation and synchronization with the main grid. In order to connect from the islanded to grid connected mode, the magnitude and the frequency of the AC side PCC voltage has to be in synchronism with the grid voltage magnitude and frequency. From the case study results presented in Fig. 3.17, it can be observed that DC bus voltage, AC bus RMS voltage and frequency remain in synchronism even in the transition period from islanded to grid connected mode.

3.5 Chapter Summary

In this chapter, a novel coordinated control strategy is proposed which facilitates the V2G capability of three-phase AC and DC type EV charging stations in an islanded commercial hybrid AC/DC microgrid. The main objective of the coordinated control is to improve the performance of the microgrid in terms of voltage and frequency regulation, active/reactive power management in both balanced and unbalanced systems. Realistic EV availability constraints are considered for the design process. Three concurrently operating and non-overlapping layers of coordination have been developed. The first layer manages the DC subgrid of the hybrid AC/DC microgrid and ensures stiff DC bus voltage regulation by coordinating DC type EV chargers. The second and third layer coordinate three-phase EV charging station that has the V2G four quadrant operational capability which are responsible for frequency and AC bus RMS voltage regulation respectively. As a single entity, the coordination algorithm is embedded into the microgrid central controller (MGCC) which generates necessary active/reactive power command for microgrid local controllers such as interlinking and interfacing controllers. The designed controller

with proposed algorithm has been tested considering PV with fluctuating output and random commercial loads. Based on the comparative simulation results, improved voltage regulation and power sharing performance have been observed even with the presence of homogeneous and heterogeneous single-phase EV charging.

The centralized control structure presented in this chapter is well suited when there is a few number of DG units or multiple interconnected microgrids are involved. However, for larger interconnected or isolated microgrids with multiple EVs, distributed control techniques are a better alternative due to less computational burden and the avoidance of single-point communication link failure. As a result, in the next chapter, coordination for multiple EV storages are done in a distributed fashion with an improve inverter control topology.

Chapter 4

A Need-Based Distributed Coordination Strategy for Multiple EVs in a Commercial Microgrid

This chapter presents a need-based distributed coordination strategy (NDCS) for multiple electric vehicle (EV) storages in an islanded commercial hybrid alternating-current (AC)/direct-current (DC) microgrid. The control capacity of the interlinking converter is enhanced by incorporating combined power-droop and voltage-droop strategies to leverage the coupling of AC and DC voltages. Therefore, the AC bus voltage can be regulated simultaneously by regulating only the DC bus voltage without affecting the power-sharing capabilities of the converter. The NDCS is proposed to coordinate the EV storages to regulate the DC bus voltage. The main objective of the NDCS is to decide whether the coordination of the available EV storages is to be done in a decentralized or a distributed manner. The mathematical model and the algorithm to deploy NDCS are developed to realize its application to a real system. The effectiveness of the control system is verified in a commercial hybrid AC/DC microgrid comprising one photovoltaic (PV) unit and four EV

storages directly connected to the DC bus via DC/DC converters and four distributed-generation (DG) units connected to the AC bus using the conventional droop-control scheme. The performance of both controllers is tested under variable irradiation, commercial loading and various fault conditions. The results of the case studies demonstrate the efficacy of the overall system in terms of robustness for a variable generation-demand scenario, time delay, EV plug-and-play and fault conditions.

4.1 Introduction

With a view to leveraging the advantages of both alternating current (AC) and direct current (DC) types of power systems, recently a hybrid AC/DC microgrid structure is proposed in [24]– [25]. This particular structure is gaining momentum due to its several advantages including minimum AC/DC conversion loss, higher efficiency, less effort in voltage synchronization and feasibility of source-load connection [50]– [160]. However, the control structure of a hybrid microgrid is more complex due to the coexistence of multiple buses of different electric natures. Supplementary complexities are introduced when dynamic energy-storage systems (ESS) like electric vehicles (EVs) are plugged in on a massive scale, either to charge themselves or to provide ancillary vehicle-to-grid (V2G) services, such as active and reactive power support, voltage and frequency regulation, valley filling, peak-load shaving etc. [14]– [161]. Consequently, the hybrid AC/DC microgrid is unlikely to be implemented in residential areas in the near future, because of higher uncertainties and complexities [2]. Thus, suitable applications for a hybrid AC/DC microgrid structure could be commercial or industrial vicinities [17]– [1]. Moreover, commercial buildings are using nearly 32% of the overall energy generation, and at the same time these buildings are responsible for emitting almost 30% of the CO_2 related to energy consumption. Sustainable sources like photovoltaic (PV) units, fuel cells and small-scale

wind turbines can be incorporated to reduce this emission. The efficiency of the overall system can be further improved by utilizing the power generated from the EVs parked in a commercial vicinity [125]– [162]. However, additional research attention is required for the effective utilization and control of EVs in a commercial-grade microgrid.

Microgrids require a definite control structure due to the presence of power electronic converters and non-inertial sources as well as their ability to work in both islanded and grid-tied modes. The concept of a hierarchical control structure for both conventional power systems and for all types of microgrids (*i.e.* AC, DC and hybrid AC/DC) is well-accepted in the literature [150]. This structure involves a hierarchy of primary, secondary and tertiary layers of control. Of those layers the primary control layer is well researched and various types of decentralized droop controls are predominantly studied and used for this layer. The main objectives of both the primary and secondary control layers are to ensure voltage and frequency stability by compensating for respective deviations, whereas the tertiary control layer is more focused on optimal power flow and economic dispatch operation in the grid-tied mode. Both secondary and tertiary control layers can achieve their individual objectives by adopting either a centralized (for small-scale microgrids) or a distributed approach (commercial-grade microgrids or interconnected microgrids) [150]– [163]. However, the centralized approach has some limitations such as single-point failures, extensive computational burden for the processing units and expensive communication networks. As a result, distributed control approaches are gaining attention particularly for the secondary and tertiary control layers. This control structure requires sparse communication among neighboring distributed-generation (DG) units and utilizes local parameters, such as voltage, frequency and power requirements to regulate them, which in turns reduces the computational burden of the processing units and reduces the overall cost with improved reliability [164]– [82].

Recently application of distributed control in microgrids has been a topic of interest

due to the above-mentioned advantages over centralized control structures. For instance, these controllers are developed for AC microgrids [102]– [74] to achieve proportional power sharing and voltage regulation. The controller has been applied to DC microgrids [165] and is later extended for multiple DC microgrid clusters [166]– [167]. The performance of the developed controller is later improved to consider the impacts of communication latency [81]– [168], uncertain communication topology [169], communication link failure and parameter uncertainties [82]. Consensus-based distributed control structures for ESS are developed in some recent literature [80]– [170] to achieve certain objectives, such as state-of-charge (SOC) balancing and energy-level balancing. An SOC-based distributed cooperative controller is developed to reduce distribution feeder-voltage swelling due to high PV penetration [171]– [172]. A distributed consensus algorithm is utilized for PV-battery based single-phase islanded microgrids [173]. However, none of these analyses considered simultaneous AC and DC bus voltage regulation, which is a primary requirement, particularly for an islanded hybrid AC/DC microgrid. Moreover, effective utilization of EV storage in a microgrid through proper coordination requires additional research.

Several distributed control schemes are proposed to coordinate ESSs considering them as active cooperative agents. However, most of these literature consider the controllers used, either in the primary or the secondary layer to be fully distributed in nature. Distributed controllers are indeed attractive options to coordinate multiple storages; nevertheless, problems the use of communication and the extent of computational burden persist. As a result, an efficient algorithm is required, which will ensure the period and the scenario when the distributed controllers need to be activated. Motivated by these challenges, this research presents a need-based distributed coordination strategy (NDCS) for the V2G-capable EV storages connected to the DC bus of the microgrid to regulate the DC bus voltage of the hybrid AC/DC microgrid. Firstly, the correlation between the AC-bus RMS voltage and the DC bus voltage is established using a voltage-based droop

control method [174]– [175]. The conventional interlinking converter (IC) control structure is extended with combined power- and voltage-droop control schemes. As a result, one type of voltage regulation ensures regulation of other types of voltage without affecting the power-sharing capabilities of the converters. The main contributions presented in this chapter can be summarized as follows:

1. An improved IC-control structure is proposed by unifying proportional-derivative (PD) power-based and voltage-based droop control structures. This improved control topology ensures better transient performance and provides coupling between the AC-bus RMS and the DC bus voltage without affecting the power-sharing capability of the converter. This control topology is cost-effective as it substantially utilizes the apparent-power (kVA) ratings of the converter without overloading it.
2. An integrated EV storage controller is proposed which can work in both decentralized and distributed manner. This controller ensures DC-bus voltage regulation, which results in zero circulating currents. As a result, the efficiency and the lifetime of the EV storages are improved. Additionally, this controller interacts with the IC to aid in regulating the AC bus voltage. As a result, simultaneous AC and DC bus voltage regulation is achieved.
3. A novel strategy named NDCS is proposed that takes the EV availability into account to activate need-based distributed coordination of multiple EVs. By utilizing this algorithm, the advantages of both decentralized and distributed controllers can be obtained.
4. Unlike existing distributed controllers, the proposed need-based controller exhibits robust fault-tolerance while operating in pair with the improved IC-control structure, which ensures reliable control framework.

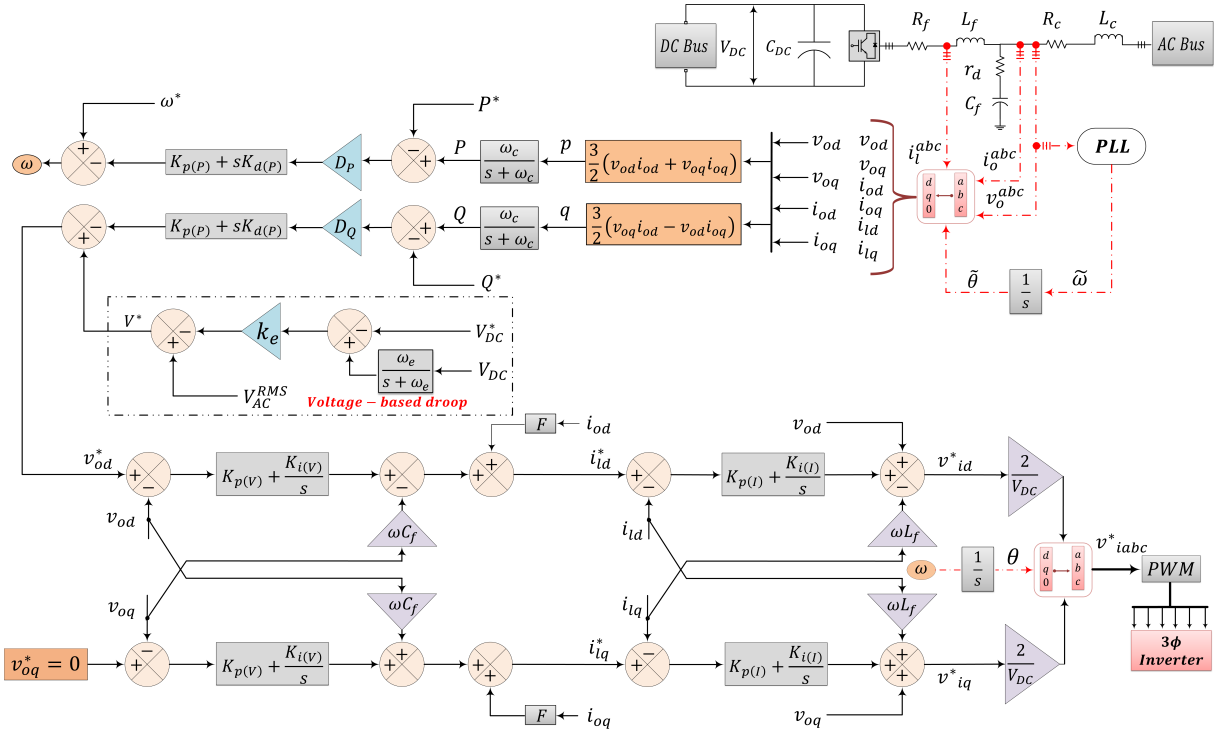


Figure 4.1: IC control structure with voltage-based droop.

- Interaction between the EV storage controllers and the IC controller affects the dynamic response of the hybrid microgrid. Moreover, there are substantial effects of time delay on the performance of the IC when the EV storages are controlled in a distributed manner. Therefore, a dynamic mathematical model for the IC controller is derived considering the interaction and the delay effects.

The remainder of the chapter is organized as follows. Section 4.2 presents the proposed IC control topology and its mathematical model. The general formulation of the proposed NDCS for the EV storages is presented in Section 4.3. In Section 4.4, case studies involving a commercial hybrid AC/DC microgrid with four EV storages in various scenarios are presented to demonstrate the controller performance. Finally, concluding remarks are presented in Section 4.5.

4.2 Proposed IC Control Topology

The IC acts as an interface between the AC and DC subgrids while the microgrid enters into a hybrid AC/DC microgrid operational mode. The IC controller has three inner control loops namely power controller, voltage controller and current controller as shown in Fig. 4.1. The dynamic modeling of these control loops is briefly described in the following subsections.

4.2.1 Power-Based Droop Control

The instantaneous voltage v_o^{abc} and current i_o^{abc} after the LC filter and the inverter output current v_l^{abc} are measured and transformed through the Park transformation. The real and reactive power calculations are carried out as follows [102, 149]:

$$\begin{aligned} p &= \frac{3}{2} (v_{od}i_{od} + v_{oq}i_{oq}) \\ q &= \frac{3}{2} (v_{oq}i_{od} - v_{od}i_{oq}) \end{aligned} \quad (4.1)$$

The fundamental components of p and q are extracted using a low-pass filter (LPF) with a cutoff frequency ω_c . The filtered active and reactive power are as follows:

$$\begin{aligned} P &= \frac{\omega_c}{s + \omega_c} p \\ Q &= \frac{\omega_c}{s + \omega_c} q \end{aligned} \quad (4.2)$$

Voltage and frequency are regulated via droop control during islanded microgrid operation. The usual X/R ratio of a microgrid is very high due to the high inductance of the inductors present in LC filters, particularly for a commercial-grade microgrid. As a result, the well-known P/f and Q/V droop control can be applied to regulate the frequency and the voltage of the system as follows [150]:

$$\begin{aligned} \omega &= \omega^* - D_P(P - P^*) \\ V &= V^* - D_Q(Q - Q^*) \end{aligned} \quad (4.3)$$

It should be noted that the designed controller can also be applied to microgrids with a low X/R ratio using the inverse droop equations. The dynamic performance of the conventional droop controllers is poor and can be improved by implementing PD-compensated droop control, which enables robust microgrid mode transitions and improved fault tolerance capabilities [176]. Now, assuming the d -axis to be aligned with the line voltage measured by the phase-locked-loop (PLL), we get $v_{oq}^* = 0$. Therefore, $V \approx v_{od}^*$. Then the droop equations become:

$$\begin{aligned} \omega &= \omega^* - K_{p(P)}D_P(P - P^*) - K_{d(P)}D_P\frac{d}{dt}(P - P^*) \\ V = v_{od}^* &= V^* - K_{p(Q)}D_Q(Q - Q^*) - K_{d(Q)}D_Q\frac{d}{dt}(Q - Q^*) \end{aligned} \quad (4.4)$$

ω^* is a global parameter, and a constant value can be assigned to it. For instance, for the system frequency of 50 Hz, $\omega^* = 314.16$ rad/s. Conventionally V^* , P^* and Q^* are taken as constants as well. However, for this chapter all of these three parameters are adaptive. This method ensures robustness in dynamic load changing, uninterrupted active/reactive power-sharing capabilities of the converter, and simultaneous AC and DC bus voltage regulation. The following subsection will discuss how P^* , Q^* and V^* are dynamically generated.

4.2.2 Generation of P^* , Q^* and V^*

The references for the active power (P^*), reactive power (Q^*) and the AC-side voltage (V^*) need to be adaptive, so that the IC controller performs robustly in changing network dynamics. Let us define three variables (\mathcal{A} , \mathcal{B} , \mathcal{C}) $\subseteq \mathbf{R}$ as follows:

$$\mathcal{A} = P_{AC(load)}^{Tot} - P_{AC(gen)}^{Tot} \quad (4.5)$$

$$\mathcal{B} = Q_{AC(load)}^{Tot} - Q_{AC(gen)}^{Tot} \quad (4.6)$$

$$\mathcal{C} = P_{DC(load)}^{Tot} - P_{DC(gen)}^{Tot} \quad (4.7)$$

Line losses should be added, if known, to all of (4.5)-(4.7). However, line losses are not considered in this chapter. The normal operation of a hybrid AC/DC microgrid refers to zero energy transfer between the AC and DC subgrids. In order to preserve the KVA ratings of the converters, the normal operation requires $\sqrt{\mathcal{A}^2 + \mathcal{B}^2} = \mathcal{C}$; however, deviations might occur due to overloading or surplus energy generation. These deviations will lead to hybrid AC/DC microgrid operation. Then P^* and Q^* for the hybrid AC/DC microgrid operation are to be defined as follows:

$$P^* = \begin{cases} 0 & \text{for } \sqrt{\mathcal{A}^2 + \mathcal{B}^2} = \mathcal{C} \\ \mathcal{A} & \text{for } \sqrt{\mathcal{A}^2 + \mathcal{B}^2} > \mathcal{C} \\ \mathcal{C} & \text{for } \sqrt{\mathcal{A}^2 + \mathcal{B}^2} < \mathcal{C} \end{cases} \quad (4.8)$$

$$Q^* = \begin{cases} 0 & \text{for } \sqrt{\mathcal{A}^2 + \mathcal{B}^2} = \mathcal{C} \\ \mathcal{B} & \text{for } \sqrt{\mathcal{A}^2 + \mathcal{B}^2} > \mathcal{C} \\ 0 & \text{for } \sqrt{\mathcal{A}^2 + \mathcal{B}^2} < \mathcal{C} \end{cases} \quad (4.9)$$

The inverter output AC voltage is proportionally related to the DC link voltage. The relation is presented in [158] and later elaborated in [17]. Vandoorn *et al.* in [174]–[175] utilize this relationship of voltages of different electric natures to control the inverters of DG units. This relation can be expressed as

$$V_{DC} \approx \underbrace{2 \times \left(\frac{\Lambda}{m}\right) \times \left(\frac{\sqrt{2}}{\sqrt{3}}\right)}_{\alpha} \times V_{L-L}^{AC} \quad (4.10)$$

where V_{L-L}^{AC} = peak-to-peak magnitude of the phase-to-phase voltage of the AC bus and α = slope of the linear relation presented in (4.10).

Then the V^{AC}/V^{DC} droop equation presented in [174]–[175] can be expressed as

$$V^* = V_{AC}^{RMS} + K_e(V_{DC} - V_{DC}^*) \quad (4.11)$$

Implementation of the control scheme in (4.11), combined with the power-based droop in the power control loop of the IC controller gives the opportunity, particularly for the islanded microgrid scenario, to achieve simultaneous quasi-decoupled power sharing and AC and DC bus-voltage regulation. Representing the delay using an LPF with the cutoff frequency of ω_e where $\omega_e > \omega_c$, the proposed IC control topology is illustrated in Fig. 4.1. It can be seen from Fig. 1 that if the DC bus voltage is tightly regulated (*i.e.* $V_{DC} - V_{DC}^* \approx 0$) then the whole IC control structure operates under the conventional strategy. As a result, the power sharing remains unaffected. Herein, by utilizing the information obtained from (4.8) – (4.9); and by the perturbing (4.2), (4.4) and (4.11) the state-space dynamic model of the proposed power-control loop of the IC controller can be obtained as follows:

$$\begin{aligned}
 \begin{bmatrix} \dot{Q} - Q^* \\ \dot{P} - P^* \\ \dot{V}^* \end{bmatrix} &= A \begin{bmatrix} Q - Q^* \\ P - P^* \\ V^* \end{bmatrix} + B \begin{bmatrix} q - Q \\ p - P \\ V_{DC} - V_{DC}^* \\ V_{AC}^{RMS} \\ \omega^* \end{bmatrix} \\
 \begin{bmatrix} v_{od}^* \\ \omega \end{bmatrix} &= C \begin{bmatrix} Q - Q^* \\ P - P^* \\ V^* \end{bmatrix} + D \begin{bmatrix} q - Q \\ p - P \\ V_{DC} - V_{DC}^* \\ V_{AC}^{RMS} \\ \omega^* \end{bmatrix} \tag{4.12} \\
 A &= \begin{bmatrix} 0 & 0 & 0 \\ 0 & 0 & 0 \\ 0 & 0 & -\omega_e \end{bmatrix}; B = \begin{bmatrix} \omega_c & 0 & 0 & 0 & 0 \\ 0 & \omega_c & 0 & 0 & 0 \\ 0 & 0 & K_e \omega_e & \omega_e & 0 \end{bmatrix}; \\
 C &= \begin{bmatrix} -K_{p(P)} D_Q & 0 & 1 \\ 0 & -K_{p(P)} D_P & 0 \end{bmatrix}; \\
 D &= \begin{bmatrix} -K_{d(P)} D_Q \omega_c & 0 & 0 & 0 & 0 \\ 0 & -K_{d(P)} D_P \omega_c & 0 & 0 & 1 \end{bmatrix}
 \end{aligned}$$

It is evident from the A matrix of the proposed power control loop that the system is only dependent upon the time delay attributed to the distributed controllers of EVs. It is also clear that $eig(A) < 0$ for all values of ω_e . As a result, the system is inherently stable for acceptable time delays. However, the controller, operating in the distributed mode can reach critical stability for unlikely large time delays in range of seconds.

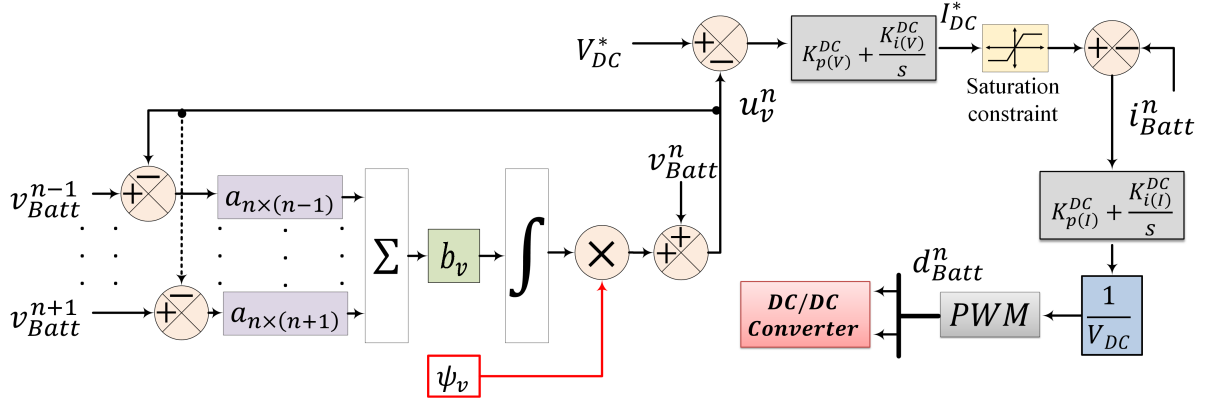


Figure 4.2: EV converter controller with distributed cooperative control loop.

4.2.3 Voltage and Current Controllers

Voltage and current controllers are developed utilizing decoupled d-q axis PI controllers with feed-forward gains [80, 102]. The combined dynamic equations for both voltage and current controllers can be obtained as follows:

$$\begin{aligned}
 \dot{\phi}_{od} &= v_{od}^* - v_{od} \\
 \dot{\phi}_{oq} &= v_{oq}^* - v_{oq} \\
 \dot{\lambda}_{ld} &= i_{ld}^* - i_{ld} \\
 \dot{\lambda}_{lq} &= i_{lq}^* - i_{lq} \\
 i_{ld}^* &= F i_{od} - \omega C_f v_{oq} + K_{p(V)} \dot{\phi}_{od} + K_{i(V)} \phi_{od} \\
 i_{lq}^* &= F i_{oq} - \omega C_f v_{od} + K_{p(V)} \dot{\phi}_{oq} + K_{i(V)} \phi_{oq} \\
 v_{id}^* &= v_{od} - \omega L_f i_{lq} + K_{p(I)} \dot{\lambda}_{ld} + K_{i(I)} \lambda_{ld} \\
 v_{iq}^* &= v_{oq} + \omega L_f i_{ld} + K_{p(I)} \dot{\lambda}_{lq} + K_{i(I)} \lambda_{lq}
 \end{aligned} \tag{4.13}$$

where $\dot{\phi}_{od}$ and $\dot{\phi}_{oq}$ are state variables corresponding to the PI controller of the voltage controller whereas $\dot{\lambda}_{ld}$ and $\dot{\lambda}_{lq}$ are state variables corresponding to the PI controller of the current controller.

4.3 Need-Based Distributed Coordination Strategy

Let us consider a microgrid of N number of EV storages communicating with each other through a sparse communication network. The communication graph, also known as a weighted directed graph (digraph), representing the interconnection of nodes can be denoted by $\mathcal{G} = (\mathcal{V}_{\mathcal{G}}, \mathcal{E}_{\mathcal{G}}, \mathcal{A}_{\mathcal{G}})$, where $\mathcal{V}_{\mathcal{G}} = \{\mathcal{V}_1, \mathcal{V}_2, \mathcal{V}_3, \dots, \mathcal{V}_n\}$ is the set of all nodes, $\mathcal{E}_{\mathcal{G}} \subset \mathcal{V}_{\mathcal{G}} \times \mathcal{V}_{\mathcal{G}}$ is the set of pairs of nodes also known as edges, $\mathcal{A}_{\mathcal{G}} = [a_{ij}]_{N \times N}$ is the weighted adjacency matrix of dimension $N \times N$ that gives information regarding the interconnectivity of nodes. The communication between node i and node j can be presented as follows:

$$a_{i \times j} = \begin{cases} 1 & \text{if } (i, j) \in \mathcal{E}_{\mathcal{G}} \\ 0 & \text{otherwise} \end{cases} \quad (4.14)$$

The in-degree matrix is $D_G^{in} = \text{diag}\{d_i^{in}\}$, i.e. the diagonal matrix of $d_i^{in} = \sum_{j=0}^n a_{ij}$. Similarly the out-degree matrix is $D_G^{out} = \text{diag}\{d_i^{out}\}$, i.e. the diagonal matrix of $d_i^{out} = \sum_{i=0}^n a_{ji}$. For an undirected communication network with bidirectional information flow, $D_G^{out} = D_G^{in}$. As a result, the Laplacian matrix $\mathcal{L}_{\mathcal{G}}$, defined as $\mathcal{L}_{\mathcal{G}} = D_G^{in} - \mathcal{A}_{\mathcal{G}}$, is considered *balanced* [59].

All EV storages are designed with the distributed dynamic average consensus protocols shown in Fig. 4.2. This protocol uses local information of the n^{th} EV storage and the information measured from its neighbors to converge to an average output voltage u_v^n , given by:

$$\begin{aligned} u_v^n(t) &= v_{Batt}^n(t) + \underbrace{\psi_v b_v \int_0^t \sum_{j \in N} a_{n \times j} (v_{batt}^j(\tau) - u_v^n(\tau)) d\tau}_{\Delta v} \\ &= v_{Batt}^n(t) + \Delta v \end{aligned} \quad (4.15)$$

Following this protocol, the output voltages of the EV storages for any step changes will converge at an average value of the neighboring units at $t \rightarrow \infty$, as long as there

exists a spanning tree and the communication delay (T_d) satisfies the condition [177]

$$T_d \leq \frac{\pi}{2\lambda_{max}(\mathcal{L}_G)} \quad (4.16)$$

The nominal value of the DC bus voltage is fixed for a particular application. As a result, without loss of generality it can be considered that all the EV storages connected to the DC bus have access to this reference value. This enables the entire controller to act in a leaderless manner. Fig. 4.3 illustrates the NDCS for cooperative V2G-capable EV storages. Each EV storage collects the terminal voltage information of its neighboring units $n-1$ and $n+1$. The DC bus voltage deviation, ΔV_{DC} is checked for the acceptable operating range, i.e. $-3\% - +5\%$ [17]. If ΔV_{DC} is within the acceptable operating range then zero is assigned for ψ_v . This results in $\Delta v = 0$ such that $u_v^n = v_{Batt}^n$. As a result, the EV storage controllers start operating in the decentralized mode. On the other hand, when ΔV_{DC} exceeds the acceptable range, then a substantial number of EV storages need to work cooperatively to regulate the DC bus voltage. As a result, when this situation occurs, NDCS will check the availability of V2G-capable EV storages. The availability constraints can be set as follows:

- Storage-capacity constraints for the n th EV can be set as $(SOC_n^{max} - SOC_n^{initial})Q_n^{Rated} \leq \Delta Q_n^{\Delta T_n} \leq (SOC_n^{initial} - SOC_n^{min})Q_n^{Rated}$; where, SOC_n^{max} , SOC_n^{min} , $SOC_n^{initial}$ are the maximum, minimum and the initial state-of-charge (SOC) of the n th EV storage respectively; Q_n^{Rated} and $\Delta Q_n^{\Delta T_n}$ are the rated capacity and the capacity for the duration of V2G operation (ΔT_n) of the n th EV storage respectively.
- The converter capacity for the n th EV storage can be depicted as $-P_n^{max} \leq P_n^{EV} \leq P_n^{max}$ and $-Q_n^{max} \leq Q_n^{EV} \leq Q_n^{max}$; where P_n^{max} and Q_n^{max} are the maximum allowable active and reactive power respectively and P_n^{EV} and Q_n^{EV} are the output active and reactive powers respectively for

the n th EV storage. However, the reactive power capacity will not be a concern when EVs are operating through DC/DC converters.

- A flexible user experience can be preserved by setting a constraint such as $SOC_n^{final} \geq SOC_n^{pre-set}$; where SOC_n^{final} and $SOC_n^{pre-set}$ are the SOC of the n th EV storage after the V2G participation and the user-defined pre-set SOC respectively.

Now if all the constraints are satisfied then $\psi_v = 1$ will be assigned which enables the EV storage controllers to operate in the distributed mode. However, if the constraints are not satisfied then the NDCS will keep the EV storage controller in the decentralized mode by preserving $\psi_v = 0$. Later on, it will initiate non-critical load curtailment to keep ΔV_{DC} within the limit. The grid reconnection command will be initiated for the microgrid as the last resort of regulation. For both decentralized and distributed modes of operation, u_v^n is updated according to (4.15) and I_{DC}^* is generated using (4.17), which results in the generation of d_{Batt}^n for the DC/DC converters of the EV storages using (4.18). In the final step the output voltage, v_{Batt}^n of the EV storage is broadcast to its neighboring units $n - 1$ and $n + 1$.

$$I_{DC}^* = (V_{DC}^* - u_v^n) \left(K_{p(V)}^{DC} + \frac{K_{i(V)}^{DC}}{s} \right) \quad (4.17)$$

$$d_{Batt}^n = \frac{(I_{DC}^* - i_{Batt}^n) \left(K_{p(I)}^{DC} + \frac{K_{i(I)}^{DC}}{s} \right)}{V_{DC}} \quad (4.18)$$

Storage lives can be enhanced by preserving pre-defined SOC levels for all EVs. As a result, it is important to maintain that level when EVs are operating in the decentralized mode. According to [178], the SOC of a battery is a function of time and output current

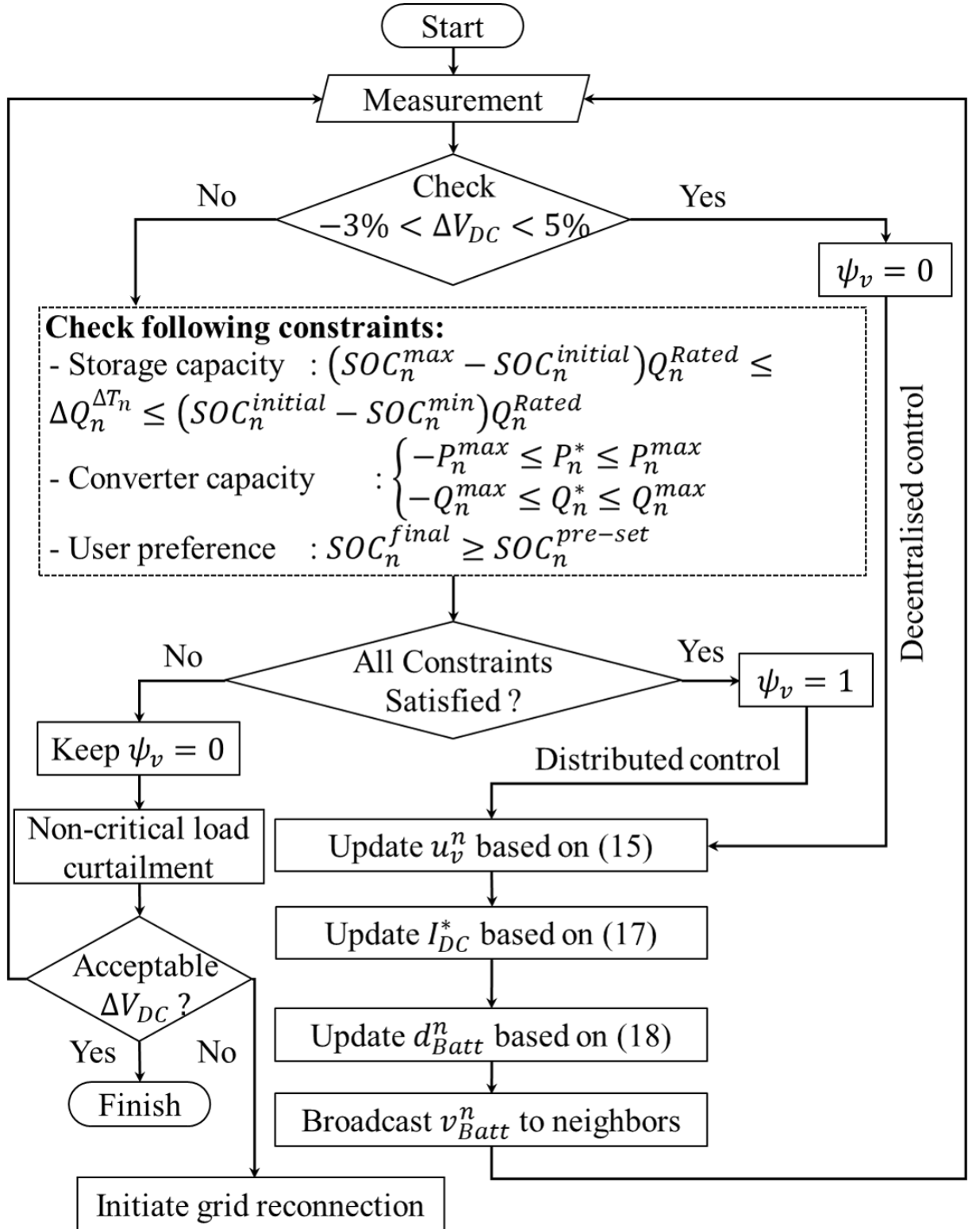


Figure 4.3: Need-based distributed coordination strategy of EV storages.

of the battery i.e. $SOC_n = f(t, i_{Batt}^n)$. It can be observed from (4.17) and (4.18) that $i_{Batt}^n = f(I_{DC}^*)$. It implies that, by limiting the dynamic value of I_{DC}^* , the SOC level can be maintained during the decentralized mode. Assuming that each EV has the maximum power capacity of 20 kW with the output reference DC bus voltage 520 V, in this chapter we have assumed the maximum and minimum values of I_{DC}^* to be ± 40 A.

4.4 Case Studies

Several case studies are carried out to demonstrate the performance of the developed controller. For all the case studies, the microgrid is considered to be islanded. Case A is carried out considering islanded operation, with step load changes to verify the performance of the proposed NDCS. Concurrent variable PV generation and real commercial loading are considered for case B to demonstrate the efficacy of the controller under intermittent supply and demand. This case study also demonstrates the efficacy of the proposed controller in the distributed mode with the conventional one presented in [25]. In case C, the effects of time delay on the controller performance are demonstrated. EVs are mobile storages in contrast to the static ESS and their operations also rely on their owners. As a result, in case D, the impacts of user-preferred disconnection is explored to demonstrate plug-and-play features.

The designed hybrid AC/DC microgrid model is an extended version of the university-based commercial hybrid AC/DC microgrid as presented in [17]. A simplified single-line diagram of the model is illustrated in Fig. 4.4. The AC subgrid consists of four DG units controlled by the conventional droop-control scheme [163] without any inter-unit communication. All DG units are connected to the AC bus through respective LCL filters. The DC subgrid is designed with four EV storages and one PV unit. The EV storages are connected to the DC bus through DC fast chargers which are controlled by the developed

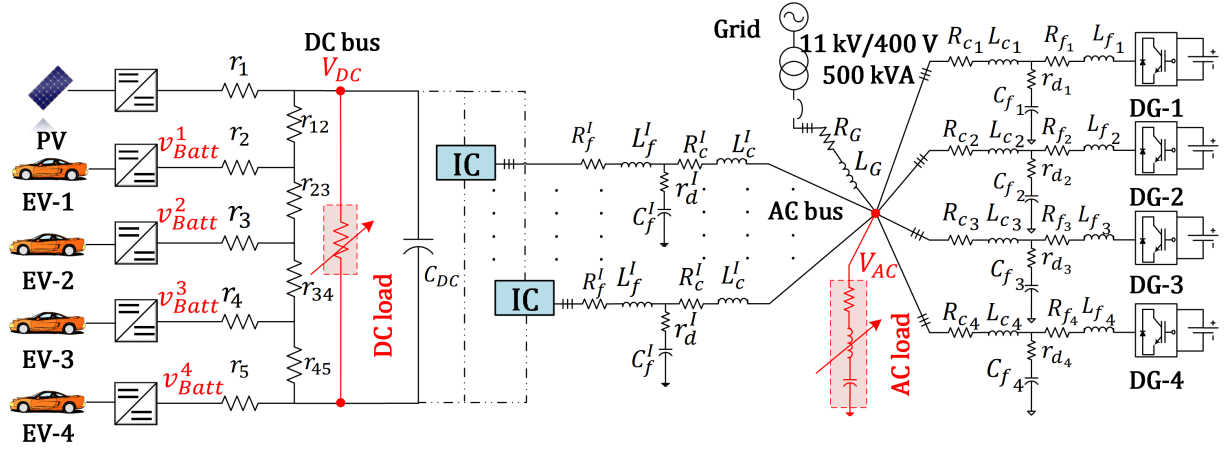


Figure 4.4: Single-line diagram of the test hybrid AC/DC microgrid.

distributed cooperative controllers. The bidirectional connectivity graph among the four EVs is shown in Fig. 4.5. The DC/DC converter of the PV unit is controlled by a maximum-power-point tracking (MPPT) controller. The DC bus is interfaced with the AC bus through the IC. DC loads are connected at the DC bus terminal and AC loads are connected at the AC bus terminal. The load profile as shown in Fig. 4.7 and the solar irradiation data used for the case studies of this chapter are obtained using OSI PI software that uses a centralized communication structure. The system parameters and ratings of all units are given in Table 4.1. Additional information regarding the hardware setups, communication protocols used for data collection and monitoring along with building schematics can be obtained from [17].

4.4.1 Case A: Step Load Change

The objective of this case study was to compare the performance of NDCS with the decentralized coordination of EVs under sudden load change. From $t = 0$ s to 4 s EVs were operating under the decentralized mode. During this period, the DC bus was loaded with 40 kW DC load. All EV converters were designed to generate or consume a

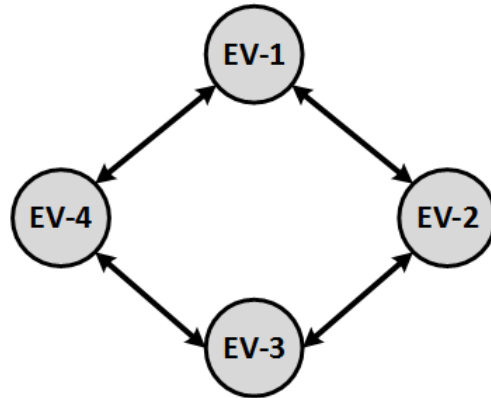


Figure 4.5: Communication graph of EVs.

Table 4.1: System parameters

Energy nodes			
PV	30 kW		
EV-(1,2,3,4)	24, 41, 30 and 23 kWh	Initial EV battery voltages, (v_{Batt}^1 , v_{Batt}^2 , v_{Batt}^3 and v_{Batt}^4)	465, 580, 500 and 520 V
DG-(1,2,3,4)	17 kVA		
Line parameters			
Nominal V_{AC}^{RMS}	240 V	L_f	10×10^{-3} H
V_{DC}^*	520 V	C_f	250×10^{-6} F
Frequency	50 Hz	R_c, R_G	0.03Ω
C_{DC}	150×10^{-4} F	L_c, L_G	3.5×10^{-4} H
R_f	$2 \times 10^{-3}\Omega$	r_d	0.65Ω
r_1, r_2, r_3, r_4	0.02Ω	$r_{12}, r_{23}, r_{34}, r_{45}$	0.05Ω
Control parameters			
Power controller		Voltage controller	
ω_c, ω_e	31.42, 314.16 rad/s	F	0.19
ω^*	314.16 rad/s	$K_{p(V)}$	0.11
D_P	3.14×10^{-4}	$K_{i(V)}$	2.2
D_Q	1.36×10^{-3}	Current controller	
k_e	1	$K_{p(I)}$	0.16
$K_{p(P)}$	2×10^{-5}	$K_{i(I)}$	200
$K_{d(P)}$	2×10^{-7}		
EV storage controller			
$K_{p(V)}^{DC}$	1.3	$K_{p(I)}^{DC}$	0.03
$K_{i(V)}^{DC}$	6	$K_{i(I)}^{DC}$	1.1
b_v	1.5		

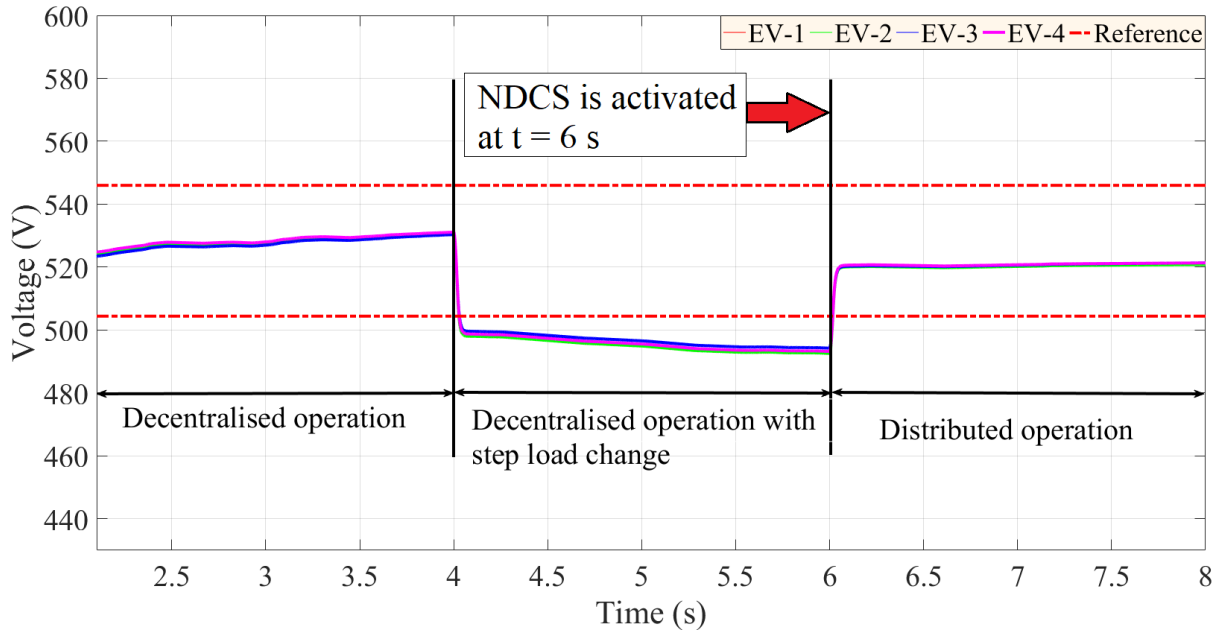


Figure 4.6: $v_{Batt}^1, v_{Batt}^2, v_{Batt}^3$ and v_{Batt}^4 for case A. At $t = 4$ s, a step load is applied at the DC bus for 2 s. At $t = 6$ s NDCS is activated to initiate the distributed operation.

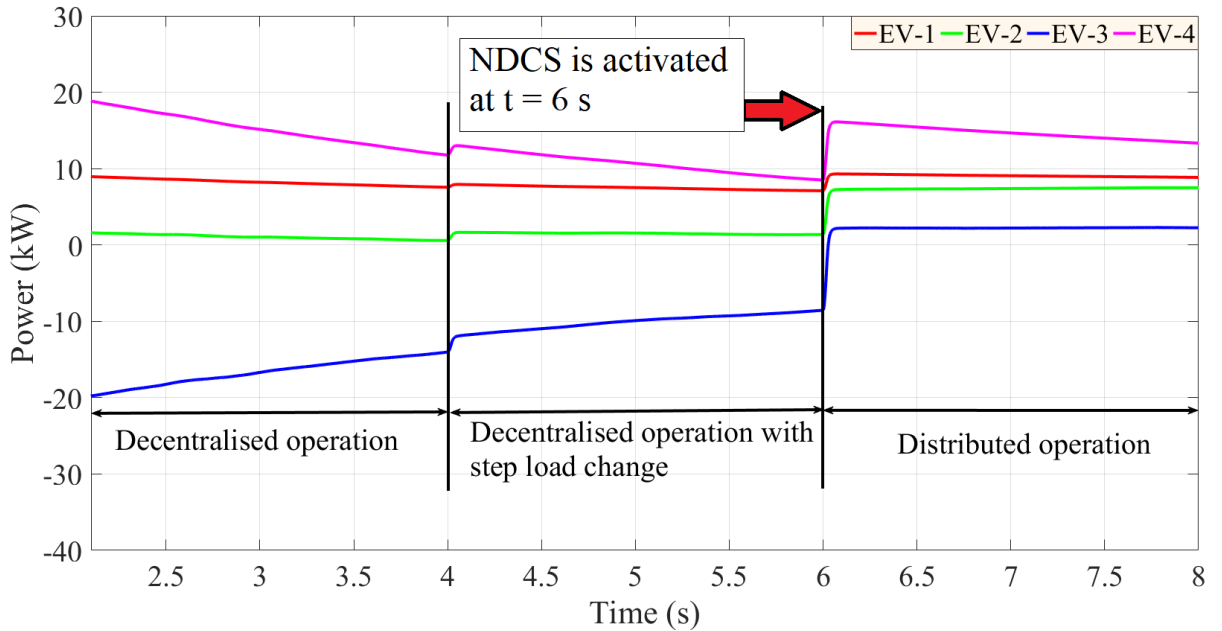


Figure 4.7: Power supplied or consumed by the EVs for case A. Saturation constraints were applied to ensure that the EV powers do not exceed the maximum allowable limit of ± 20 kW for both decentralized and distributed operation.

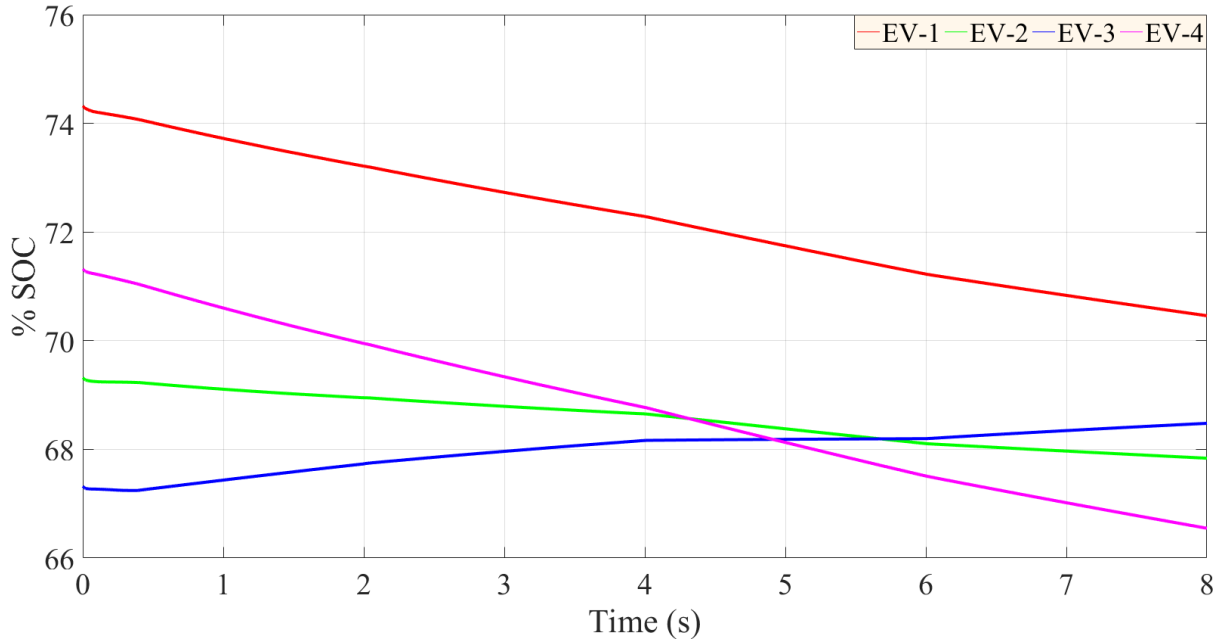


Figure 4.8: %SOC for all EVs for case A during both decentralized and distributed operation.

maximum of 20 kW power. As a result, the maximum and minimum saturation points for I_{DC}^* , as mentioned earlier, were chosen as ± 40 A. Over utilization of EV converters, particularly during decentralized operation, can be avoided by putting this limit in the current-control loops of EV converters. At $t = 4$ s, a step load of 25 kW was switched on for the duration of 2 s. As a result, the DC bus voltage dropped down below the lower reference level as shown in Fig. 4.6. The standard acceptable voltage ranges for the AC and DC bus voltages are shown in dotted red lines. The standard references for the AC bus voltage is in between 0.94 per-unit (pu) to 1.1 pu [80]. For the DC bus voltage, this range is in between -3% – +5% of the nominal voltage [17]. In order to restore the DC bus voltage to its reference value, at $t = 6$ s NDCS was activated. The objective of the NDCS was to provide regulation-up service by ensuring that all EVs generate additional power by discharging. The generated or consumed power of all EVs and their corresponding %SOC are shown in Fig. 4.7 and Fig. 4.8 respectively. As can be seen there, initially

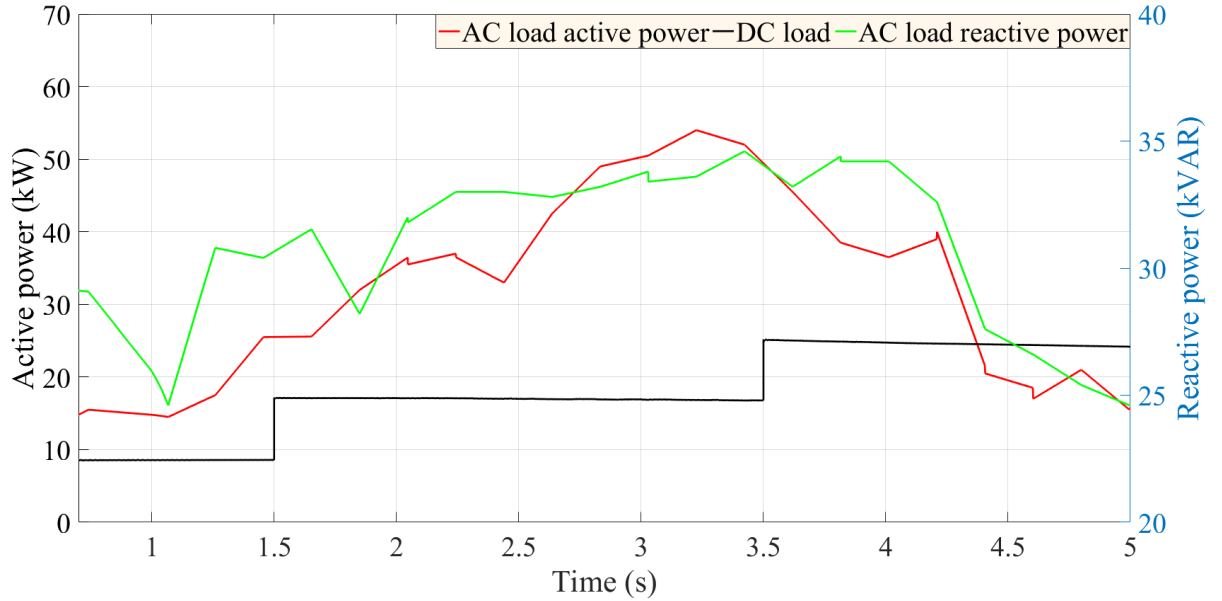


Figure 4.9: Commercial AC and DC load profiles

EV-1, EV-2 and EV-4 were in the discharging mode, whereas EV-3 was in the charging mode. When the NDCS was activated, all EVs including EV-3 checked their individual constraints and started discharging. This results in a restored DC bus voltage. Apart from the voltage restoration, it can be observed from Fig. 4.6 that NDCS demonstrates more stable DC bus voltage regulation capability than the decentralized operation.

4.4.2 Case B: Variable PV Generation and Commercial Loading

For case B, the islanded hybrid AC/DC microgrid was exposed to variable PV generation due to fluctuating irradiation. The main aim of this case study was to verify the performance of the designed controller under variable PV generation, as its output is random and variable in nature. The DC bus and AC bus were loaded with commercial load profiles as shown in Fig. 4.9. Both conditions (*i.e.* variable PV generation and load profile) were considered simultaneously to accurately represent a realistic scenario. The NDCS for the EV storages was activated at $t=0$ s. The communication links among neighbors

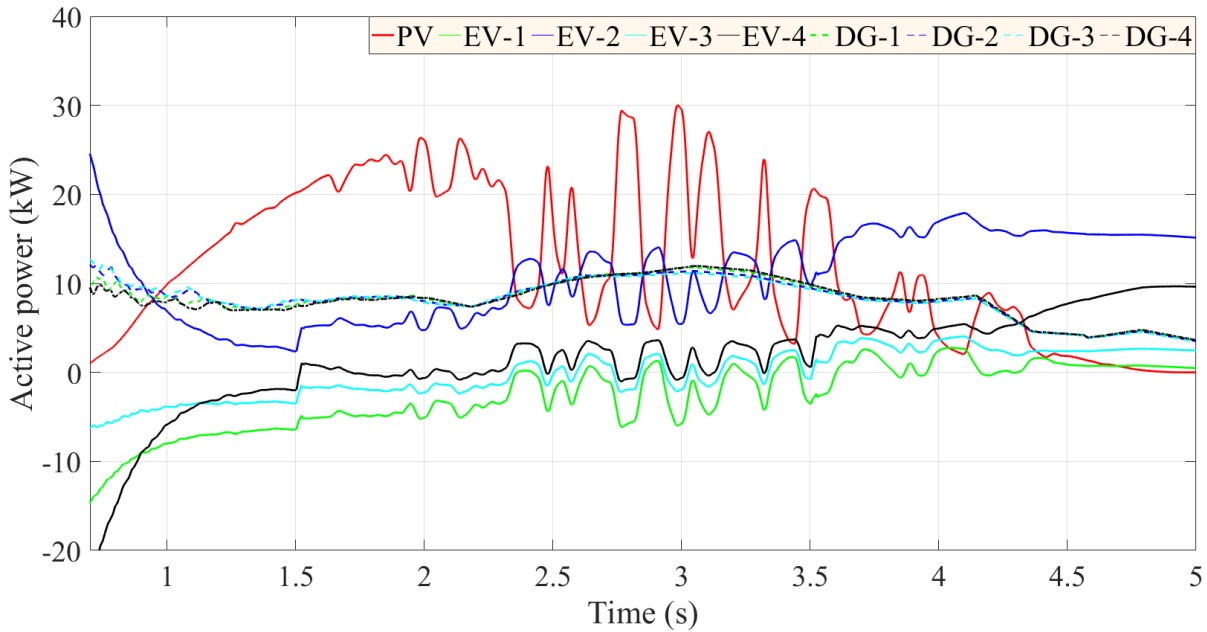


Figure 4.10: Varying output power of all DG units. DC type DG units are shown in solid lines and the AC type DG units are shown in dotted lines.

were considered ideal without time delay. The output active powers of all the DG units are shown in Fig. 4.10. The output powers of all the DG units at the AC side were alike because of their fixed droop coefficients. The output voltages of the EV storage converters and the AC bus RMS voltages are shown respectively in Fig. 4.11 and 4.12. It can be observed from Fig. 4.11 that, despite the differences in the initial terminal voltages, all of the EV storages eventually converged to the desired voltage level. Likewise, due to the coupling of the DC bus voltage with the AC bus RMS voltage, the convergence of the DC side voltage assists in controlling the AC bus RMS voltage to be within the acceptable range.

During islanded microgrid condition, it is important that all operating ICs should have four-quadrant operational capability. This means that the converter can transfer both active and reactive power in between two subgrids. As a result, the inverter will have four modes of operation (rectifier, inverter, capacitive and inductive modes). During

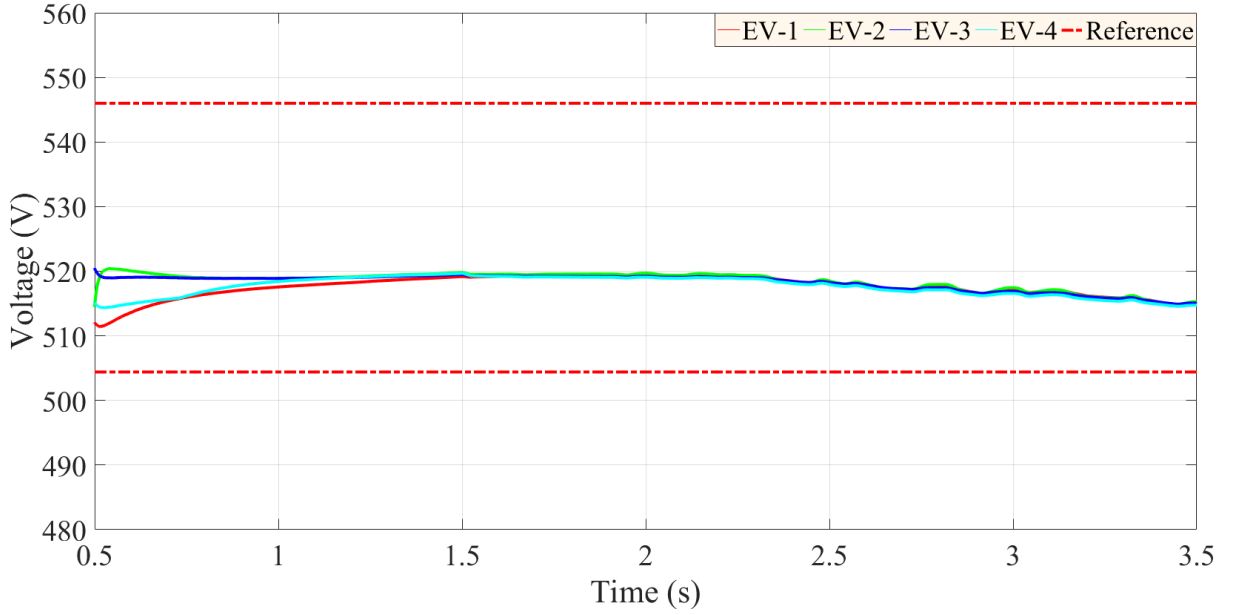


Figure 4.11: $v_{Batt}^1, v_{Batt}^2, v_{Batt}^3$ and v_{Batt}^4 for case B.

the rectifier mode, the inverter will transfer power to the DC subgrid from the AC subgrid, whereas, during the inverter mode it will transfer power to the AC subgrid from the DC subgrid. The normalized DC bus voltage for all the cases are shown in Fig. 4.17. The DC bus voltage for this case is shown in red in Fig. 4.17. It can be seen that the voltage is properly regulated through the proposed control scheme. The tracking performance of the proposed controller for the reactive power reference is shown in Fig. 4.14 in comparison with the conventional control scheme presented in [25]. It can be observed that the proposed controller provides superior reference-tracking performance without any steady-state error.

4.4.3 Case C: Effects of Time Delay

EV storage controllers need to withstand an obvious latency while operating under the distributed mode, which requires sparse communication among neighbors. The main purpose of this case study is to evaluate the controller performance under a communication

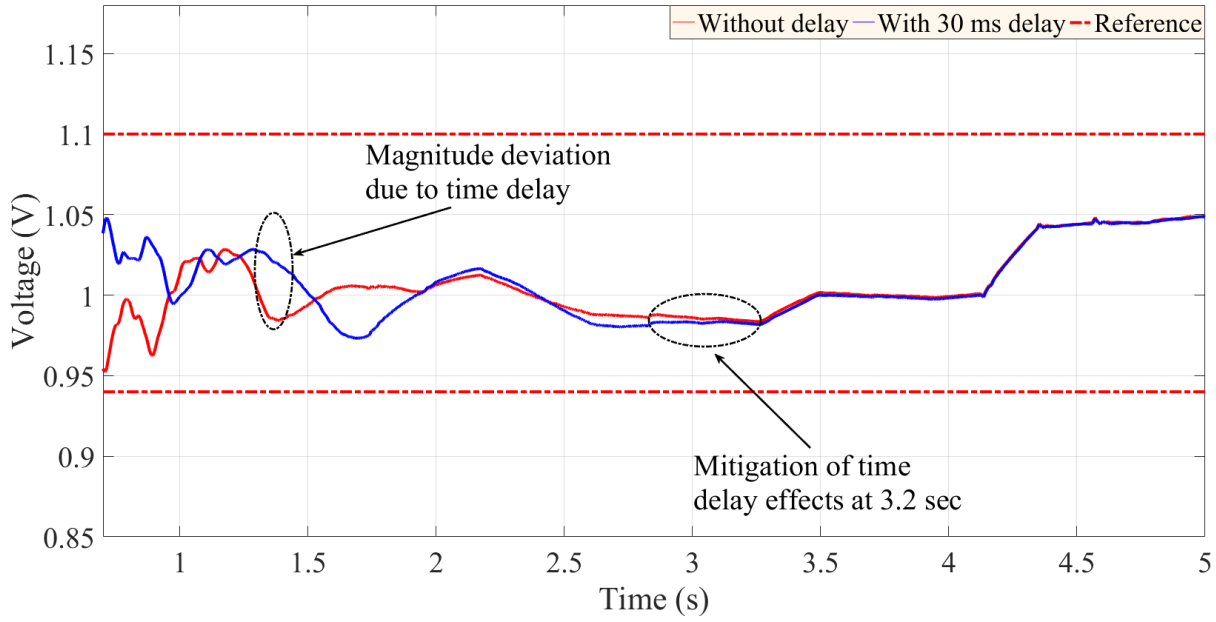


Figure 4.12: AC-bus RMS voltage case B (red) and case C (blue).

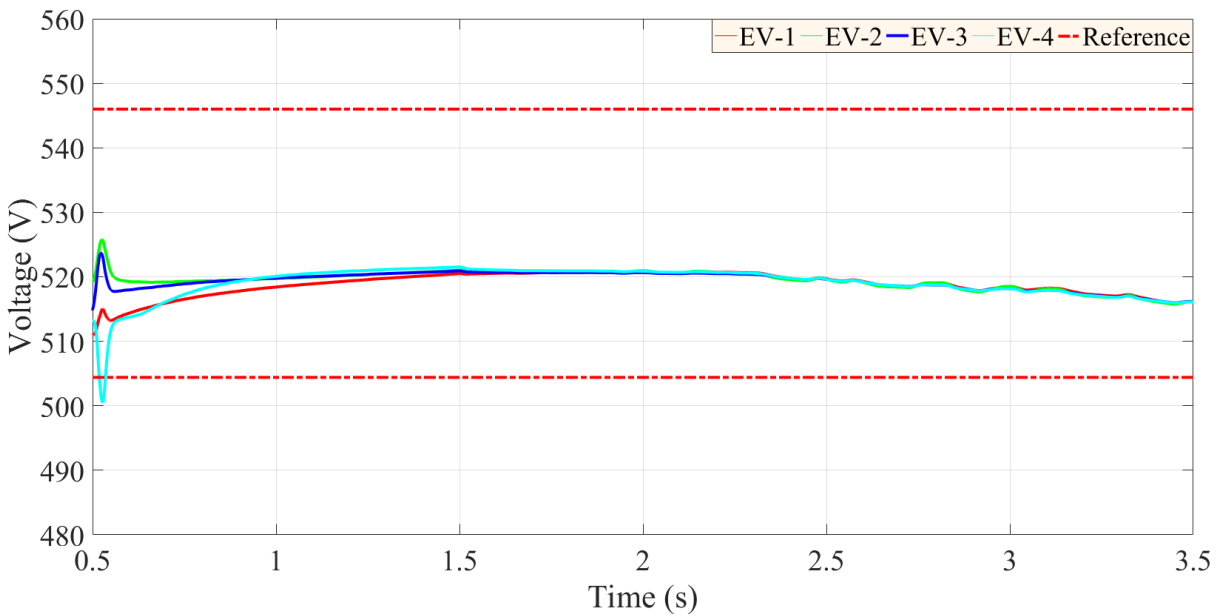


Figure 4.13: v^1_{Batt} , v^2_{Batt} , v^3_{Batt} and v^4_{Batt} for case C.

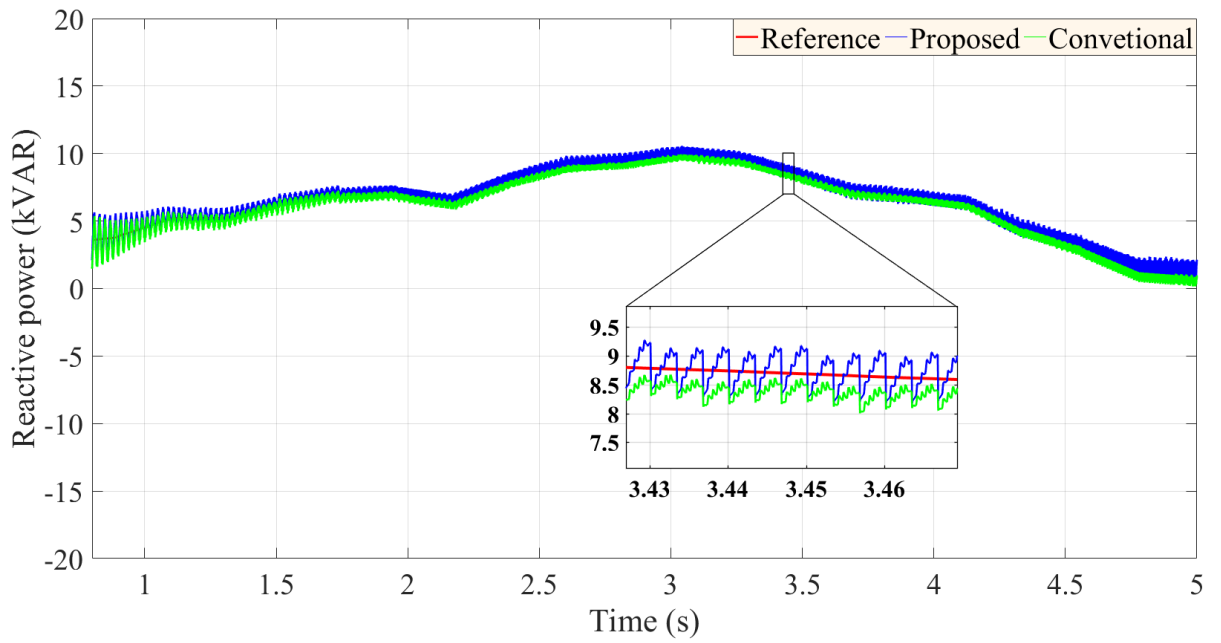


Figure 4.14: Reference-tracking performance of the proposed controller.

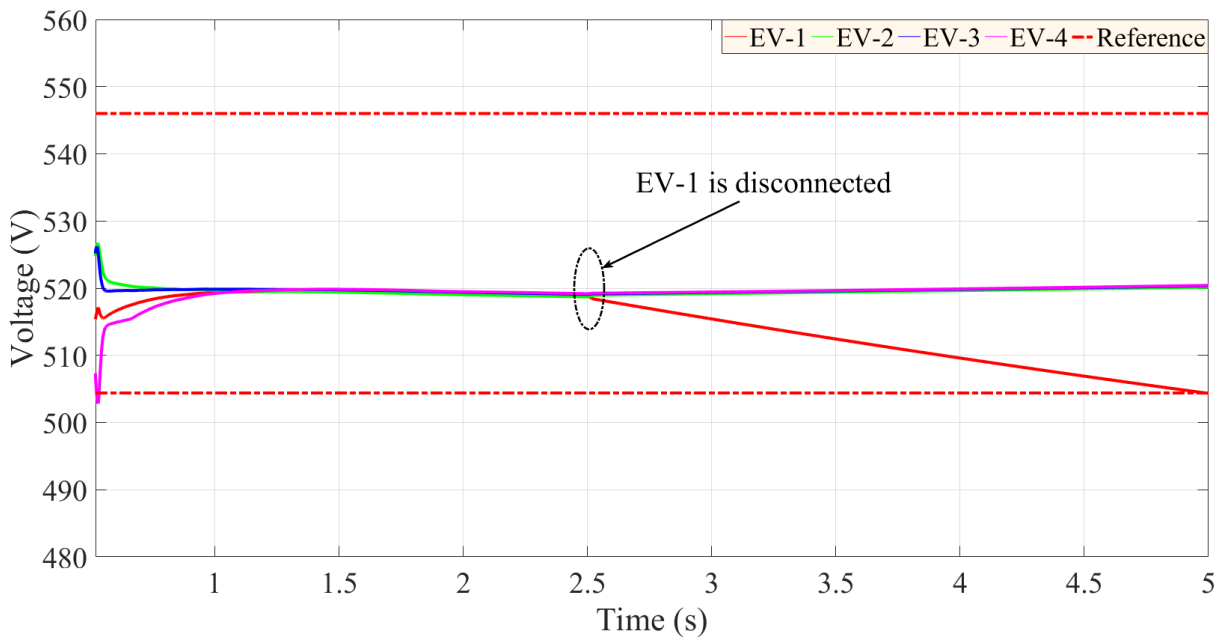


Figure 4.15: $v_{Batt}^1, v_{Batt}^2, v_{Batt}^3$ and v_{Batt}^4 for case D.

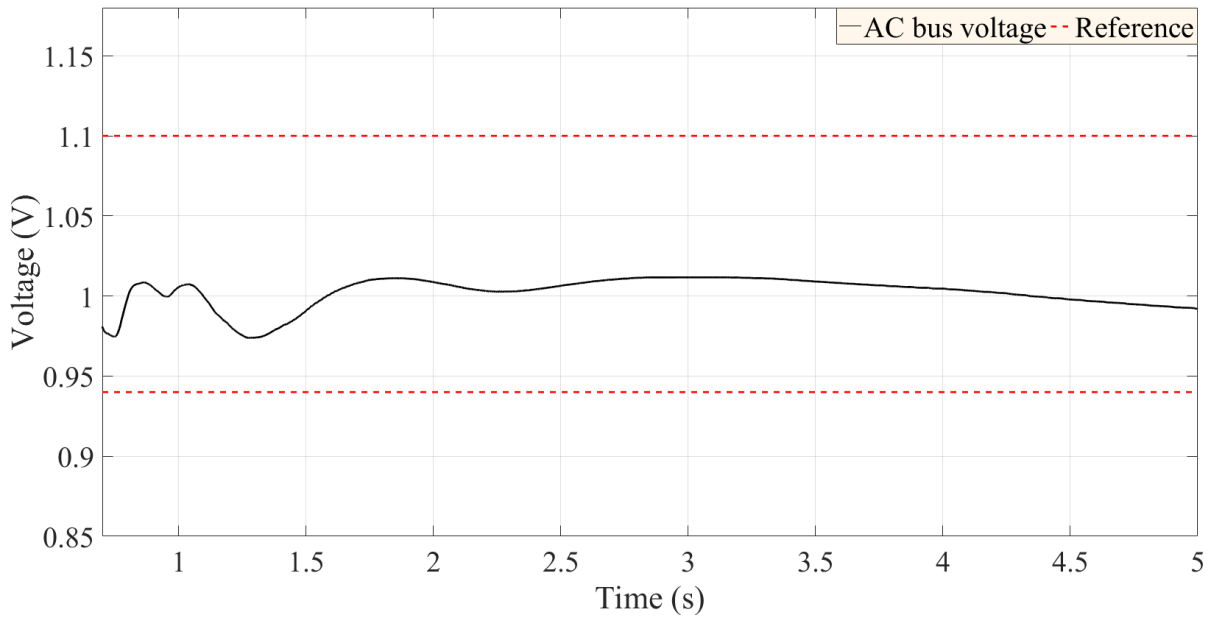


Figure 4.16: AC-bus RMS voltage for case D.

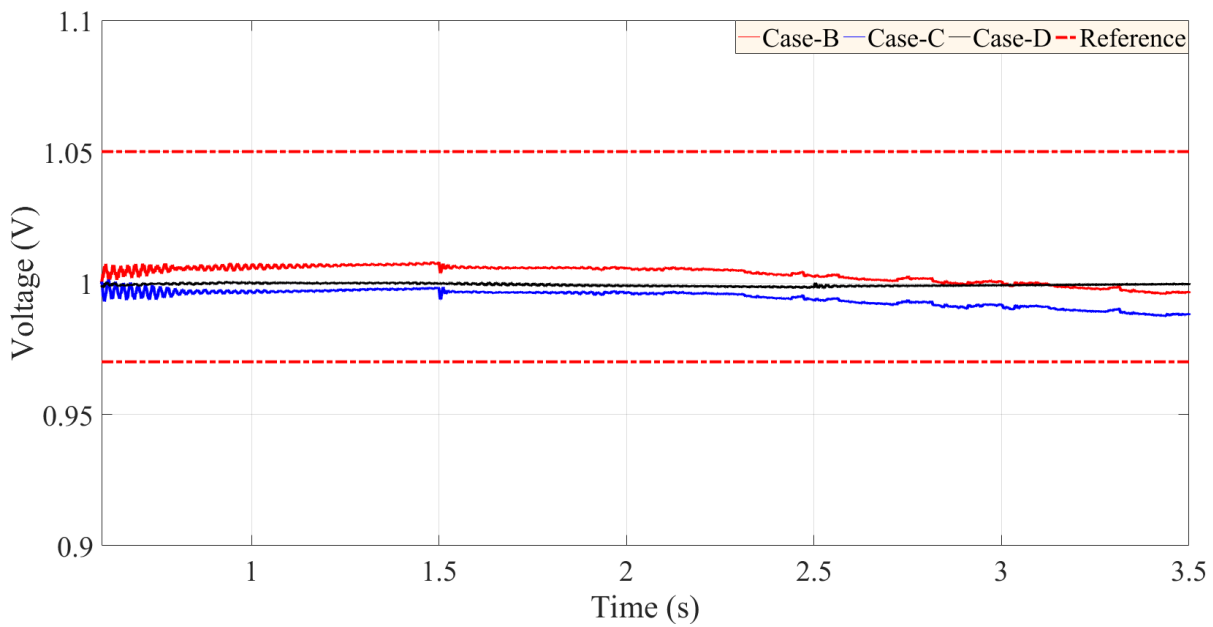


Figure 4.17: Normalized DC bus voltage for cases B, C and D.

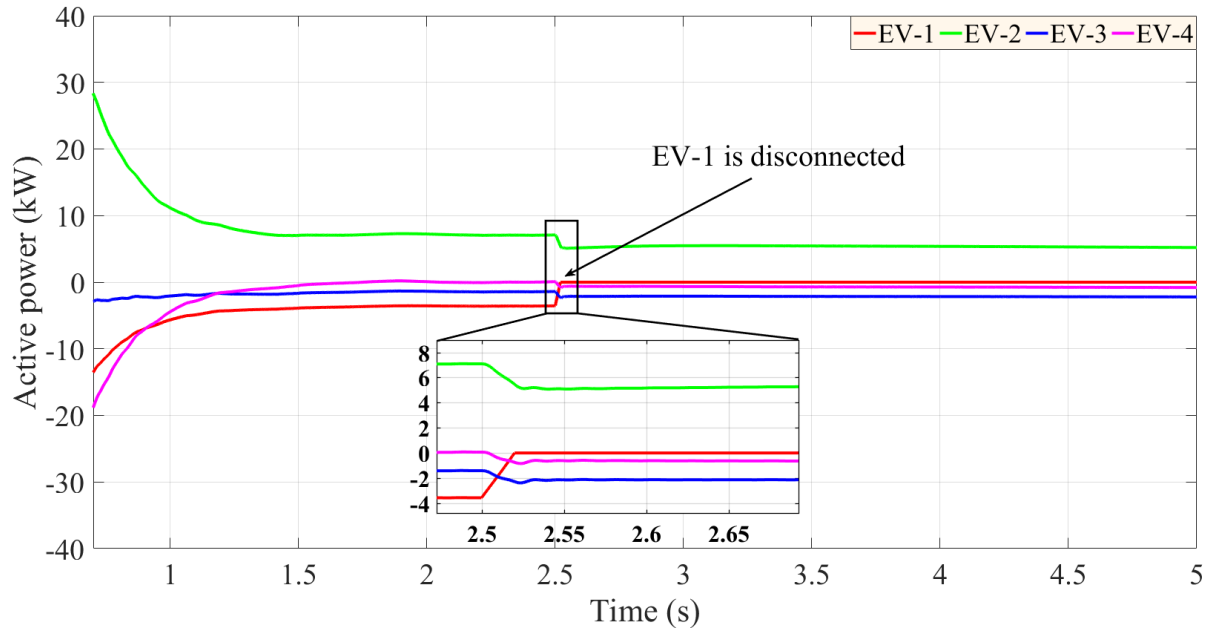


Figure 4.18: Output power of EV storages for case D.

time delay. It should be noted that the usual communication delays for WiFi-based networks are typically 20 ms [179]. However, for this case study a 30 ms time delay was assumed and the effects on the controller performance were observed. NDCS were considered active at $t = 0$ s. The AC bus RMS voltage for this case is shown in blue color in Fig. 4.12. Fig. 4.13 presents the output voltages of the EV storages for this case study. The output voltages of all EVs took approximately 1.5 s to converge when the time delay is 30 ms. It can be observed from Fig. 4.13 that due to the 30 ms delay there were slight magnitude deviations in the beginning for the voltages of the EV storages, which also impacted the AC bus voltage as shown in Fig. 4.12. Nevertheless, the AC bus voltage remained in acceptable range as shown in Fig. 4.12. The DC bus voltage also maintained the acceptable range for this case as presented in Fig. 4.17 in blue color. It should be noted that the performance of the controller in terms of convergence speed can be further improved by increasing the level of connectivity. However, this will increase the communication-based cost [177]. Overall, it is evident from the result that both the

IC controller and the distributed cooperative controller are robust to time-delay effects.

4.4.4 Case D: User-Preferred Disconnection

The objective of this case study is to evaluate the controller performance when participating EV users disconnect the V2G service without sending any notification signal. The controller should work in a dynamic condition where EV owners will have the flexibility to include or exclude their EVs for V2G operations. For this case study, both types of loads were kept constant. For the AC load a fixed $70 \text{ kW} + j30 \text{ kvar}$ was used and for the DC load a fixed 30 kW was used.

The NDCS was activated at the beginning of the simulation. At $t = 2.5 \text{ s}$, user of EV-1 decided to disconnect the V2G service while EV-2, EV-3 and EV-4 was active under the NDCS. The output voltages of EV storages maintain the required voltage level as shown in Fig. 4.15 to regulate the DC-bus voltage as shown in black in Fig. 4.17. As the DC bus voltage is properly regulated, it keeps the AC-bus RMS voltage within the acceptable limit as presented in Fig. 4.16. The output powers of the EVs for this case study are shown in Fig. 4.18. It can be observed that the output power of EV-1 becomes zero when disconnected. However, the load, EV-3 and EV-4, is supported partially by the high-capacity EV storage EV-2. The rest of the power is exported from the AC subgrid for this particular case.

4.4.5 Case E: Performance Evaluation under Faults

The robustness of the proposed distributed controller was evaluated under two types of fault scenario. At first, a short circuit fault was applied at the DC bus at $t = 3 \text{ s}$ for the duration of 30 ms . During that period, the DC bus was loaded with 55 kW and the AC bus was loaded with $200 \text{ kW} + j70 \text{ kvar}$. The load current at the DC bus experienced a spike due to the fault condition as shown in Fig. 4.19a. Due to the fault at the

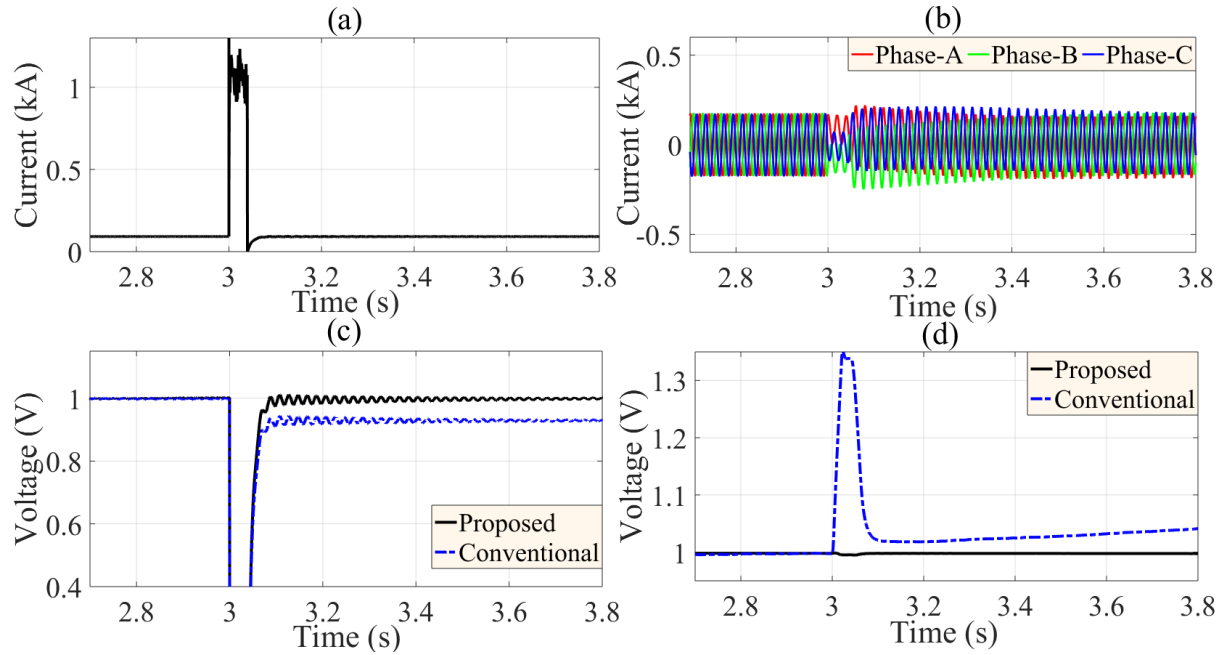


Figure 4.19: Performance evaluation of the proposed scheme under the DC short circuit fault for case E. The fault was applied at $t = 3$ s for the duration of 40 ms. (a) Load current at the DC bus. (b) Load current at the AC bus. (c) Normalized DC bus voltage with the proposed distributed controller (solid black) and with the conventional decentralized controller (dotted blue). (d) AC bus RMS voltage in per unit (pu) with the proposed distributed controller (solid black) and with conventional decentralized controller (dotted blue).

DC terminal, the load current at the AC bus was temporarily affected as presented in Fig. 4.19b. Figs. 4.19c and 4.19d represent the DC bus voltage and the AC bus RMS voltage respectively for this case study. Voltages are shown with the solid black line for the proposed distributed controller and with the dotted blue line for the conventional decentralized controller. As compared to the conventional decentralized controller, the proposed distributed controller effectively performs post-fault voltage regulation for both AC and DC bus voltages with zero steady state error.

The performance of the proposed controller was further validated under three-phase

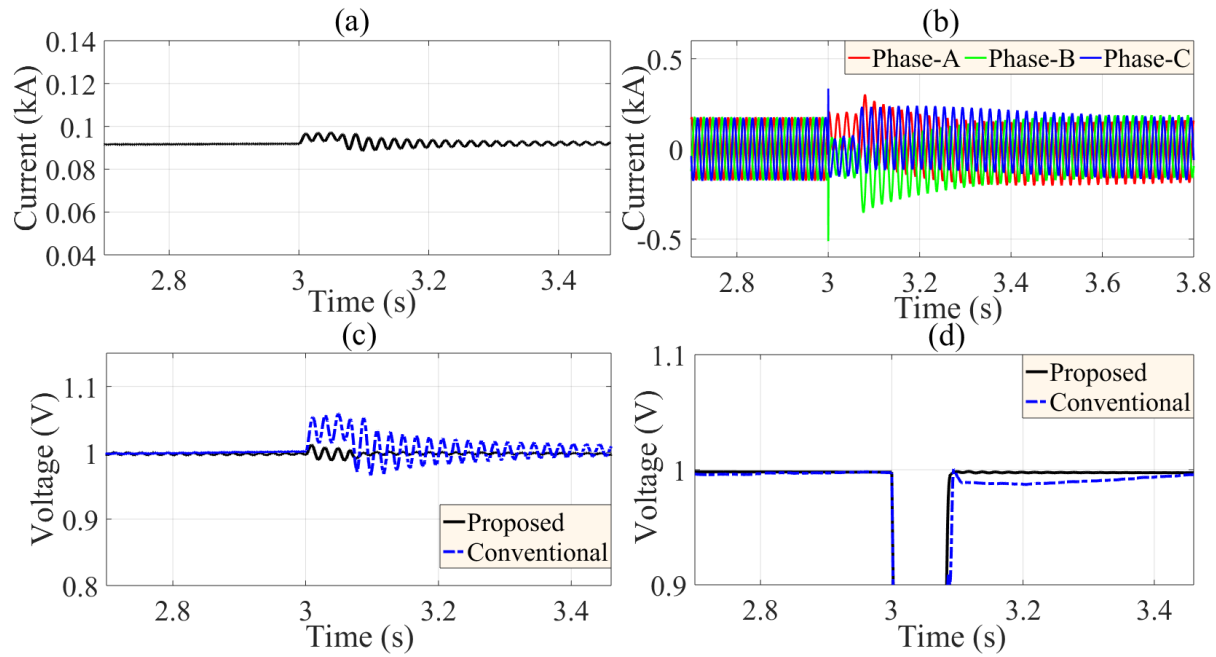


Figure 4.20: Performance evaluation of the proposed scheme under three-phase AC symmetric fault for case E. The fault was applied at $t = 3$ s for the duration 60 ms (a) Load current at the DC bus. (b) Load current at the AC bus. (c) Normalized DC bus voltage with the proposed distributed controller (solid black) and with the conventional decentralized controller (dotted blue). (d) AC bus RMS voltage in per unit (pu) with the proposed distributed controller (solid black) and with conventional decentralized controller (dotted blue).

symmetric fault applied at the AC bus. The fault was applied at $t = 3$ s for the period of 60 ms (3 cycles for a 50 Hz system). The loading conditions for both buses were kept the same. The load current at the DC bus and the AC bus are shown in Figs. 4.20a and 4.20b. The DC and the AC bus RMS voltages for this case study are shown in Figs. 4.20c and 4.20d. Both voltages are marked with solid black and dotted blue lines respectively for the proposed distributed controller and the conventional decentralized controller. It is evident from Figs. 4.20c and 4.20d that both bus voltages are effectively regulated when the fault is cleared. The conventional decentralized controller exhibited oscillatory performance for the DC bus voltage and higher settling time for the AC bus RMS voltage as compared to the proposed distributed controller.

4.5 Chapter Summary

This chapter presents a novel algorithm to coordinate EV storages in a commercial hybrid AC/DC microgrid. Based on the DC-bus voltage condition, the algorithm switches the coordination among multiple EV storages from decentralized to distributed mode or vice versa. Firstly, the conventional IC control topology is enhanced by using a combination of the PD-compensating power-droop and voltage-droop control schemes. This development ensures improved transient response along with the coupling between the AC-bus RMS voltage and the DC-bus voltage. This results in the capability of regulating one bus voltage by regulating the other. Secondly, a mode-changing EV storage controller is designed which can operate in decentralized or distributed mode. Finally, a new coordination strategy namely NDCS, is proposed that ensures when and how long the EV storages need to operate in distributed mode to regulate the DC bus voltage. The NDCS also takes into account the storage and converter capacities along with the user preferences for both decentralized and distributed operation. Case studies are carried out to demonstrate

the performance of the developed controller under concurrent variable PV generation and commercial loading. The effects of time delay and user-preferred disconnection of operating EVs are explored through case studies. It is evident from the comparative analysis that the developed controller operated by NDCS can provide robust performance for voltage regulation and power sharing within a hybrid AC/DC microgrid.

Considering the economic aspects, in the next chapter, real-time optimization techniques are incorporated with the distributed EV storage control topology.

Chapter 5

V2M via Optimization-Incorporated Distributed EV Coordination Strategies

An improved vehicle-to-microgrid (V2M) framework is proposed for a commercial locality operating as a hybrid alternating-current (AC) / direct-current (DC) microgrid, which optimally coordinates electric-vehicle (EV) storages in a distributed manner. An aggregator model is proposed that solves the economic dispatch problem of parked EV storages in a centralized manner and generates the power reference for the designed distributed EV storage controller. The proposed optimization-incorporated distributed controller (ODC) for the EV storages ensures DC bus voltage regulation by supplying the demand in a cost-effective way by utilizing a sparse vehicle-to-vehicle (V2V) communication network. The power flow between the AC and DC subgrids is managed by interlinking converters (IC). The IC control structure is augmented by combining voltage- and power-based droop-control schemes in the power-control loop. This modification enables simultaneous AC and DC bus voltage regulation. Case studies are carried out to validate the efficacy of

the developed framework with a real commercial network and loads. The results exhibit robust performance of the overall system for generation-demand variability, transitions between islanded and grid-tied conditions, and user-preferred EV disconnections and time delay.

5.1 Introduction

The concept of a direct-current (DC) power distribution network is gaining momentum due to the increased number of photovoltaic (PV) installations along with the rapid growth in electric vehicles (EV) as promising energy storage systems (ESS). The DC distribution system can provide a cost-effective solution to integrate DC technologies such as light-emitting diodes (LED), DC motors, data centers etc. with minimum conversion losses. Commercial buildings, that consume nearly 61% of the total electric energy in the United States, are emerging as zero-net energy (ZNE) buildings by adopting DC distribution systems [180]. As a result, islanded DC distribution systems or inter-tied DC microgrids are possible by expanding the capacities of rooftop PV and ESS in commercial buildings. However, the installation of a DC-only distribution system is unlikely in the near future due to the AC-dominated legacy electric system. Therefore, an intermediate solution would be hybrid AC/DC microgrids [24, 25]. Hybrid microgrids combine the aptness of both AC and DC systems. They have emerged with advantages such as minimum AC/DC conversion loss, increased efficiency, and reduced voltage synchronization effort, to ensure improved connectivity for AC and DC technologies [50, 160]. However, they come along with convoluted network and control topologies. Due to the intricate nature of their structures and control methodologies, hybrid microgrids are well suited for commercial neighborhood rather than residential localities.

Contemporary commercial buildings are equipped with state-of-the-art technologies

such as smart EV parks, intelligent power-electronic-interfaced variable-speed drives (VSDs), four-quadrant inverters and smart high-voltage air-conditioning (HVAC) systems. Utilizing these technologies, commercial buildings can contribute to both electric power grids and the electricity market by providing ancillary services [16]. However, coordination among multiple technologies such as EV storages is a difficult task, particularly when these buildings are operating as autonomous microgrids. Furthermore, peak load for commercial areas occurs during mid-daytime; therefore, parked EV storages in commercial neighborhoods can be utilized to provide ancillary services during office hours, which typically range between 9:00 am to 6:30 pm [17, 18]. Considering the above-mentioned possibilities of vehicle-to-microgrid (V2M) application in commercial vicinities, several pieces of literature have explored this research area. In [19], an economic analysis is presented to show the feasibility of using EV storages in commercial-building microgrids. An energy-management system (EMS) for a building with PV units and EV storages is presented in [20], designed to minimize the operating cost considering different charging and discharging profiles. A real-time peak-shaving model to reduce high peak demand combining demand response and load control is presented in [21]. A four-stage optimization algorithm is proposed in [22] for a PV-assisted EV charging station in a commercial building to minimize operation costs associated with customer satisfaction by the optimal scheduling of EV storages. However, all the optimization approaches to coordinate EV storages for V2M operations follows either the hourly or the daily forecasting methods. As a result, these approaches are only suitable for the planning purposes of the V2M. Conversely, a dynamic framework to ensure EV coordination in conjunction with the real-time optimization technique can provide both technical and economic optimality.

The V2M connection can be achieved by centralized, decentralized or distributed approaches for AC, DC or hybrid AC/DC microgrids. The centralized structure provides improved controllability with reduced scalability. The decentralized structure ensures

modularity, however, optimal operation cannot be guaranteed due to the limited information exchange among units. Conversely, a distributed structure combines the advantages of both centralized and decentralized structures. As a result, distributed control in microgrids with EV storages is gaining momentum. Distributed controllers are developed for AC microgrids [74, 102], for DC microgrids [165–167] and for hybrid AC/DC microgrids [18, 181]. The application of distributed control for ESS is presented in [80, 170–173] to achieve voltage control, state-of-charge balancing and power-sharing considering time delays and uncertainties in PV output power generation. However, these analyses do not specifically concentrate on commercial-grade V2M applications, and the concept of incorporating a solution for the EV economic dispatch problem in their real-time control has not been explored. Some recent work [182, 183], has attempted to unify optimization-based economic dispatch with real-time distributed control for DC microgrids. However, their feasibility and efficacy for hybrid-microgrid operations are not explored. Moreover, from a realistic point of a view, an EV aggregator would like to have a certain control over the EV storages under its operational vicinity, but at the same time, EV storages are parked in a spatially dispersed form. Therefore, from the perspective of an EV aggregator and EV owners, a combination of the centralized and distributed control framework would be an optimal approach for commercial-grade V2M operation.

Considering all the above issues, this chapter presents a novel V2M framework suitable for commercial neighborhoods. The framework involves three core components: (i) a centralized EV economic-dispatch optimizer, (ii) a distributed EV storage controller and (iii) an interlinking converter (IC) with modified control topology. The optimizer generates the reference power for each EV storage as a function of the incremental cost (λ) by solving an economic dispatch problem. Later, it adjusts the power reference accordingly, which ensures proper power management within the microgrid through a cost-effective and distributed vehicle-to-grid (V2G) operation. The IC is responsible to control the

power flow between the AC and DC subgrids. The IC control topology is augmented by combining the voltage-based droop- [174,175] and power-based droop-control techniques. This augmentation enables simultaneous AC and DC bus voltage regulation without affecting the power-sharing capabilities of the converter. Overall, the salient contributions of this chapter can be summarized as follows:

1. An aggregator model is developed that provides a centralized solution for the EV economic dispatch problem considering a bounded EV output power. The aggregator/optimizer generates a reference power signal for the designed distributed controller. A generalized mathematical expression of the optimal reference power is presented as a function of the optimal incremental cost, defined by the slope of the cost function.
2. A distributed EV storage controller is designed that can operate in both decentralized and distributed manner based on a situation-aware signal. The designed controller communicates with other neighboring EV units through a sparse communication network with a spanning tree to exchange output-power information. Later, it utilizes a local voting protocol for dynamic averaging.
3. In order to ensure voltage regulation and to maintain power flow between the AC and DC subgrids, a modified IC control strategy combining power- and voltage-based droop techniques is developed. The transient performance of the IC is further enhanced by utilizing a proportional-derivative (PD) controller within the power-control loop of the IC as proposed in [176]. This approach facilitates a smooth transition between islanded and grid-tied microgrid operation.

The remainder of the chapter is organized as follows: Section 5.2 presents the proposed V2M framework, which includes a description of the optimizer operating as a centralized EV aggregator, the distributed EV storage controller and the IC controller. Case studies

5.2 Proposed V2M framework

5.2.1 EV Economic-Dispatch Problem Formulation

During V2G operation within a hybrid AC/DC microgrid, EV units operate as dispatchable sources. With a view to minimizing the generation cost of EV units while preserving all other flexibilities, the optimization problem can be formulated as similar to that of a conventional power system. Now let us consider that the aggregated cost function, $C(p)$ of N EV storages operating in V2G mode is a quadratic function of their corresponding output powers with coefficients of α , β and γ . Therefore, the optimization problem for EV economic dispatch can be presented as follows [182]:

$$\begin{aligned}
 \min \quad & C(p) = \sum_{n \in N} \alpha_n + \beta_n p_n + \gamma_n p_n^2 \\
 \text{s.t.} \quad & G = \sum_{n \in N} = P_{total}^{load} - P_{total}^{gen}, \quad n = 1, 2, \dots, N., \\
 & H_1 = -p_n + p_n^{min} \leq 0, \\
 & H_2 = p_n - p_n^{max} \leq 0
 \end{aligned} \tag{5.1}$$

where, $P_{total}^{load} = \sum S_{AC}^{load} + \sum P_{DC}^{load}$,

$P_{total}^{gen} = \sum S_{AC}^{gen} + \sum P_{DC}^{gen}$,

$\sum S_{AC}^{load}$ = the aggregated demand of the apparent power by AC loads,

$\sum P_{DC}^{load}$ = the aggregated demand of the active power by DC loads,

$\sum S_{AC}^{gen}$ = the aggregated apparent power generated by dispatchable AC sources,

$\sum P_{DC}^{gen}$ = the aggregated active power generated by non-dispatchable DC sources,

p_n^{max} and p_n^{min} = the allowable maximum and minimum power of the n th EV storage respectively.

Therefore, the economic dispatch problem can be formulated as a Lagrange function with Lagrange (λ) and Karush–Kuhn–Tucker (KKT) multipliers (μ_1 and μ_2) for each EV

storage as below

$$L(p_n, \lambda, \mu_1, \mu_2) = C(p) + \lambda G + \mu_1 H_1 + \mu_2 H_2 \quad (5.2)$$

The solution of the aforementioned optimization problem is a stationary point where the partial derivative of $L(p_n, \lambda)$ is zero with respect to all variables. Now, for the time being, if we neglect the EV output power constraints H_1 and H_2 then

$$\begin{aligned} \frac{\partial L}{\partial p_n} &= \frac{\partial C(p)}{\partial p_n} - \lambda = 0 \\ \implies \lambda &= \frac{\partial C(p)}{\partial p_n} = \beta_n + 2\gamma_n p_n \end{aligned} \quad (5.3)$$

In order to achieve optimality, it is necessary that the Lagrange multiplier or the incremental cost (λ) of each EV storage converges to the optimal incremental cost (λ^*). This convergence can be achieved only when all EV storages generate the optimal power (p_n^*). Considering small perturbations of both AC and DC load demands, the optimal output power of each EV storage can be obtained with simple mathematical manipulation of (5.3), as below [184]

$$\begin{cases} \lambda^* = \frac{\Delta \mathcal{P} + \sum_{n \in N} \frac{\beta_n}{2\gamma_n}}{\sum_{n \in N} \frac{1}{2\gamma_n}} \\ p_n^* = \frac{\lambda^* - \beta_n}{2\gamma_n} \end{cases} \quad (5.4)$$

where, $\Delta \mathcal{P} = P_{total}^{gen} - P_{total}^{load}$. Moreover, by considering the output power constraints, the necessary minimum-cost operating condition can be extended to represent the reference power for the distributed EV storage controller.

$$p_n^{ref} = \begin{cases} p_n^* & \text{for } p_n^{min} \leq p_n \leq p_n^{max} \\ p_n^{min} & \text{for } p_n \leq p_n^{min} \\ p_n^{max} & \text{for } p_n \geq p_n^{max} \end{cases} \quad (5.5)$$

5.2.2 Optimization-Incorporated Distributed Control (ODC) for EV Storages

Let us consider a commercial neighborhood operating as a hybrid microgrid with N V2G-capable EV storages. Additionally, all active EV storages communicate through a sparse communication network with each other. The interaction among active EV storages can be represented via a weighted directed graph (digraph). The interconnection nodes can be represented by $\mathcal{G} = (\mathcal{V}_{\mathcal{G}}, \mathcal{E}_{\mathcal{G}}, \mathcal{A}_{\mathcal{G}})$, where $\mathcal{V}_{\mathcal{G}} = \{\mathcal{V}_1, \mathcal{V}_2, \mathcal{V}_3, \dots, \mathcal{V}_n\}$ is the set of all nodes, $\mathcal{E}_{\mathcal{G}} \subset \mathcal{V}_{\mathcal{G}} \times \mathcal{V}_{\mathcal{G}}$ is the set of pairs of nodes also known as edges, and $\mathcal{A}_{\mathcal{G}} = [a_{ij}]_{N \times N}$ is the weighted adjacency matrix of dimension $N \times N$ that gives information regarding the interconnectivity of nodes. The communication between node i and node j can be presented as follows:

$$a_{i \times j} = \begin{cases} 1 & \text{if } (i, j) \in \mathcal{E}_{\mathcal{G}} \\ 0 & \text{otherwise} \end{cases} \quad (5.6)$$

The in-degree matrix is defined as $D_G^{in} = \text{diag}\{d_i^{in}\}$, i.e. the diagonal matrix of $d_i^{in} = \sum_{j=0}^n a_{ij}$. Likewise the out-degree matrix is defined as $D_G^{out} = \text{diag}\{d_i^{out}\}$, i.e. the diagonal matrix of $d_i^{out} = \sum_{i=0}^n a_{ji}$. The Laplacian matrix $\mathcal{L}_{\mathcal{G}}$, defined as $\mathcal{L}_{\mathcal{G}} = D_G^{in} - \mathcal{A}_{\mathcal{G}}$, provides useful insights regarding the stability of the communication network. For an undirected communication network with bidirectional information flow, $D_G = D_G^{out} = D_G^{in}$, which results in $\mathcal{L}_{\mathcal{G}}$ being *balanced* for this particular case [59].

All EV storages are designed with the local voting protocol shown in Fig. 5.1a. This protocol uses local information of the n th EV storage and the information observed from its neighbors to converge to an average output power u_p^n , given by

$$u_p^n(t) = p_{EV}^n(t) + \psi_p b_p \int_0^t \sum_{j \in N} a_{n \times j} (p_{EV}^j(\tau) - u_p^n(\tau)) d\tau \quad (5.7)$$

where p_{EV}^n = measured output power of n^{th} EV storage,

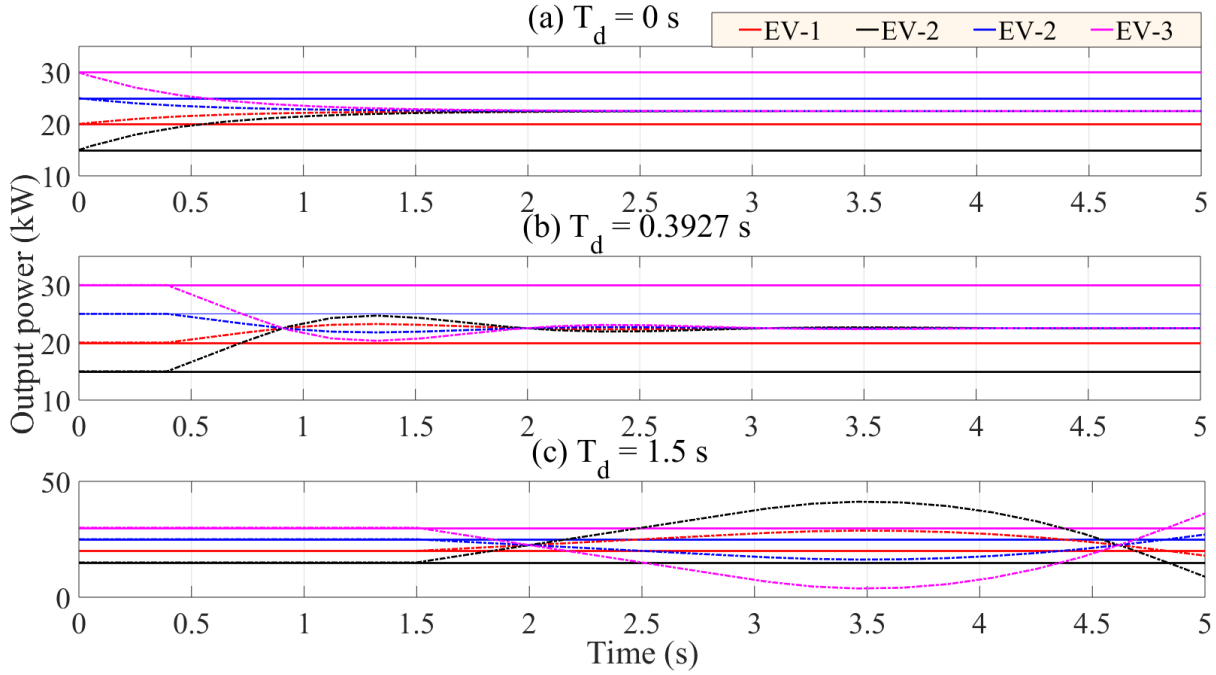


Figure 5.2: Convergence of output powers with the distributed controller for various time delays. (a) Time delay, $T_d = 0$ s. (b) Time delay, $T_d = 0.3927$ s. (c) Time delay, $T_d = 1.5$ s. Dotted lines are the outputs measured from the distributed controller

ψ_p = acknowledgement signal for the distributed operation which is governed by the need-based distributed coordination strategy (NDCS) [18],

b_p = coupling gain of the cooperative control loop.

The local voting protocol ensures that the output power of all EV storages for any step changes will converge at an average value of the neighboring units at $t \rightarrow \infty$, considering a spanning tree is present and the communication delay (T_d) satisfies the condition [177]

$$T_d \leq \frac{\pi}{2 \max(\text{eig}(\mathcal{L}_G))} \quad (5.8)$$

Now by introducing an uniform time delay of T_d in (5.7), the following relation can be obtained

$$u_p^n(t) = p_{EV}^n(t) + \psi_p b_p \int_0^t e^{-T_d \tau} \sum_{j \in N} a_{n \times j} (p_{EV}^j(\tau) - u_p^n(\tau)) d\tau \quad (5.9)$$

Example: let us consider that the output powers of four EV storages for any instant are 20 kW, 15 kW, 25 kW and 30 kW – represented by EV-1, EV-2, EV-3 and EV-4 respectively. The communication network illustrated in Fig. 5.3 can be presented as follows:

$$\mathcal{A}_{\mathcal{G}} = \begin{bmatrix} 0 & 1 & 0 & 1 \\ 1 & 0 & 1 & 0 \\ 0 & 1 & 0 & 1 \\ 1 & 0 & 1 & 0 \end{bmatrix}; \mathcal{D}_{\mathcal{G}} = \begin{bmatrix} 2 & 0 & 0 & 0 \\ 0 & 2 & 0 & 0 \\ 0 & 0 & 2 & 0 \\ 0 & 0 & 0 & 2 \end{bmatrix};$$

$$\mathcal{L}_{\mathcal{G}} = \begin{bmatrix} 2 & -1 & 0 & -1 \\ -1 & 2 & -1 & 0 \\ 0 & -1 & 2 & -1 \\ -1 & 0 & -1 & 2 \end{bmatrix}.$$

Therefore, the output power of all EV storages will converge to an average consensus value of 22.5 kW following (5.7) as long as the time delay T_d is less than 0.3927 s, calculated using (5.8). The results of this example are presented in Fig. 5.2, where Figs. 2a, 2b and 2c represents the performance of the distributed controller for $T_d = 0$ s, 0.3927 s and 1.5 s respectively.

By differentiating (5.7) and taking the Laplace transformation with zero initial conditions, we can obtain a generalized model for the cooperative power controller:

$$\mathbf{U}_{\mathbf{p}} = s(s\mathbf{I}_{N \times N} + G_{TD}\psi_p b_p \mathcal{L}_{\mathcal{G}})^{-1} \mathbf{P}_{\mathbf{EV}} \quad (5.10)$$

where the cooperative control output, $\mathbf{U}_{\mathbf{p}} = [u_p^1 \ u_p^2 \ \dots \ u_p^n]^T$, the measured output powers of EV storages, $\mathbf{P}_{\mathbf{EV}} = \text{diag}\{p_{EV}^n\}$, and $G_{TD} = \frac{1}{1+T_d s}$. $\mathbf{I}_{N \times N}$ represents an identity matrix of dimension $N \times N$. Overall, the general formulation of the voltage references, $\mathbf{V}^{\text{ref}} = [v_1^{\text{ref}} \ v_2^{\text{ref}} \ \dots \ v_n^{\text{ref}}]^T$ for the optimization-incorporated distributed EV storage controller can be expressed as

$$\mathbf{V}^{\text{ref}} = [\mathbf{P}^{\text{ref}} (\mathbf{I}_{N \times N} + \mathbf{G}_{\text{pi}(\mathbf{P})}^{\text{EV}}) - \mathbf{U}_{\mathbf{p}} \mathbf{G}_{\text{pi}(\mathbf{P})}^{\text{EV}}] \mathbf{I}_{\mathbf{EV}}^{-1} \quad (5.11)$$

where $\mathbf{G}_{\mathbf{pi}(\mathbf{P})}^{\text{EV}} = \text{diag}\{G_{pi(P)}^{\text{EV}}\}$, $\mathbf{P}^{\text{ref}} = \text{diag}\{p_n^{\text{ref}}\}$ and $\mathbf{I}_{\text{EV}} = \text{diag}\{i_{EV}^n\}$ considering $G_{pi(P)}^{\text{EV}}$ to be the transfer function of the proportional-integral (PI) controller in the power-control loop of the ODC and i_{EV}^n is the output current of the n th EV storage.

Overall, the design procedure of the proposed ODC can be summarized as below:

Step 1: From smart meters collect load and generation data then check output powers of active EV storages.

Step 2: Find values of α , β and γ for all EV storages.

Step 3: Calculate p_n^{ref} using (5.5).

Step 4: Calculate \mathbf{V}^{ref} using (5.11).

Step 5: Repeat the process until $|p_n^{\text{ref}} - p_{EV}^n| \approx 0$.

5.2.3 Power-Flow Control between Subgrids via IC

The objective of the IC is to ensure accurate active and reactive power flow between the AC and DC subgrids to maintain the bus voltages and the frequency stability. The single-line circuit diagram of the IC is shown in Fig. 5.1b. The IC controller consists of three control loops, i.e. power, voltage and current-control loops with bandwidths (BW) of 2-10 Hz, 400-600 Hz and 1.5 kHz or above respectively as illustrate in Fig. 5.1c. The voltage and current controllers are designed utilizing a conventional decoupled topology with voltage and current feed-forward techniques, whereas the power-control loop is extended with the combined voltage- and power-based droop techniques proposed in [18]. This augmentation improves concurrent DC and AC bus voltage regulation. The algebraic expression of the inverter voltage references in $d - q$ reference frame (v_{id}^* and

v_{iq}^*) and the input angle θ for the $d-q$ to abc converter can be presented as below

$$\begin{cases} v_{id}^* = v_{od} - \omega L_f i_{lq} + [\{V^* - D_Q(Q - Q^*)G_{pd} - v_{od}\}G_{pi}^V \\ \quad - \omega C_f v_{oq} + F i_{od} - i_{ld}]G_{pi}^I \\ v_{iq}^* = v_{oq} + \omega L_f i_{ld} + \{\omega C_f v_{od} + (v_{oq}^* - v_{oq})G_{pi}^V \\ \quad + F i_{oq} - i_{lq}\}G_{pi}^I \\ \theta = \frac{1}{s}\{\omega^* - D_P(P - P^*)G_{pd}\} \end{cases} \quad (5.12)$$

where P and Q are the filtered output active and reactive power whereas P^* and Q^* are the respective references. v_{ldq} and v_{odq} are the inverter filter input and output voltages, i_{ldq} and v_{odq} are the inverter filter input and output currents in the $d-q$ reference frame. D_P and D_Q are active and reactive power droop coefficients. V^* is the output of the voltage-based droop-control loop [18] and F is the feed-forward gain. ω is the angular frequency measured from the phase-locked loop (PLL). L_f and C_f are the inductance and capacitance values of the LC filter. G_{pd} , G_{pi}^V and G_{pi}^I are the transfer functions of the PD controller of the power-control loop, the PI controllers of the voltage and current-control loops respectively. Considering V_{DC} to be the measured DC bus voltage, finally, the pulse-width modulation (PWM) generator of the IC generates the modulation index in the natural abc reference frame as follows:

$$\mathbf{M}_{abc} = \frac{2}{V_{DC}} \mathbf{T}_{dq0-abc}(\theta) \mathbf{V}_{idq}^* \quad (5.13)$$

where, $\mathbf{M}_{abc} = [m_a \ m_b \ m_c]^T$, $\mathbf{V}_{idq}^* = [v_{id}^* \ v_{iq}^*]^T$ and $\mathbf{T}_{dq0-abc}(\theta)$ is the $dq0-abc$ transformation matrix.

5.3 Case Studies

The designed commercial hybrid AC/DC microgrid is illustrated in Fig. 5.3, and consists of four V2G-capable EV storages parked at the parking area with individual capacities

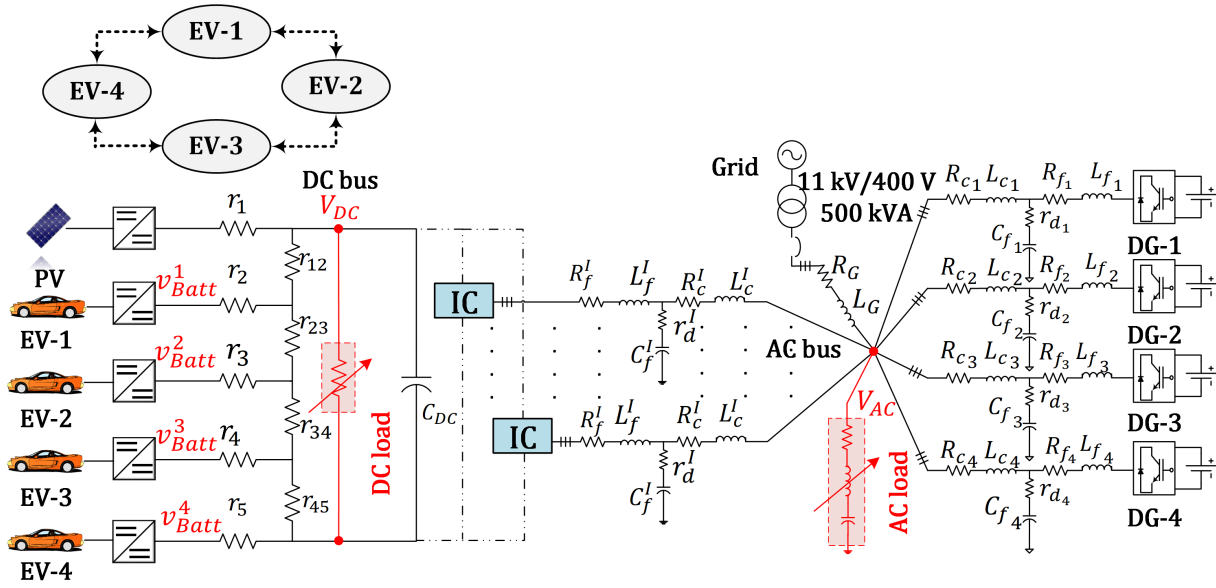


Figure 5.3: Single-line circuit diagram of the test hybrid AC/DC microgrid.

of 24 kWh, one rooftop solar PV unit with a rated capacity of 30 kW and four 17 kVA dispatchable-power electronic-based AC sources. The model is the extended and modified version of the university-based microgrid presented in [1, 2, 17, 18]. All the EV storages and the PV unit are connected to the DC bus of the microgrid. The PV unit is designed to provide maximum power, whereas the EV storages are equipped with the designed ODC. The dispatchable AC sources are connected to the AC bus via four-quadrant inverters, which are controlled by decentralized droop control scheme as presented in [163]. It should be noted that due to large-value inductors present at the inverter terminals, commercial localities usually have a higher X/R ratio. Thus, decentralized $P - f$ and $Q - V$ droop-control schemes are adopted. Both the AC and DC buses are interfaced through a bidirectional interlinking converter, which is controlled by the combined voltage- and power-based droop-control scheme.

Three case studies are carried out to demonstrate the efficacy of the proposed V2M framework. The first case study demonstrates the voltage-regulation and power-sharing

capabilities of the proposed scheme considering irradiation and load variability. The second case study provides insights on the performance of the framework during and subsequent to grid reconnection. The final case study is performed to show the effects of a sudden V2M service disruption due to the disconnection of particular EV storages. This case study also explores the effects of time delay on the output powers of the EV storages. Parameters relevant to the design of the system are depicted in Table 5.1. The load and solar irradiation data are obtained using OSI PI software which gathers sensor data from the smart meters installed at the university premises.

5.3.1 Case A: Variable Solar Insolation and Commercial Loading

For Case A, the designed V2M framework is tested considering PV generation and commercial load variability. The main objective of this case study is to assess the robustness of the developed framework. Both AC and DC buses are loaded with commercial load data obtained from the OSI PI software. Concurrent PV power and load variabilities ensure genuine conditions that the controller needs to withstand. EV storages communicate through a vehicle-to-vehicle (V2V) communication network illustrated in Fig. 5.3. As was mentioned before, the designed distributed controller can provide stable operation as long as there exists a spanning tree and the time delay is within a specified limit. The interaction graph among the four EV storages shown in Fig. 5.3. has one spanning tree. The optimal incremental cost (¢/kW) and the dynamic cost for all EV storages for this case are presented in Figs. 5.4a and 5.4c respectively. It can be observed from the dynamic-cost profiles of all EV storages that EV-1 and EV-4 require higher incentives to provide V2G operation than EV-2 and EV-3. Therefore, from Fig. 5.4e, it can be observed that

Table 5.1: Specifications of the Framework

Energy nodes			
PV	30 kW	DG-(1,2,3,4)	17 kVA
EV-(1,2,3,4)	24 kWh		
Line parameters			
Nominal V_{AC}^{RMS}	240 V	L_f	20×10^{-3} H
V_{DC}^*	600 V	C_f	200×10^{-6} F
Frequency	50 Hz	R_c, R_G	0.03Ω
C_{DC}	130×10^{-4} F	L_c, L_G	3.5×10^{-4} H
R_f^I	0.1Ω	r_d	0.65Ω
$r_1, r_2,$ r_3, r_4	0.02Ω	$r_{12}, r_{23},$ r_{34}, r_{45}	0.05Ω
Control parameters			
Power controller		Voltage controller	
ω_c, ω_e	31.42, 314.16 rad/s	F	0.19
ω^*	314.16 rad/s	K_p	0.11
D_P	3.14×10^{-4}	K_i	2.2
D_Q	1.36×10^{-3}	Current controller	
K_p	2×10^{-5}	K_p	0.16
K_d	2×10^{-7}	K_i	200
EV storage controller			
Power control loop		Voltage control loop	
K_p	1.3	K_p	0.03
K_i	6	K_i	1.1
b_p	1.5		
Cost functions of EV storages			
EV-1	$120 + 0.80p_1 + 0.017p_1^2$		
EV-2	$80 + 0.65p_2 + 0.012p_2^2$		
EV-3	$90 + 0.60p_3 + 0.010p_3^2$		
EV-4	$100 + 0.90p_4 + 0.018p_4^2$		

the EV storages with higher dynamic costs discharge less power for V2G operation. As a result, the highest power is discharged by EV-3 and then EV-2 descending from EV-1 towards EV-4. Figs. 5.4b, 5.4d and 5.4f represent electrical parameters such as the AC bus voltage, the normalized DC bus voltage and the system frequency respectively. It can be concluded from the results that the designed V2M framework can provide stable and efficient hybrid microgrid operations in a cost-effective manner.

5.3.2 Case B: Effects of Grid Reconnection

Case B is carried out to demonstrate the efficacy of the designed system during and subsequent to grid reconnection. Microgrids can operate in both islanded and grid-tied modes. However, an intentional islanding or grid reconnection have certain effects on the electrical parameters of the concerned microgrid. For this case study, at $t = 2.5$ s the islanded hybrid AC/DC microgrid is reconnected with the grid. During the islanded operational mode, the EV storages provide ancillary V2M services by power sharing and voltage regulation to ensure stable microgrid operation. However, if the microgrid is reconnected with a stiff grid then further V2G operation might not be essential. As a result, EV storages are typically expected to be in charging mode during grid-tied microgrid operation. Furthermore, due to the support of the grid, the operating cost or incentives required for V2M operation are reduced. This phenomenon can be observed in Figs. 5.5a and 5.5c, which represent the optimal incremental cost and the operating cost of all EV storages. It can be observed from both Figs. 5.5a and 5.5c that the overall cost is steeply reduced due to the presence of a stiff grid. Therefore, all EV storages enter into charging modes also known as grid-to-vehicle (G2V) mode, for most of the period after $t = 2.5$ s. The negative values of the cost function in Fig. 5.5c represents the dynamic cost required to charge a vehicle. The output charging or discharging power for all EV storages are shown in Fig. 5.5e. The electrical parameters such as the AC bus voltage,

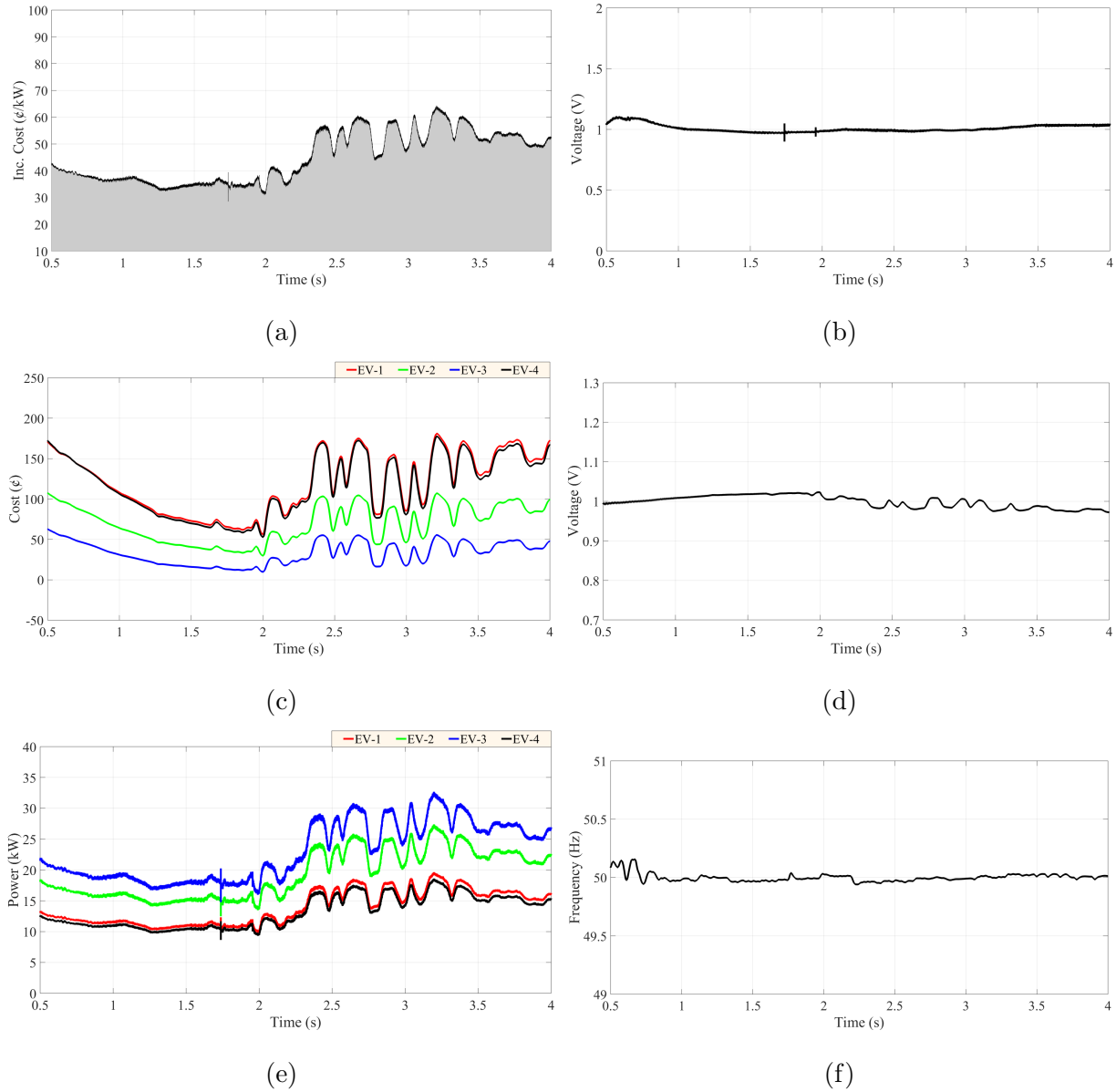


Figure 5.4: Performance evaluation under variable solar insolation and commercial load profile. (a) Optimal incremental cost in ¢/kW. (b) AC bus voltage in per unit (p. u.). (c) Dynamic cost of all EV storages. (d) Normalized DC bus voltage. (e) Output power of all EV storages. (f) Frequency of the system.

the DC bus voltage and the system frequency for this case are shown in Figs. 5.5b , 5.5d and 5.5f respectively. Due to grid reconnection, the AC bus voltage and the frequency quickly settle down by tracking the grid-enforced reference values. The DC bus voltage exhibits a dip during the reconnection but quickly settles down due to the efficacy of the designed ODC for EV storage.

5.3.3 Case C: Effects of EV Disconnection and Time Delay

Case C is dedicated to analyzing the effects of intentional EV service disruption on the system. As EV storages are individually owned, the designed V2M network needs to withstand sudden EV disconnection based on owners' desires. The designed framework should be robust enough to endure dynamic situations where EV owners possess the flexibility of including or excluding EV storages for V2M operations. The load profiles and the solar insolation used in the previous case are kept similar for this case study. At $t = 2$ s, EV-4 is disconnected from the system, emulating a fault at the V2M terminal or a service disruption condition. Figs. 5.6 and 5.7 present the dynamic operating cost and the output power profile for all EV storages before and after the disconnection of EV-4. As there is a shortage of supply due to this disconnection, other EV storages need to cover this additional power requirement to make the system stable. As a result, the output powers of all EV storages have increased after $t = 2$ s. However, active EV storages require higher incentives to supply this additional discharged power. Therefore, it can be observed from Fig. 5.6 that there is an escalation in the operating cost profile after $t = 2$ s.

The effects of a time delay on the power profiles of EV storages are presented in Fig. 5.8. A time delay of 30 ms is introduced at the distributed power-control loop. It can be observed from Fig. 5.8a that the outputs of the distributed controller for all EV storages, i.e. u_p^1, u_p^2, u_p^3 and u_p^4 , converge to an average value of output power with time delay $T_d = 0$

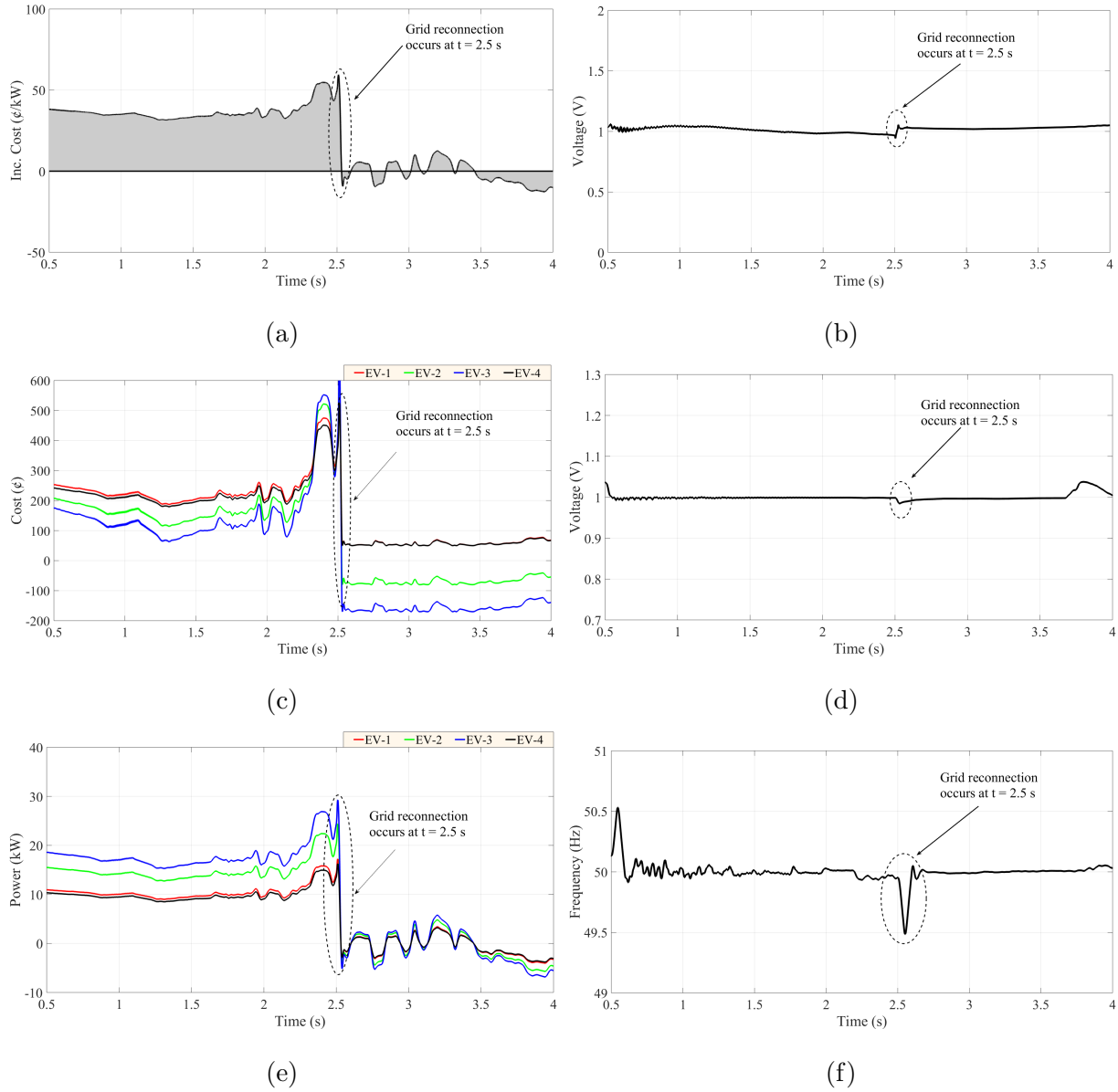


Figure 5.5: Performance evaluation during and subsequent to grid reconnection. (a) Optimal incremental cost in ¢/kW . (b) AC bus voltage in per unit (p. u.). (c) Dynamic cost of all EV storages. (d) Normalized DC bus voltage. (e) Output power of all EV storages. (f) Frequency of the system.

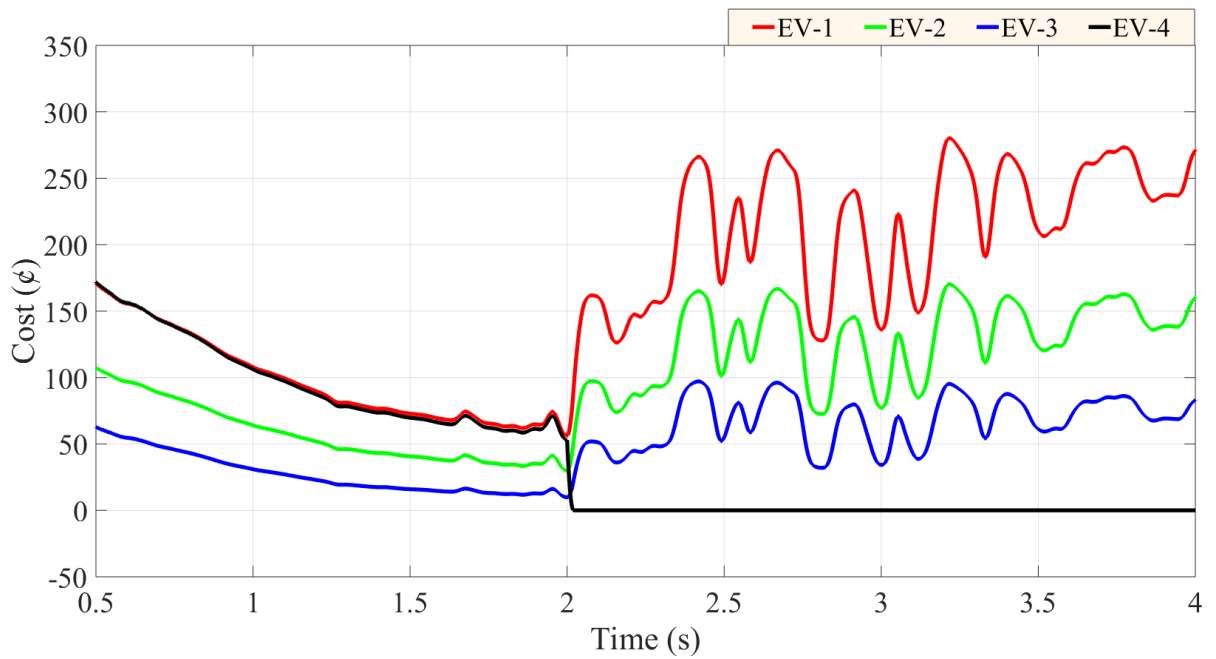


Figure 5.6: Costs of all EV storages when EV-4 is intentionally disconnected at $t = 2$ s.

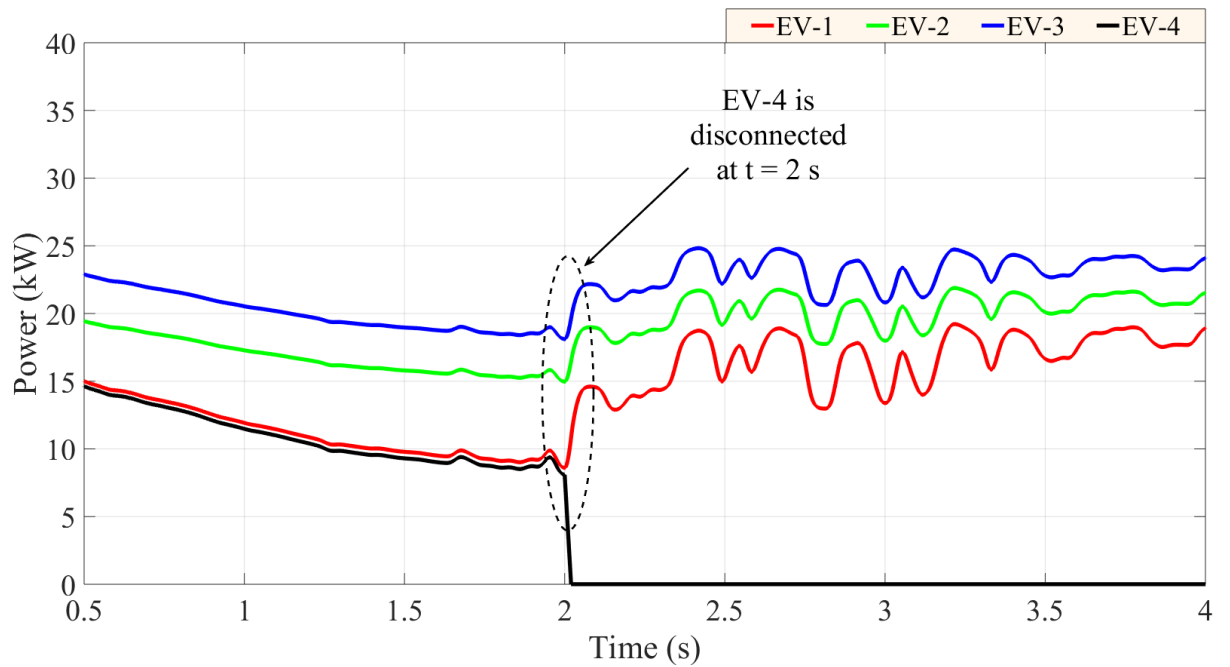
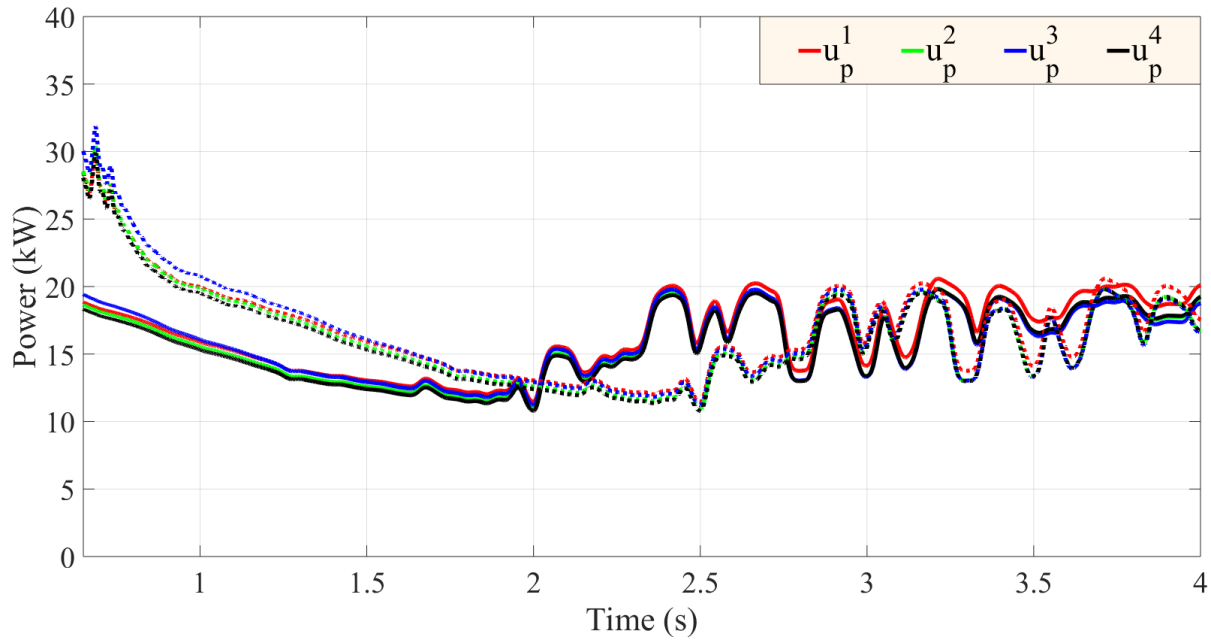
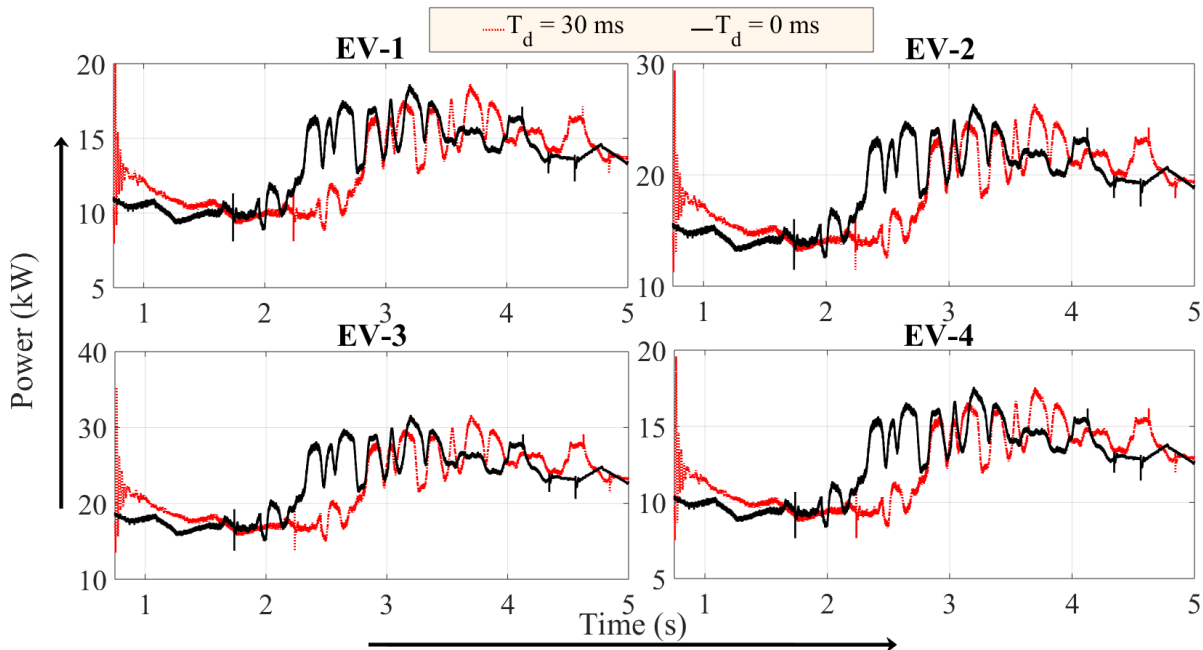


Figure 5.7: Output powers of all EV storages when EV-4 is intentionally disconnected at $t = 2$ s.



(a)



(b)

Figure 5.8: Effects of 30 ms time delay on the system power profile. (a) Output u_p^n of the distributed controllers for all EV storages with time delay (dotted) and without time delay (solid). (b) Discharged power of all EV storages with time delay (red) and without time delay (black)

ms. Conversely, introducing a delay of 30 ms deteriorates the controller performance on convergence. However, the response is stable, as T_d is within the specified limit given in (5.8). As the output powers of all EV storages are driven by the values u_p^n , the discharged output powers from all EV storages are also affected by the time delay as shown in Fig. 5.8.

5.4 Conclusion

A novel V2M framework combining the centralized economic dispatch problem with the distributed EV coordination strategy is presented for optimal power sharing and voltage regulation for a commercial neighborhood to operate as an autonomous electric entity. An aggregator model is developed that generates reference powers for all EV storages utilizing a centralized optimization technique to solve an economic dispatch problem. An EV storage controller is developed that tracks the reference power generated by the EV aggregator and has the capability to operate in either decentralized or distributed mode. Finally, a modified interlinking converter is designed that ensures proper power transportation between the AC and DC subgrids of a hybrid AC/DC microgrid designed for a commercial locality. The developed model is tested considering various scenarios such as generation-load variability, intentional EV disconnection, time delay, and grid reconnection. It is evident from the critical analyses of the case studies that the proposed V2M framework ensures stable microgrid operation in terms of voltage/frequency regulation, power sharing, and cost effectiveness.

Chapter 6

Conclusions and Future Work

This dissertation has extended the conceptual framework of hybrid alternating current (AC)/ direct current (DC) microgrids for an autonomous electrical network for commercial vicinities. This research has analyzed the impacts of electric vehicle (EV) storages in commercial hybrid microgrids and has proposed novel coordinated control schemes for EV storages to mitigate the potential issues by ensuring robust power control and management in presence of renewable energy resources (RERs). General concluding remarks of this dissertation and research directions for the future are provided below.

6.1 Thesis Conclusions

This thesis has discussed the prospects and challenges of EV integration in commercial vicinities by forming them as autonomous microgrids. In order to facilitate this, novel control strategies are proposed to coordinate multiple EV storages in presence of intermittent RERs and real commercial load profiles. The main purpose of the case studies presented in this dissertation is to assess the performance of the developed control and coordination strategies. However, an extensive literature survey is carried out before applying the proposed techniques in simulation results. The survey is composed of the

state-of-the-art of the prospects and feasibilities of hybrid microgrids, hierarchical control strategies, EV charging/ discharging control during grid-tied and islanded operations and distributed control techniques. Different electricity connection standards are also studied for different operational modes and their feasibilities are discussed keeping special attention to the integration of RER integration and vehicle-to-grid (V2G) applications. This comprehensive and structured literature survey is presented in **Chapter 2**.

A simulation benchmark model for a commercial hybrid AC/DC microgrid is developed in **Chapter 3**. A novel approach to coordinate EV storages is presented in the designed microgrid. The potential impacts of EV chargers with different configurations such as DC, three-phase (3P) AC and single-phase (1P) AC EV chargers are studied. The effects of concurrent fluctuating photovoltaic (PV) output power and the variable commercial load profile on the microgrid performance are analyzed. A modified interlinking/interfacing converter controller is designed to improve the transient response of the microgrid during transient from grid-tied to islanded mode or vice versa. A centralized three-layered coordinated control algorithm is proposed to mitigate the impacts caused by different EV chargers and to improve the overall efficacy of the microgrid operation. Finally, several case studies such as variable irradiation and commercial loading, homogeneous single-phase EV allocation, heterogeneous single-phase EV allocation and grid synchronization are carried out to quantify the performance of the proposed approach.

Research challenges associated with the coordination of EV storages in hybrid microgrids with extended geographical size and spatially dispersed EV storages are considered in **Chapter 4**. The centralized EV coordination is vulnerable to single-point failure and subsidiary computational burden. As a result, an innovative need-based distributed coordination strategy (NDCS) for several spatially dispersed EV storages is proposed to avoid the abovementioned problems associated with the centralized coordination technique. The control capacity of the interlinking converter is augmented by utilizing both

voltage- and power-based droop control techniques. With this modification, simultaneous regulation of AC and DC bus voltages and robust power-sharing among distributed generation (DG) units are achieved. An improved distributed controller for DC EV chargers is developed that requires fewer communication interactions as compared to the previously developed centralized technique. Furthermore, unnecessary distributed coordination is avoided utilizing NDCS, which decides whether the coordination of the available EV storages is to be performed in a decentralized or a distributed manner. A mathematical model is developed to assess the controller performance during communication delays. The performance of the proposed approach is validated by performing several case studies such as step load change, variable PV generation and commercial loading, effects of time delay, user-preferred EV disconnection and severe 3P fault at the DC and AC buses.

A cost-effective and optimized solution of the distributed EV coordination scheme is presented in **Chapter 5**. An optimizer is unified with the previously developed distributed EV storage controller. The reference power for each EV storage is generated as function of the incremental cost (λ) by solving an economic dispatch problem. The optimizer adjusts the power reference for each EV storages, which ensures proper power management within the microgrid through a cost-effective distributed V2G operation.

Overall, the following conclusions can be drawn from this research work:

- Hybrid AC/DC microgrids can be a feasible solution to form commercial vicinities into microgrids. Additionally, these microgrids can be interconnected with neighboring microgrids to form the internet of energy (IoE) network.
- Different configurations of EV storages such as DC, 3P, and 1P AC chargers have different impacts on the performance of a microgrid.
- Aggregated EV storages parked in commercial vicinities can be utilized as smart power parks to improve the microgrid performance.

- With the application of the existing microgrid controllers, uncoordinated DC EV chargers severely affect the DC bus voltage whereas the AC bus voltage is minimally affected.
- The incorporation of an additional proportional-derivative (PD) in the power control loop of the microgrid controller enhances the transient stability. This augmentation also stabilizes the system frequency during and subsequent to a fault and transition from grid-tied to islanded modes of operation or vice versa. The effects of phase unbalance caused by heterogeneous allocation of 1P chargers as constant power loads are also minimized due to the abovementioned enhancement.
- The proposed centralized EV coordination is a feasible solution to improve the performance of medium-sized commercial microgrids. The optimal voltage and frequency regulation can be achieved when both 3P and DC EV chargers participate in V2G operations.
- The proposed distributed controllers is an effective EV coordination scheme for commercial microgrids with extended geographical size and spatially dispersed EV storages.
- The conventional distributed controller that uses average consensus method has the inherent capability to withstand time delay effects.
- The augmented interlinking converter control topology by combining voltage- and power-based droop control techniques and the designed distributed EV storage controllers provide robust fault tolerances and improved AC and DC bus voltage regulations. Furthermore, user-preferred EV disconnection has minimal effects on the system voltages with the proposed approach.

- Unification of optimization techniques related to economic dispatch with the microgrid controllers is possible. This union provides cost-effective distributed control solution.

6.2 Future Research Directions

With the increasing RERs and EV penetration, particularly in Australia, there are several challenges that require further research and developments. The future research directions of this dissertation are summarized below.

- Research problems related to harmonics due to nonlinear loads, unbalanced phase voltage conditions could be incorporated with the proposed approaches.
- Circulating current can be minimized by the proposed approach in the dissertation; however, mitigation of the circulating current among multiple interlinking converters connected in parallel requires further attention.
- Model-free adaptive controllers also known as the data-driven controllers (DDC) can be feasible solutions to develop robust controllers for large interconnected and converter-dominated power systems. These controllers do not require extensive system modeling and only utilize the information obtained from the system outputs for given inputs.
- There are several promising research areas such as transactive energy management and control, blockchain-based peer-to-peer energy trading, advanced data management with cyber resiliency, Internet of Energy (IoE), vehicle-to-vehicle (V2V) power sharing can be explored to enhance the present research.
- Utilizing of nonlinear controllers in the inner control loop of the microgrid controller can provide better performance.

- The hardware implementation can be organized utilizing small-scale microgrid systems with two or more battery-energy storage systems (BESS) and bi-directional inverters to validate proposed approaches. However, the experimental setup would require expensive installations and interdisciplinary aptitudes in the field of communication, optimization, power electronics, control theory and power systems.

Appendix A

Commercial Microgrid Testbed

Table A.1: N44 microgrid testing facility equipment

Identifier	Description
A	Allocated location for D-STATCOM
B	10 kW SMA inverter
C	DC marshalling, micro-inverter and DC/DC converter enclosure
D	2 kW SMA Inverter
E	160 A distribution board
F	1.5 kW SMA inverter
G	3-phase monitoring enclosure
H	3-phase monitoring and protection unit
I	Red-lion communication adapter
J	Single-phase monitoring enclosure
K	Data connection point with SMA Webbox
L	DC bus
M	AC bus

Table A.2: Installed solar PV specification

Identifier	Description
A	10 kW peak SunPower E20 series solar panels in 6 strings of 5 panels
B	2 kW peak SunPower E20 series solar panels
C	2 kW peak SunPower E20 series solar panels
D	1.5 kW peak Kyocera modules in series configuration

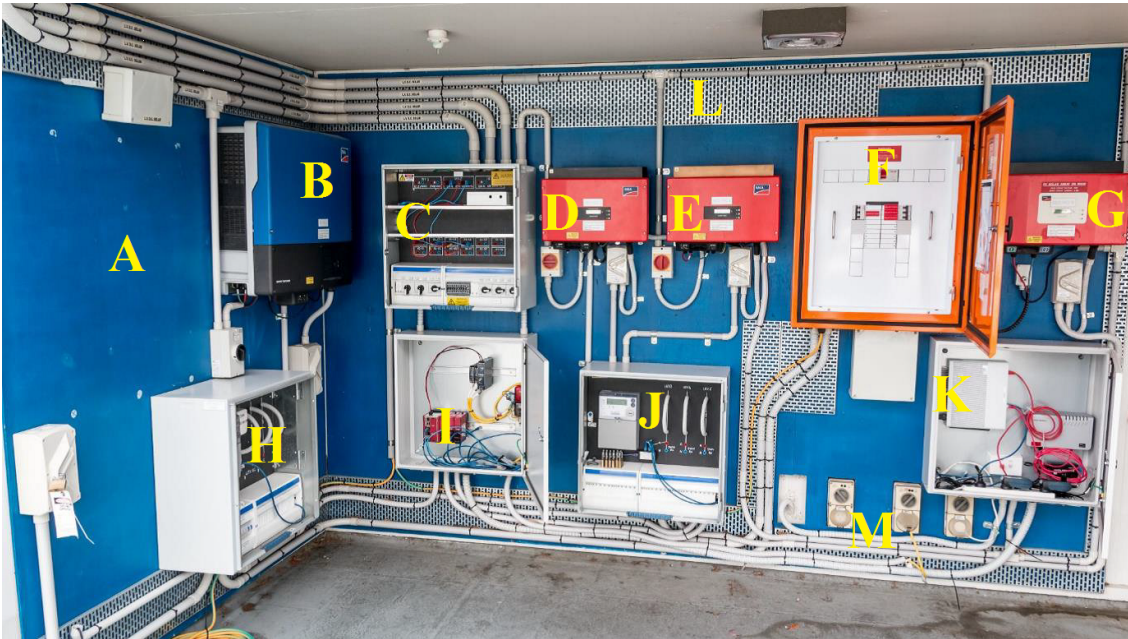


Figure A.1: Microgrid components in N44 building of the Griffith University

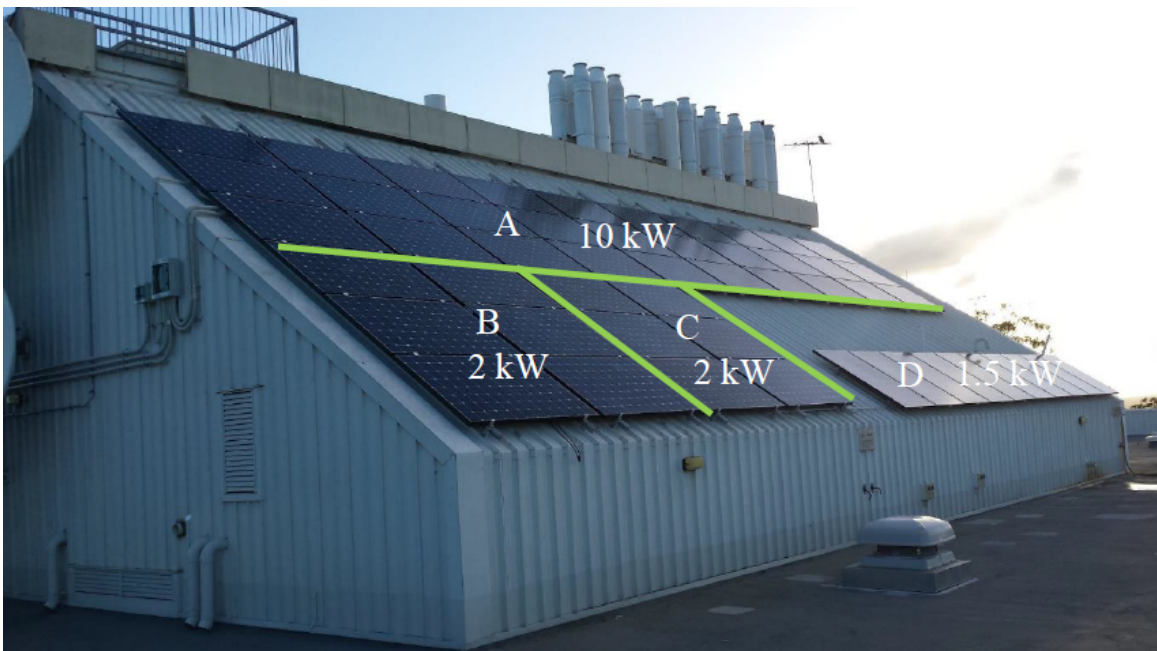


Figure A.2: Rooftop PV installation on N44 building of the Griffith University

Appendix B

List of Acronyms

ADM	Alternating direction method
AC	Alternating-current
ACE	Area control error
ACS	Area control signal
AEMO	Australian Energy Market Operator
AGC	Automatic gain controller
APP	Auxiliary problem principle
BEV	Battery electric vehicles
BESS	Battery energy storages
CEDP	Centralized economic dispatch problem
CERTS	Consortium for Electric Reliability Technology Solutions
CCL	Current control loop
CCVSI	Current-controlled voltage source inverter
DSM	Demand side management
DAE	Differential algebraic equations
DC	Direct-current
DER	Distributed energy resources
DG	Distributed generation
DMPC	Distributed model predictive control
D-STATCOM	Distribution static synchronous compensators
DSO	Distribution System Operators
EV-ESS	Electric vehicle - energy storage systems
EV	Electric vehicles
EPS	Electrical power system
HVDC	High voltage DC
HEV	Hybrid electric vehicles
HTTP	Hypertext Transfer Protocol
ICC	Incremental cost consensus
IC	Interlinking converter
JADE	Java agent development framework
LFC	Load-frequency controller
LC	Local controller

LPF	Low pass filter
LV	Low voltage
MPPT	Maximum power point tracking
MV	Medium voltage
MGCC	Microgrid central controller
MAS	Multi-agent system
MIMO	Multi-input-multi-output
NDCS	Need-based distributed coordination strategy
NEM	National Electricity Market
OPF	Optimal power flow
PLL	Phase-locked-loop
PV	Photovoltaic
PHEV	Plug-in hybrid electric vehicles
PCC	Point of common coupling
PCL	Power control loop
PCPM	Predictor-corrector proximal multiplier method
PWM	Pulse width modulation
RTU	Remote terminal unit
SLB	Sensitive load bus
SOC	State-of-charge
SCADA	Supervisory control and data acquisition
SRF	Synchronous reference frame
3P	Three-phase
THD	Total harmonic distortion
TCP/IP	Transmission Control Protocol/Internet Protocol
UPS	Uninterruptable power supply
UCTE	Union for the Coordination of Transmission of Electricity
V2G	Vehicle-to-grid
V2M	Vehicle-to-microgrid
VCL	Voltage control loop
VSC	Voltage source converters
VSI	Voltage source inverters
VCVSI	Voltage-controlled voltage source inverter

Appendix C

List of Symbols

V_{DC}	measured DC bus voltage.
V_{AC}^{RMS}	measured root-mean-square (RMS) voltage of the AC bus, also known as the point of common coupling (PCC).
V_{DC}^*	DC bus voltage reference.
L_f	filter inductance.
L_c	coupling inductance.
L_G	grid inductances.
R_f	filter resistance.
R_c	coupling resistances.
R_G	grid resistances
r	DC-side coupling resistance.
r_d	damping resistance.
C_f	filter capacitance.
C_{DC}	DC-link capacitance.
v_o^{abc}	inverter output voltage in abc frame.
i_o^{abc}	inverter output current in abc frame.
i_l^{abc}	inverter current before LCL filter in natural abc frame.
v_{od}	d -axis inverter output voltage.
i_{od}	d -axis inverter output current.
v_{oq}	q -axis inverter output voltage.
i_{oq}	q -axis inverter output current.
i_{ld}	d -axis inverter output currents before filter.
i_{lq}	q -axis inverter output currents before filter.
P	filtered active power.
Q	filtered reactive power.
ω	angular frequency.
θ	angle.
F	feed-forward gain.
D_P	droop coefficients of active power controller.
D_Q	droop coefficients of reactive power controller.
k_e	droop coefficient of voltage-based droop controllers.

Λ	voltage compensation factor for inverter interconnection loss.
d_{Batt}^n	duty cycle of n^{th} EV storage.
m	modulation index of the inverter pulse-width-modulation (PWM) controller.
λ_{max}	the largest eigen value of a particular matrix.
*	reference values for corresponding variables.
v_{Batt}^n	measured voltage of n^{th} EV before their corresponding DC/DC converter.
i_{Batt}^n	measured current of n^{th} EV before their corresponding DC/DC converter.
u_v	cooperative-control input for voltage control loop.
$a_{i \times j}$	weight of the communication link from unit j to i .
b_v	coupling gain of the cooperative voltage control loop.
ψ_v	acknowledgement signal for the voltage cooperation.
$K_{p(.)}, K_{i(.)}, K_{d(.)}$	proportional-integral-derivative (PID) gains of interlinking inverter. P, V and I within parentheses represent control loops for power, voltage and current respectively.
$K_{p(.)}^{DC}, K_{i(.)}^{DC}$	PI gains of EV storage DC/DC converters. V and I within parentheses represent control loops for voltage and current respectively
$P_{AC(load)}^{Tot}$	total active power drawn from the AC bus by the AC-type loads.
$Q_{AC(load)}^{Tot}$	total reactive power drawn from the AC bus by the AC-type loads.
$P_{DC(load)}^{Tot}$	total active power drawn from the DC bus by the DC-type loads.
$P_{AC(gen)}^{Tot}$	total active power generations by AC-type DG units.
$Q_{AC(gen)}^{Tot}$	total reactive power generations by AC-type DG units.
$P_{DC(gen)}^{Tot}$	total active power generation by DC-type DG units.

Appendix D

Reuse Permissions of Published Papers for Chapters **2**, **3** and **4**

4/16/2018

Rightslink® by Copyright Clearance Center



RightsLink®

Home

Account Info

Help



Title: Utilization of parked EV-ESS for power management in a grid-tied hybrid AC/DC microgrid

Conference Proceedings: Power Engineering Conference (AUPEC), 2015 Australasian Universities

Author: Md Shamiur Rahman

Publisher: IEEE

Date: Sept. 2015

Copyright © 2015, IEEE

Logged in as:
Md Shamiur Rahman
Account #:
3001249849

LOGOUT

Thesis / Dissertation Reuse

The IEEE does not require individuals working on a thesis to obtain a formal reuse license, however, you may print out this statement to be used as a permission grant:

Requirements to be followed when using any portion (e.g., figure, graph, table, or textual material) of an IEEE copyrighted paper in a thesis:

- 1) In the case of textual material (e.g., using short quotes or referring to the work within these papers) users must give full credit to the original source (author, paper, publication) followed by the IEEE copyright line © 2011 IEEE.
- 2) In the case of illustrations or tabular material, we require that the copyright line © [Year of original publication] IEEE appear prominently with each reprinted figure and/or table.
- 3) If a substantial portion of the original paper is to be used, and if you are not the senior author, also obtain the senior author's approval.

Requirements to be followed when using an entire IEEE copyrighted paper in a thesis:

- 1) The following IEEE copyright/ credit notice should be placed prominently in the references: © [year of original publication] IEEE. Reprinted, with permission, from [author names, paper title, IEEE publication title, and month/year of publication]
- 2) Only the accepted version of an IEEE copyrighted paper can be used when posting the paper or your thesis on-line.
- 3) In placing the thesis on the author's university website, please display the following message in a prominent place on the website: In reference to IEEE copyrighted material which is used with permission in this thesis, the IEEE does not endorse any of [university/educational entity's name goes here]'s products or services. Internal or personal use of this material is permitted. If interested in reprinting/republishing IEEE copyrighted material for advertising or promotional purposes or for creating new collective works for resale or redistribution, please go to http://www.ieee.org/publications_standards/publications/rights/rights_link.html to learn how to obtain a License from RightsLink.

If applicable, University Microfilms and/or ProQuest Library, or the Archives of Canada may supply single copies of the dissertation.

BACK

CLOSE WINDOW

Copyright © 2018 Copyright Clearance Center, Inc. All Rights Reserved. [Privacy statement](#). [Terms and Conditions](#). Comments? We would like to hear from you. E-mail us at customercare@copyright.com

Figure D.1

4/16/2018

Rightslink® by Copyright Clearance Center



RightsLink®

Home

Account
Info

Help



Title: A multi-purpose interlinking converter control for multiple hybrid AC/DC microgrid operations

Logged in as:
Md Shamiur Rahman
Account #:
3001249849

Conference Proceedings: Innovative Smart Grid Technologies - Asia (ISGT-Asia), 2016 IEEE

Author: Md. Shamiur Rahman

Publisher: IEEE

Date: Nov. 2016

Copyright © 2016, IEEE

LOGOUT

Thesis / Dissertation Reuse

The IEEE does not require individuals working on a thesis to obtain a formal reuse license, however, you may print out this statement to be used as a permission grant:

Requirements to be followed when using any portion (e.g., figure, graph, table, or textual material) of an IEEE copyrighted paper in a thesis:

- 1) In the case of textual material (e.g., using short quotes or referring to the work within these papers) users must give full credit to the original source (author, paper, publication) followed by the IEEE copyright line © 2011 IEEE.
- 2) In the case of illustrations or tabular material, we require that the copyright line © [Year of original publication] IEEE appear prominently with each reprinted figure and/or table.
- 3) If a substantial portion of the original paper is to be used, and if you are not the senior author, also obtain the senior author's approval.

Requirements to be followed when using an entire IEEE copyrighted paper in a thesis:

- 1) The following IEEE copyright/ credit notice should be placed prominently in the references: © [year of original publication] IEEE. Reprinted, with permission, from [author names, paper title, IEEE publication title, and month/year of publication]
- 2) Only the accepted version of an IEEE copyrighted paper can be used when posting the paper or your thesis on-line.
- 3) In placing the thesis on the author's university website, please display the following message in a prominent place on the website: In reference to IEEE copyrighted material which is used with permission in this thesis, the IEEE does not endorse any of [university/educational entity's name goes here]'s products or services. Internal or personal use of this material is permitted. If interested in reprinting/republishing IEEE copyrighted material for advertising or promotional purposes or for creating new collective works for resale or redistribution, please go to http://www.ieee.org/publications_standards/publications/rights/rights_link.html to learn how to obtain a License from RightsLink.

If applicable, University Microfilms and/or ProQuest Library, or the Archives of Canada may supply single copies of the dissertation.

BACK

CLOSE WINDOW

Copyright © 2018 [Copyright Clearance Center, Inc.](#) All Rights Reserved. [Privacy statement](#). [Terms and Conditions](#).
Comments? We would like to hear from you. E-mail us at customercare@copyright.com

4/16/2018

Rightslink® by Copyright Clearance Center



RightsLink®

Home

Account Info

Help



Title: EV charging in a commercial hybrid AC/DC microgrid: Configuration, control and impact analysis

Conference Proceedings: Power Engineering Conference (AUPEC), 2016 Australasian Universities

Author: Md Shamiur Rahman

Publisher: IEEE

Date: Sept. 2016

Copyright © 2016, IEEE

Logged in as:
Md Shamiur Rahman
Account #:
3001249849

LOGOUT

Thesis / Dissertation Reuse

The IEEE does not require individuals working on a thesis to obtain a formal reuse license, however, you may print out this statement to be used as a permission grant:

Requirements to be followed when using any portion (e.g., figure, graph, table, or textual material) of an IEEE copyrighted paper in a thesis:

- 1) In the case of textual material (e.g., using short quotes or referring to the work within these papers) users must give full credit to the original source (author, paper, publication) followed by the IEEE copyright line © 2011 IEEE.
- 2) In the case of illustrations or tabular material, we require that the copyright line © [Year of original publication] IEEE appear prominently with each reprinted figure and/or table.
- 3) If a substantial portion of the original paper is to be used, and if you are not the senior author, also obtain the senior author's approval.

Requirements to be followed when using an entire IEEE copyrighted paper in a thesis:

- 1) The following IEEE copyright/ credit notice should be placed prominently in the references: © [year of original publication] IEEE. Reprinted, with permission, from [author names, paper title, IEEE publication title, and month/year of publication]
- 2) Only the accepted version of an IEEE copyrighted paper can be used when posting the paper or your thesis on-line.
- 3) In placing the thesis on the author's university website, please display the following message in a prominent place on the website: In reference to IEEE copyrighted material which is used with permission in this thesis, the IEEE does not endorse any of [university/educational entity's name goes here]'s products or services. Internal or personal use of this material is permitted. If interested in reprinting/republishing IEEE copyrighted material for advertising or promotional purposes or for creating new collective works for resale or redistribution, please go to http://www.ieee.org/publications_standards/publications/rights/rights_link.html to learn how to obtain a License from RightsLink.

If applicable, University Microfilms and/or ProQuest Library, or the Archives of Canada may supply single copies of the dissertation.

BACK

CLOSE WINDOW

Copyright © 2018 Copyright Clearance Center, Inc. All Rights Reserved. [Privacy statement](#). [Terms and Conditions](#). Comments? We would like to hear from you. E-mail us at customercare@copyright.com

Figure D.3

4/16/2018

Rightslink® by Copyright Clearance Center

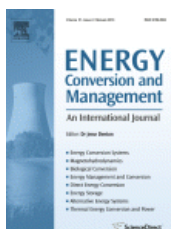


RightsLink®

Home

Account
Info

Help



Title: Coordinated control of three-phase AC and DC type EV-ESSs for efficient hybrid microgrid operations

Author: Md Shamiur Rahman, M.J. Hossain, Junwei Lu

Publication: Energy Conversion and Management

Publisher: Elsevier

Date: 15 August 2016

© 2016 Elsevier Ltd. All rights reserved.

Logged in as:
Md Shamiur Rahman
Account #:
3001249849

LOGOUT

Please note that, as the author of this Elsevier article, you retain the right to include it in a thesis or dissertation, provided it is not published commercially. Permission is not required, but please ensure that you reference the journal as the original source. For more information on this and on your other retained rights, please visit: <https://www.elsevier.com/about/our-business/policies/copyright#Author-rights>

BACK

CLOSE WINDOW

Copyright © 2018 [Copyright Clearance Center, Inc.](#) All Rights Reserved. [Privacy statement](#). [Terms and Conditions](#).
Comments? We would like to hear from you. E-mail us at customercare@copyright.com

4/16/2018

Rightslink® by Copyright Clearance Center



RightsLink®

Home

Account Info

Help



Title: A Need-Based Distributed Coordination Strategy for EV Storages in a Commercial Hybrid AC/DC Microgrid with an Improved Interlinking Converter Control Topology

Author: Md Shamiur Rahman

Publication: Energy Conversion, IEEE Transactions on

Publisher: IEEE

Date: Dec 31, 1969

Copyright © 1969, IEEE

Logged in as:
Md Shamiur Rahman
Account #:
3001249849

LOGOUT

Thesis / Dissertation Reuse

The IEEE does not require individuals working on a thesis to obtain a formal reuse license, however, you may print out this statement to be used as a permission grant:

Requirements to be followed when using any portion (e.g., figure, graph, table, or textual material) of an IEEE copyrighted paper in a thesis:

- 1) In the case of textual material (e.g., using short quotes or referring to the work within these papers) users must give full credit to the original source (author, paper, publication) followed by the IEEE copyright line © 2011 IEEE.
- 2) In the case of illustrations or tabular material, we require that the copyright line © [Year of original publication] IEEE appear prominently with each reprinted figure and/or table.
- 3) If a substantial portion of the original paper is to be used, and if you are not the senior author, also obtain the senior author's approval.

Requirements to be followed when using an entire IEEE copyrighted paper in a thesis:

- 1) The following IEEE copyright/ credit notice should be placed prominently in the references: © [year of original publication] IEEE. Reprinted, with permission, from [author names, paper title, IEEE publication title, and month/year of publication]
- 2) Only the accepted version of an IEEE copyrighted paper can be used when posting the paper or your thesis on-line.
- 3) In placing the thesis on the author's university website, please display the following message in a prominent place on the website: In reference to IEEE copyrighted material which is used with permission in this thesis, the IEEE does not endorse any of [university/educational entity's name goes here]'s products or services. Internal or personal use of this material is permitted. If interested in reprinting/republishing IEEE copyrighted material for advertising or promotional purposes or for creating new collective works for resale or redistribution, please go to http://www.ieee.org/publications_standards/publications/rights/rights_link.html to learn how to obtain a License from RightsLink.

If applicable, University Microfilms and/or ProQuest Library, or the Archives of Canada may supply single copies of the dissertation.

BACK

CLOSE WINDOW

Copyright © 2018 Copyright Clearance Center, Inc. All Rights Reserved. [Privacy statement](#). [Terms and Conditions](#). Comments? We would like to hear from you. E-mail us at customercare@copyright.com

Figure D.5

References

- [1] M. S. Rahman, M. J. Hossain, F. H. M. Rafi, and J. Lu, “EV charging in a commercial hybrid AC/DC microgrid: Configuration, control and impact analysis,” in *2016 Australasian Universities Power Engineering Conference (AUPEC)*, September 2016, pp. 1–6.
- [2] M. Rahman, M. Hossain, and J. Lu, “Utilization of parked ev-ess for power management in a grid-tied hybrid ac/dc microgrid,” in *2015 Australasian Universities Power Engineering Conference (AUPEC)*, Sept 2015, pp. 1–6.
- [3] N. Mahmud, A. Zahedi, and M. Shamiur Rahman, *Control of Renewable Energy Systems*. Singapore: Springer Singapore, 2018, pp. 207–231.
- [4] A. Bidram and A. Davoudi, “Hierarchical Structure of Microgrids Control System,” *IEEE Transactions on Smart Grid*, vol. 3, no. 4, pp. 1963–1976, Dec. 2012.
- [5] D. E. Olivares, A. Mehrizi-Sani, A. H. Etemadi, C. a. Cañizares, R. Iravani, M. Kazerani, A. H. Hajimiragha, O. Gomis-Bellmunt, M. Saeedifard, R. Palma-Behnke, G. a. Jiménez-Estévez, and N. D. Hatziargyriou, “Trends in microgrid control,” *IEEE Transactions on Smart Grid*, vol. 5, no. 4, pp. 1905–1919, 2014.
- [6] A. M. Bouzid, J. M. Guerrero, A. Cheriti, M. Bouhamida, P. Sicard, and M. Benghanem, “A survey on control of electric power distributed generation systems for

- microgrid applications,” *Renewable and Sustainable Energy Reviews*, vol. 44, no. 0, pp. 751 – 766, 2015.
- [7] T. Panel, N. E. M. Mainland, and A. A. This, “The Frequency operating standard,” vol. 3, no. November, pp. 1–11, 2017.
- [8] E. Standards, “Voltage & equipment standards,” pp. 1–3, 2010.
- [9] J. Momoh, *Smart Grid. Fundamental of design and analysis*, 2012.
- [10] J. Lazar and M. Mckenzie, “Australian Standards for Smart Grids – Standards Roadmap,” no. June, 2012.
- [11] U.S. Department of Energy, “the SMART GRID,” *Communication*, vol. 99, p. 48, 2010. [Online]. Available: <http://www.oe.energy.gov/SmartGridIntroduction.htm>
- [12] REN21, “Renewables 2017: global status report,” Tech. Rep. October 2016, 2017. [Online]. Available: http://www.ren21.net/wp-content/uploads/2017/06/17-8399_GSR.2017_Full_Report_0621_Opt.pdf
- [13] N. Cost and B. Assessment, “Shaping Australia ’ s Energy Future,” no. July, 2014.
- [14] M. Yilmaz and P. T. Krein, “Review of the impact of vehicle-to-grid technologies on distribution systems and utility interfaces,” *IEEE Trans. Power Electron.*, vol. 28, no. 12, pp. 5673–5689, December 2013.
- [15] Iec, “Executive summary.” *Grid integration of large-capacity Renewable Energy sources and use of large-capacity Electrical Energy Storage*, vol. 39, pp. 11–12, 2009.
- [16] Y. J. Kim, D. H. Blum, N. Xu, L. Su, and L. K. Norford, “Technologies and magnitude of ancillary services provided by commercial buildings,” *Proc. IEEE*, vol. 104, no. 4, pp. 758–779, April 2016.

- [17] M. S. Rahman, M. J. Hossain, and J. Lu, "Coordinated control of three-phase AC and DC type EV-ESSs for efficient hybrid microgrid operations," *Energy Conversion and Management*, vol. 122, pp. 488 – 503, 2016.
- [18] M. S. Rahman, J. Hossain, J. Lu, and H. R. Pota, "A need-based distributed coordination strategy for ev storages in a commercial hybrid ac/dc microgrid with an improved interlinking converter control topology," *IEEE Trans. Energy Convers.*, vol. PP, no. 99, pp. 1–1, 2017.
- [19] S. Beer, T. Gomez, D. Dallinger, I. Momber, C. Marnay, M. Stadler, and J. Lai, "An economic analysis of used electric vehicle batteries integrated into commercial building microgrids," *IEEE Transactions on Smart Grid*, vol. 3, no. 1, pp. 517–525, March 2012.
- [20] G. Byeon, T. Yoon, S. Oh, and G. Jang, "Energy management strategy of the dc distribution system in buildings using the ev service model," *IEEE Trans. Power Electron.*, vol. 28, no. 4, pp. 1544–1554, April 2013.
- [21] G. Zhang, T. Tan, and G. Wang, "Real-time smart charging of electric vehicles for demand charge reduction at non-residential sites," *IEEE Trans. Smart Grid*, vol. PP, no. 99, pp. 1–1, 2017.
- [22] Q. Yan, B. Zhang, and M. Kezunovic, "Optimized operational cost reduction for an ev charging station integrated with battery energy storage and pv generation," *IEEE Trans. Smart Grid*, vol. PP, no. 99, pp. 1–1, 2018.
- [23] D. Kondoleon, L. Ten-Hope, T. Surles, and R. L. Therakelsen, "The CERTS MicroGrid Concept," *Integration of Distributed Energy Resources – The CERTS MicroGrid Concept*, no. October, p. 32, 2003. [Online]. Available: <http://certs.lbl.gov/pdf/50829.pdf>

-
- [24] X. Liu, P. Wang, and P. C. Loh, "A hybrid ac/dc microgrid and its coordination control," *IEEE Transactions on Smart Grid*, vol. 2, no. 2, pp. 278–286, June 2011.
- [25] P. C. Loh, D. Li, Y. K. Chai, and F. Blaabjerg, "Autonomous control of interlinking converter with energy storage in hybrid ac/dc microgrid," *IEEE Transactions on Industry Applications*, vol. 49, no. 3, pp. 1374–1382, May 2013.
- [26] T. S. Ustun, C. Ozansoy, and A. Zayegh, "Recent developments in microgrids and example cases around the world - A review," *Renewable and Sustainable Energy Reviews*, vol. 15, no. 8, pp. 4030–4041, 2011.
- [27] C. Wang and M. H. Nehrir, "Power management of a stand-alone wind/photo-voltaic/fuel cell energy system," *IEEE Transactions on Energy Conversion*, vol. 23, no. 3, pp. 957–967, 2008.
- [28] C. Alvial-Palavicino, N. Garrido-Echeverría, G. Jiménez-Estévez, L. Reyes, and R. Palma-Behnke, "A methodology for community engagement in the introduction of renewable based smart microgrid," *Energy for Sustainable Development*, vol. 15, no. 3, pp. 314–323, 2011.
- [29] B. Bahrani, "Islanding Detection and Control of Islanded Single and Two-Parallel Distributed Generation Units," 2008.
- [30] Ieee, *IEEE Standard Conformance Test Procedure for Equipment Interconnecting Distributed Resources with Electric Power Systems*, 2005, no. July.
- [31] J. Rocabert, A. Luna, F. Blaabjerg, and P. Rodríguez, "Control of power converters in ac microgrids," *IEEE Transactions on Power Electronics*, vol. 27, no. 11, pp. 4734–4749, Nov 2012.

-
- [32] R. Ambrosio and S. Widergren, "A framework for addressing interoperability issues," *2007 IEEE Power Engineering Society General Meeting, PES*, pp. 1–5, 2007.
- [33] J. M. Guerrero, J. C. Vasquez, J. Matas, M. Castilla, and L. G. de Vicuna, "Control strategy for flexible microgrid based on parallel line-interactive ups systems," *IEEE Transactions on Industrial Electronics*, vol. 56, no. 3, pp. 726–736, March 2009.
- [34] J. M. Guerrero, J. C. Vasquez, J. Matas, L. G. de Vicuna, and M. Castilla, "Hierarchical Control of Droop-Controlled AC and DC Microgrids—A General Approach Toward Standardization," *IEEE Transactions on Industrial Electronics*, vol. 58, no. 1, pp. 158–172, Jan. 2011.
- [35] M. S. Rahman, F. H. M. Rafi, M. J. Hossain, and J. Lu, "Power Control and Monitoring of Smart Grid with EVs," in *Vehicle-to-Grid: Linking Electric Vehicles to the Smart Grid*. IET, no. April 2015.
- [36] C. Dharmakeerthi and N. Mithulananthan, "Pev load and its impact on static voltage stability," in *Plug In Electric Vehicles in Smart Grids*. Springer Singapore, 2015, pp. 221–248.
- [37] W. Kempton and J. Tomić, "Vehicle-to-grid power fundamentals: Calculating capacity and net revenue," *Journal of Power Sources*, vol. 144, no. 1, pp. 268–279, 2005.
- [38] C. Guille and G. Gross, "Design of a Conceptual Framework for the V2G Implementation," in *Energy 2030 Conference, 2008. ENERGY 2008. IEEE*, 2008, pp. 1–3.
- [39] Y. Ota, H. Taniguchi, T. Nakajima, K. M. Liyanage, J. Baba, and A. Yokoyama, "Autonomous Distributed V2G (Vehicle-to-Grid) Satisfying Scheduled Charging," *Smart Grid, IEEE Transactions on*, vol. 3, no. 1, pp. 559–564, 2012.

-
- [40] K. Mets, T. Verschueren, W. Haerick, C. Develder, and F. De Turck, "Optimizing smart energy control strategies for plug-in hybrid electric vehicle charging," in *Network Operations and Management Symposium Workshops (NOMS Wkshps), 2010 IEEE/IFIP*, 2010, pp. 293–299.
- [41] S. V. Chakraborty, S. K. Shukla, and J. Thorp, "A detailed analysis of the effective-load-carrying-capacity behavior of plug-in electric vehicles in the power grid," in *Innovative Smart Grid Technologies (ISGT), 2012 IEEE PES*, 2012, pp. 1–8.
- [42] A. De Los Rios, J. Goentzel, K. E. Nordstrom, and C. W. Siegert, "Economic analysis of vehicle-to-grid (V2G)-enabled fleets participating in the regulation service market," in *Innovative Smart Grid Technologies (ISGT), 2012 IEEE PES*, 2012, pp. 1–8.
- [43] S. B. Peterson, J. F. Whitacre, and J. Apt, "The economics of using plug-in hybrid electric vehicle battery packs for grid storage," *Journal of Power Sources*, vol. 195, no. 8, pp. 2377–2384, 2010.
- [44] W. Kempton and T. Kubo, "Electric-drive vehicles for peak power in Japan," *Energy Policy*, vol. 28, no. 1, pp. 9–18, 2000.
- [45] N. Bottrell, M. Prodanovic, and T. C. Green, "Dynamic stability of a microgrid with an active load," *IEEE Transactions on Power Electronics*, vol. 28, no. 11, pp. 5107–5119, Nov 2013.
- [46] S. Golestan, M. Monfared, J. M. Guerrero, and M. Joorabian, "A d-q synchronous frame controller for single-phase inverters," in *Power Electronics, Drive Systems and Technologies Conference (PEDSTC), 2011 2nd*, Feb 2011, pp. 317–323.

-
- [47] F. Blaabjerg, R. Teodorescu, M. Liserre, and A. Timbus, "Overview of control and grid synchronization for distributed power generation systems," *Industrial Electronics, IEEE Transactions on*, vol. 53, no. 5, pp. 1398–1409, Oct 2006.
- [48] Y. A. R. I. Mohamed and E. F. El-Saadany, "Adaptive decentralized droop controller to preserve power sharing stability of paralleled inverters in distributed generation microgrids," *IEEE Transactions on Power Electronics*, vol. 23, no. 6, pp. 2806–2816, Nov 2008.
- [49] C. Schauder and H. Mehta, "Vector analysis and control of advanced static var compensators," *Generation, Transmission and Distribution, IEE Proceedings C*, vol. 140, no. 4, pp. 299–306, Jul 1993.
- [50] N. Eghtedarpour and E. Farjah, "Power control and management in a hybrid ac/dc microgrid," *IEEE Transactions on Smart Grid*, vol. 5, no. 3, pp. 1494–1505, May 2014.
- [51] M. Yazdanian and A. Mehrizi-Sani, "Distributed control techniques in microgrids," *Smart Grid, IEEE Transactions on*, vol. 5, no. 6, pp. 2901–2909, Nov 2014.
- [52] T. Morstyn, B. Hredzak, and V. G. Agelidis, "Control strategies for microgrids with distributed energy storage systems: An overview," *IEEE Transactions on Smart Grid*, vol. PP, no. 99, pp. 1–1, 2016.
- [53] D. K. Molzahn, F. Dörfler, H. Sandberg, S. H. Low, S. Chakrabarti, R. Baldick, and J. Lavaei, "A survey of distributed optimization and control algorithms for electric power systems," *IEEE Transactions on Smart Grid*, vol. 8, no. 6, pp. 2941–2962, Nov 2017.
- [54] P. McNamara, R. R. Negenborn, B. De Schutter, and G. Lightbody, "Optimal Coordination of a Multiple HVDC Link System Using Centralized and Distributed

- Control,” *Control Systems Technology, IEEE Transactions on*, vol. 21, no. 2, pp. 302–314, Mar. 2013.
- [55] M. Moradzadeh, R. Boel, and L. Vandeveldel, “Voltage Coordination in Multi-Area Power Systems via Distributed Model Predictive Control,” *Power Systems, IEEE Transactions on*, vol. 28, no. 1, pp. 513–521, Feb. 2013.
- [56] M. Falahi, K. Butler-Purpy, and M. Ehsani, “Dynamic Reactive Power Control of Islanded Microgrids,” *Power Systems, IEEE Transactions on*, vol. 28, no. 4, pp. 3649–3657, Nov. 2013.
- [57] K. T. Tan, P. L. So, Y. C. Chu, and M. Z. Q. Chen, “Coordinated Control and Energy Management of Distributed Generation Inverters in a Microgrid,” *Power Delivery, IEEE Transactions on*, vol. 28, no. 2, pp. 704–713, Apr. 2013.
- [58] J. N. Tsitsiklis, D. P. Bertsekas, and M. Athans, “Distributed asynchronous deterministic and stochastic gradient optimization algorithms,” *Automatic Control, IEEE Transactions on*, vol. 31, no. 9, pp. 803–812, Sep. 1986.
- [59] R. Olfati-Saber, J. A. Fax, and R. M. Murray, “Consensus and cooperation in networked multi-agent systems,” *Proc. IEEE*, vol. 95, no. 1, pp. 215–233, January 2007.
- [60] T. Keviczky, F. Borrelli, K. Fregene, D. Godbole, and G. J. Balas, “Decentralized Receding Horizon Control and Coordination of Autonomous Vehicle Formations,” *Control Systems Technology, IEEE Transactions on*, vol. 16, no. 1, pp. 19–33, Jan. 2008.
- [61] A. Nedic and A. Ozdaglar, “Distributed Subgradient Methods for Multi-Agent Optimization,” *Automatic Control, IEEE Transactions on*, vol. 54, no. 1, pp. 48–61, Jan. 2009.

-
- [62] A. Nedic, A. Ozdaglar, and P. A. Parrilo, “Constrained Consensus and Optimization in Multi-Agent Networks,” *Automatic Control, IEEE Transactions on*, vol. 55, no. 4, pp. 922–938, Apr. 2010.
- [63] T. Vicsek, A. Czirók, E. Ben-Jacob, I. Cohen, and O. Shochet, “Novel Type of Phase Transition in a System of Self-Driven Particles,” *Phys. Rev. Lett.*, vol. 75, no. 6, pp. 1226–1229, Aug. 1995.
- [64] A. Jadbabaie, J. Lin, and A. S. Morse, “Coordination of groups of mobile autonomous agents using nearest neighbor rules,” *Automatic Control, IEEE Transactions on*, vol. 48, no. 6, pp. 988–1001, Jun. 2003.
- [65] S. P. Boyd, A. Ghosh, B. Prabhakar, and D. Shah, “Gossip algorithms: design, analysis and applications.” in *INFOCOM*. IEEE, 2005, pp. 1653–1664.
- [66] Y. Xu and W. Liu, “Novel Multiagent Based Load Restoration Algorithm for Microgrids,” *Smart Grid, IEEE Transactions on*, vol. 2, no. 1, pp. 152–161, Mar. 2011.
- [67] P. Wu and P. J. Antsaklis, “Distributed Cooperative Control System Algorithms – Simulations and Enhancements,” *University of Notre Dame, ISIS Technical Report ISIS-2009*, vol. 1, no. April, 2009.
- [68] A. Costabeber, P. Tenti, and P. Mattavelli, “Distributed Cooperative Control of Low-Voltage Residential Microgrids,” in *Power Electronics for Distributed Generation Systems (PEDG), 2012 3rd IEEE International Symposium on*, 2012, pp. 457–463.
- [69] A. Bidram, A. Davoudi, F. L. Lewis, and J. M. Guerrero, “Distributed cooperative secondary control of microgrids using feedback linearization,” *IEEE Transactions on Power Systems*, vol. 28, no. 3, pp. 3462–3470, 2013.

- [70] A. Bidram, F. L. Lewis, and A. Davoudi, “Frequency Control of Electric Power Microgrids Using Distributed Cooperative Control of Multi-agent Systems,” in *Cyber Technology in Automation, Control and Intelligent Systems (CYBER), 2013 IEEE 3rd Annual International Conference on*, 2013, pp. 223–228.
- [71] A. Bidram, F. L. Lewis, A. Davoudi, and J. M. Guerrero, “Distributed Cooperative Control of Nonlinear and Non - identical Multi - agent Systems,” in *Control & Automation (MED), 2013 21st Mediterranean Conference on*, 2013.
- [72] A. Bidram, F. L. Lewis, and A. Davoudi, “Synchronization of nonlinear heterogeneous cooperative systems using input – output feedback linearization,” *Automatica*, vol. 50, no. 10, pp. 2578–2585, 2014.
- [73] F. L. Lewis, Z. Qu, A. Davoudi, and A. Bidram, “Secondary control of microgrids based on distributed cooperative control of multi-agent systems,” *IET Generation, Transmission & Distribution*, vol. 7, no. October 2012, pp. 822–831, 2013.
- [74] A. Bidram, F. L. Lewis, and A. Davoudi, “Distributed control systems for small-scale power networks: Using multiagent cooperative control theory,” *IEEE Control Syst. Mag.*, vol. 34, no. 6, pp. 56–77, December 2014.
- [75] A. Bidram, S. Member, A. Davoudi, and F. L. Lewis, “A Multiobjective Distributed Control Framework for Islanded AC Microgrids,” *IEEE Transactions on Industrial Informatics*, vol. 10, no. 3, pp. 1785–1798, 2014.
- [76] A. Bidram, A. Davoudi, and F. L. Lewis, “Two-layer Distributed Cooperative Control of Multi- inverter Microgrids,” in *Applied Power Electronics Conference and Exposition (APEC), 2014 Twenty-Ninth Annual IEEE*, 2014, pp. 2364–2371.
- [77] D. He, S. Member, D. Shi, and R. Sharma, “Consensus-based Distributed Cooperative Control for Microgrid Voltage Regulation and Reactive Power Sharing,” in

- Innovative Smart Grid Technologies Conference Europe (ISGT-Europe), 2014 IEEE PES*, 2014, pp. 1–6.
- [78] V. Nasirian, S. Moayedi, A. Davoudi, F. L. Lewis, S. Member, S. Moayedi, S. Member, A. Davoudi, F. L. Lewis, S. Member, S. Moayedi, S. Member, A. Davoudi, and F. L. Lewis, “Distributed Cooperative Control of DC Microgrids,” *IEEE Transactions on Power Electronics*, vol. 8993, no. 4, pp. 2288–2303, 2014.
- [79] Y. Xu, W. Zhang, G. Hug, S. Kar, and Z. Li, “Cooperative Control of Distributed Energy Storage Systems in a Microgrid,” *IEEE Transactions on Smart Grid*, vol. 6, no. 1, pp. 238–248, Jan. 2015.
- [80] T. Morstyn, B. Hredzak, and V. Agelidis, “Distributed cooperative control of microgrid storage,” *IEEE Transactions on Power Systems*, vol. 30, no. 5, pp. 2780–2789, Sept 2015.
- [81] J. Lai, H. Zhou, X. Lu, X. Yu, and W. Hu, “Droop-based distributed cooperative control for microgrids with time-varying delays,” *IEEE Trans. Smart Grid*, vol. 7, no. 4, pp. 1775–1789, July 2016.
- [82] M. J. Hossain, M. A. Mahmud, F. Milano, S. Bacha, and A. Hably, “Design of robust distributed control for interconnected microgrids,” *IEEE Trans. Smart Grid*, vol. PP, no. 99, pp. 1–12, 2015.
- [83] S. J. Russell and P. Norvig, *Artificial Intelligence: A Modern Approach*. Prentice Hall, 2010.
- [84] F. Schweppe and J. Wildes, “Power system static-state estimation, part i: Exact model,” *Power Apparatus and Systems, IEEE Transactions on*, vol. PAS-89, no. 1, pp. 120–125, Jan 1970.

-
- [85] R. R. Negenborn, B. De Schutter, and J. Hellendoorn, “Multi-Agent Model Predictive Control: A Survey,” Aug. 2009.
- [86] S. D. J. McArthur, E. M. Davidson, V. M. Catterson, A. L. Dimeas, N. D. Hatziargyriou, F. Ponci, and T. Funabashi, “Multi-Agent Systems for Power Engineering Applications—Part I: Concepts, Approaches, and Technical Challenges,” *IEEE Transactions on Power Systems*, vol. 22, no. 4, pp. 1743–1752, Nov. 2007.
- [87] ———, “Multi-Agent Systems for Power Engineering Applications—Part II: Technologies, Standards, and Tools for Building Multi-agent Systems,” *IEEE Transactions on Power Systems*, vol. 22, no. 4, pp. 1753–1759, Nov. 2007.
- [88] S. Filizadeh, M. Heidari, A. Mehrizi-Sani, J. Jatskevich, and J. Martinez, “Techniques for Interfacing Electromagnetic Transient Simulation Programs With General Mathematical Tools IEEE Taskforce on Interfacing Techniques for Simulation Tools,” *IEEE Transactions on Power Delivery*, vol. 23, no. 4, pp. 2610–2622, Oct. 2008.
- [89] J. Mitra, “A decentralized control architecture for a microgrid with power electronic interfaces,” in *North American Power Symposium 2010*. IEEE, Sep. 2010, pp. 1–8.
- [90] C.-X. Dou and B. Liu, “Multi-Agent Based Hierarchical Hybrid Control for Smart Microgrid,” *IEEE Transactions on Smart Grid*, vol. 4, no. 2, pp. 771–778, Jun. 2013.
- [91] Y. Han, K. Zhang, H. Li, E. A. A. Coelho, and J. M. Guerrero, “Mas-based distributed coordinated control and optimization in microgrid and microgrid clusters: A comprehensive overview,” *IEEE Transactions on Power Electronics*, vol. PP, no. 99, pp. 1–1, 2017.

-
- [92] A. G. Beccuti, T. H. Demiray, G. Andersson, and M. Morari, “A Lagrangian Decomposition Algorithm for Optimal Emergency Voltage Control,” *Power Systems, IEEE Transactions on*, vol. 25, no. 4, pp. 1769–1779, Nov. 2010.
- [93] G. Reklaitis, A. Ravindran, and K. Ragsdell, “Engineering optimization: methods and applications,” 1983.
- [94] G. Hug-Glanzmann and G. Andersson, “Decentralized Optimal Power Flow Control for Overlapping Areas in Power Systems,” *Power Systems, IEEE Transactions on*, vol. 24, no. 1, pp. 327–336, Feb. 2009.
- [95] B. Kim and R. Baldick, “A comparison of distributed optimal power flow algorithms,” *Power Systems, IEEE Transactions on*, vol. 15, no. 2, pp. 599–604, May 2000.
- [96] R. Baldick, B. H. Kim, C. Chase, and Y. Luo, “A fast distributed implementation of optimal power flow,” *Power Systems, IEEE Transactions on*, vol. 14, no. 3, pp. 858–864, Aug. 1999.
- [97] M. Ilic-Spong, J. Christensen, and K. Eichorn, “Secondary voltage control using pilot point information,” *Power Systems, IEEE Transactions on*, vol. 3, no. 2, pp. 660–668, May 1988.
- [98] S. Anand, B. G. Fernandes, and M. Guerrero, “Distributed control to ensure proportional load sharing and improve voltage regulation in low-voltage dc microgrids,” *Power Electronics, IEEE Transactions on*, vol. 28, no. 4, pp. 1900–1913, April 2013.
- [99] B. Robbins, C. Hadjicostis, and A. Dominguez-Garcia, “A two-stage distributed architecture for voltage control in power distribution systems,” *Power Systems, IEEE Transactions on*, vol. 28, no. 2, pp. 1470–1482, May 2013.

-
- [100] M. Savaghebi, A. Jalilian, J. Vasquez, and J. Guerrero, "Secondary control for voltage quality enhancement in microgrids," *Smart Grid, IEEE Transactions on*, vol. 3, no. 4, pp. 1893–1902, Dec 2012.
- [101] A. Vaccaro, G. Velotto, and A. Zobaa, "A decentralized and cooperative architecture for optimal voltage regulation in smart grids," *Industrial Electronics, IEEE Transactions on*, vol. 58, no. 10, pp. 4593–4602, Oct 2011.
- [102] A. Bidram, A. Davoudi, F. L. Lewis, and J. M. Guerrero, "Distributed cooperative secondary control of microgrids using feedback linearization," *IEEE Trans. Power Syst.*, vol. 28, no. 3, pp. 3462–3470, August 2013.
- [103] Q. Shafiee, J. Vasquez, and J. Guerrero, "Distributed secondary control for islanded microgrids - a networked control systems approach," in *IECON 2012 - 38th Annual Conference on IEEE Industrial Electronics Society*, Oct 2012, pp. 5637–5642.
- [104] C.-H. Lin and S.-Y. Lin, "Distributed optimal power flow with discrete control variables of large distributed power systems," *Power Systems, IEEE Transactions on*, vol. 23, no. 3, pp. 1383–1392, Aug 2008.
- [105] W. Qi, J. Liu, and P. Christofides, "Distributed supervisory predictive control of distributed wind and solar energy systems," *Control Systems Technology, IEEE Transactions on*, vol. 21, no. 2, pp. 504–512, March 2013.
- [106] L. Gan, U. Topcu, and S. Low, "Optimal decentralized protocol for electric vehicle charging," *Power Systems, IEEE Transactions on*, vol. 28, no. 2, pp. 940–951, May 2013.
- [107] R. Mudumbai, S. Dasgupta, and B. Cho, "Distributed control for optimal economic dispatch of a network of heterogeneous power generators," *Power Systems, IEEE Transactions on*, vol. 27, no. 4, pp. 1750–1760, Nov 2012.

-
- [108] N. Cai, N. T. T. Nga, and J. Mitra, "Economic dispatch in microgrids using multi-agent system," in *North American Power Symposium (NAPS), 2012*, Sept 2012, pp. 1–5.
- [109] Z. Zhang and M.-Y. Chow, "The leader election criterion for decentralized economic dispatch using incremental cost consensus algorithm," in *IECON 2011 - 37th Annual Conference on IEEE Industrial Electronics Society*, Nov 2011, pp. 2730–2735.
- [110] F. Gao and M. Iravani, "A control strategy for a distributed generation unit in grid-connected and autonomous modes of operation," *Power Delivery, IEEE Transactions on*, vol. 23, no. 2, pp. 850–859, April 2008.
- [111] C. Baone and C. DeMarco, "From each according to its ability: Distributed grid regulation with bandwidth and saturation limits in wind generation and battery storage," *Control Systems Technology, IEEE Transactions on*, vol. 21, no. 2, pp. 384–394, March 2013.
- [112] J. Dai, Y. Phulpin, A. Sarlette, and D. Ernst, "Coordinated primary frequency control among non-synchronous systems connected by a multi-terminal high-voltage direct current grid," *Generation, Transmission Distribution, IET*, vol. 6, no. 2, pp. 99–108, February 2012.
- [113] "Ieee standard for interconnecting distributed resources with electric power systems," *IEEE Std 1547-2003*, pp. 1–28, July 2003.
- [114] "Ieee standard conformance test procedures for equipment interconnecting distributed resources with electric power systems," *IEEE Std 1547.1-2005*, pp. 1–62, July 2005.

-
- [115] “Ieee application guide for ieee std 1547(tm), ieee standard for interconnecting distributed resources with electric power systems,” *IEEE Std 1547.2-2008*, pp. 1–217, April 2009.
- [116] “Ieee guide for monitoring, information exchange, and control of distributed resources interconnected with electric power systems,” *IEEE Std 1547.3-2007*, pp. 1–160, Nov 2007.
- [117] “Ieee guide for design, operation, and integration of distributed resource island systems with electric power systems,” *IEEE Std 1547.4-2011*, pp. 1–54, July 2011.
- [118] “Ieee recommended practice for interconnecting distributed resources with electric power systems distribution secondary networks,” *IEEE Std 1547.6-2011*, pp. 1–38, Sept 2011.
- [119] “Ieee guide for conducting distribution impact studies for distributed resource interconnection,” *IEEE Std 1547.7-2013*, pp. 1–137, Feb 2014.
- [120] “Ieee standard for interconnecting distributed resources with electric power systems - amendment 1,” *IEEE Std 1547a-2014 (Amendment to IEEE Std 1547-2003)*, pp. 1–16, May 2014.
- [121] “Ieee standard conformance test procedures for equipment interconnecting distributed resources with electric power systems - amendment 1,” *IEEE Std 1547.1a-2015 (Amendment to IEEE Std 1547.1-2005)*, pp. 1–27, May 2015.
- [122] E. Hossain, E. Kabalci, R. Bayindir, and R. Perez, “Microgrid testbeds around the world: State of art,” *Energy Conversion and Management*, vol. 86, pp. 132 – 153, 2014.

-
- [123] J. M. Guerrero, P. C. Loh, T. L. Lee, and M. Chandorkar, “Advanced control architectures for intelligent microgrids part ii: Power quality, energy storage, and ac/dc microgrids,” *IEEE Transactions on Industrial Electronics*, vol. 60, no. 4, pp. 1263–1270, April 2013.
- [124] F. Nejabatkhah and Y. W. Li, “Overview of power management strategies of hybrid ac/dc microgrid,” *IEEE Transactions on Power Electronics*, vol. 30, no. 12, pp. 7072–7089, Dec 2015.
- [125] J. V. Roy, N. Leemput, F. Geth, J. Büscher, R. Salenbien, and J. Driesen, “Electric vehicle charging in an office building microgrid with distributed energy resources,” *IEEE Transactions on Sustainable Energy*, vol. 5, no. 4, pp. 1389–1396, Oct 2014.
- [126] N. Liu, Q. Chen, J. Liu, X. Lu, P. Li, J. Lei, and J. Zhang, “A heuristic operation strategy for commercial building microgrids containing evs and pv system,” *IEEE Transactions on Industrial Electronics*, vol. 62, no. 4, pp. 2560–2570, April 2015.
- [127] C. Guille and G. Gross, “A conceptual framework for the vehicle-to-grid (v2g) implementation,” *Energy Policy*, vol. 37, no. 11, pp. 4379 – 4390, 2009.
- [128] M. Honarmand, A. Zakariazadeh, and S. Jadid, “Integrated scheduling of renewable generation and electric vehicles parking lot in a smart microgrid,” *Energy Conversion and Management*, vol. 86, pp. 745–755, 2014.
- [129] A. Zakariazadeh, S. Jadid, and P. Siano, “Integrated operation of electric vehicles and renewable generation in a smart distribution system,” *Energy Conversion and Management*, vol. 89, pp. 99–110, 2015.
- [130] M. Hosseinzadeh and F. R. Salmasi, “Robust optimal power management system for a hybrid ac/dc micro-grid,” *IEEE Transactions on Sustainable Energy*, vol. 6, no. 3, pp. 675–687, July 2015.

- [131] M. C. Kisacikoglu, B. Ozpineci, and L. M. Tolbert, “Ev/phev bidirectional charger assessment for v2g reactive power operation,” *IEEE Transactions on Power Electronics*, vol. 28, no. 12, pp. 5717–5727, Dec 2013.
- [132] M. Kesler, M. C. Kisacikoglu, and L. M. Tolbert, “Vehicle-to-grid reactive power operation using plug-in electric vehicle bidirectional offboard charger,” *IEEE Transactions on Industrial Electronics*, vol. 61, no. 12, pp. 6778–6784, Dec 2014.
- [133] P. Mitra, G. K. Venayagamoorthy, and K. A. Corzine, “Smartpark as a virtual statcom,” *IEEE Transactions on Smart Grid*, vol. 2, no. 3, pp. 445–455, Sept 2011.
- [134] J. Zhong, L. He, C. Li, Y. Cao, J. Wang, B. Fang, L. Zeng, and G. Xiao, “Coordinated control for large-scale {EV} charging facilities and energy storage devices participating in frequency regulation,” *Applied Energy*, vol. 123, pp. 253 – 262, 2014.
- [135] C. Gouveia, C. L. Moreira, J. A. P. Lopes, D. Varajao, and R. E. Araujo, “Microgrid service restoration: The role of plugged-in electric vehicles,” *IEEE Industrial Electronics Magazine*, vol. 7, no. 4, pp. 26–41, Dec 2013.
- [136] M. F. M. Arani, Y. A. R. I. Mohamed, and E. F. El-Saadany, “Analysis and mitigation of the impacts of asymmetrical virtual inertia,” *IEEE Transactions on Power Systems*, vol. 29, no. 6, pp. 2862–2874, Nov 2014.
- [137] S. Weckx and J. Driesen, “Load balancing with ev chargers and pv inverters in unbalanced distribution grids,” *IEEE Transactions on Sustainable Energy*, vol. 6, no. 2, pp. 635–643, April 2015.
- [138] M. Mehrasa, E. Pouresmaeil, H. Mehrjerdi, B. N. Jorgensen, and J. P. Catalao, “Control technique for enhancing the stable operation of distributed generation units within a microgrid,” *Energy Conversion and Management*, vol. 97, pp. 362 – 373, 2015.

-
- [139] F. Rafi, M. Hossain, and J. Lu, "Design of a single stage transformerless vsi in a smart microgrid for pv-statcom/ess operations," in *2014 Australasian Universities Power Engineering Conference (AUPEC)*, Sept 2014, pp. 1–6.
- [140] D. Leskarac, C. Bennett, M. Moghimi, S. Stegen, and J. Lu, "Testing facility for research and development of smart-microgrid technologies," in *2015 IEEE PES Asia-Pacific Power and Energy Engineering Conference (APPEEC)*, Nov 2015, pp. 1–5.
- [141] M. Moghimi, C. Bennett, D. Leskarac, S. Stegen, and J. Lu, "Communication architecture and data acquisition for experimental microgrid installations," in *2015 IEEE PES Asia-Pacific Power and Energy Engineering Conference (APPEEC)*, Nov 2015, pp. 1–5.
- [142] N. Femia, G. Petrone, G. Spagnuolo, and M. Vitelli, "Optimization of perturb and observe maximum power point tracking method," *IEEE Transactions on Power Electronics*, vol. 20, no. 4, pp. 963–973, July 2005.
- [143] T. Alnejaili, S. Drid, D. Mehdi, L. Chrifi-Alaoui, R. Belarbi, and A. Hamdouni, "Dynamic control and advanced load management of a stand-alone hybrid renewable power system for remote housing," *Energy Conversion and Management*, vol. 105, pp. 377 – 392, 2015.
- [144] S. Koochi-Kamali, N. Rahim, and H. Mokhlis, "Smart power management algorithm in microgrid consisting of photovoltaic, diesel, and battery storage plants considering variations in sunlight, temperature, and load," *Energy Conversion and Management*, vol. 84, pp. 562 – 582, 2014.

- [145] M. Mahmud, H. Pota, and M. Hossain, “Dynamic stability of three-phase grid-connected photovoltaic system using zero dynamic design approach,” *Photovoltaics, IEEE Journal of*, vol. 2, no. 4, pp. 564–571, Oct 2012.
- [146] R. Kroeze and P. Krein, “Electrical battery model for use in dynamic electric vehicle simulations,” in *Power Electronics Specialists Conference, 2008. PESC 2008. IEEE*, June 2008, pp. 1336–1342.
- [147] R. Minciardi and M. Robba, “A dynamic model for electrical vehicles interacting with microgrids and renewables,” in *Modelling Symposium (EMS), 2013 European*, Nov 2013, pp. 420–425.
- [148] O. Tremblay and L. A. Dessaint, “Experimental validation of a battery dynamic model for ev applications,” *J. World Electric Vehicle*, vol. 3, 2009.
- [149] Amirnaser Yazdani and R. Iravani, *Voltage-sourced converters in power systems: modeling, control, and applications*. John Wiley & Sons, 2010.
- [150] J. Guerrero, J. Vasquez, J. Matas, L. de Vicuna, and M. Castilla, “Hierarchical control of droop-controlled ac and dc microgrids - a general approach toward standardization,” *IEEE Transactions on Industrial Electronics*, vol. 58, no. 1, pp. 158–172, Jan 2011.
- [151] Parliament of the Commonwealth of Australia and E. Act, “Electricity Regulation 2006,” Tech. Rep. 4, 2011. [Online]. Available: <http://www.legislation.qld.gov.au/legisltn/current/e/electricR06.pdf>
- [152] T. A. E. M. C. Reliability Panel, “Application of Frequency Operating Standards During Periods of Supply Scarcity,” Tech. Rep. April, 2009.

-
- [153] T. A. P. Association, "Pv integration on australian distribution," no. September, 2013.
- [154] N. Pogaku, M. Prodanovic, and T. Green, "Modeling, analysis and testing of autonomous operation of an inverter-based microgrid," *Power Electronics, IEEE Transactions on*, vol. 22, no. 2, pp. 613–625, March 2007.
- [155] P. H. Divshali, A. Alimardani, S. H. Hosseinian, and M. Abedi, "Decentralized cooperative control strategy of microsources for stabilizing autonomous vsc-based microgrids," *IEEE Transactions on Power Systems*, vol. 27, no. 4, pp. 1949–1959, Nov 2012.
- [156] R. J. Hamidi, H. Livani, S. Hosseinian, and G. Gharehpetian, "Distributed cooperative control system for smart microgrids," *Electric Power Systems Research*, vol. 130, pp. 241 – 250, 2016.
- [157] A. A. A. Radwan and Y. A. R. I. Mohamed, "Networked control and power management of ac/dc hybrid microgrids," *IEEE Systems Journal*, vol. PP, no. 99, pp. 1–12, 2014.
- [158] B. Singh, P. Jayaprakash, T. R. Somayajulu, and D. P. Kothari, "Reduced rating vsc with a zig-zag transformer for current compensation in a three-phase four-wire distribution system," *IEEE Transactions on Power Delivery*, vol. 24, no. 1, pp. 249–259, Jan 2009.
- [159] J. P. Torreglosa, P. G.-T. no, L. M. Fernández-Ramirez, and F. Jurado, "Decentralized energy management strategy based on predictive controllers for a medium voltage direct current photovoltaic electric vehicle charging station," *Energy Conversion and Management*, vol. 108, pp. 1 – 13, 2016.

-
- [160] P. Wang, L. Goel, X. Liu, and F. H. Choo, “Harmonizing AC and DC: A hybrid AC/DC future grid solution,” *IEEE Power Energy Mag.*, vol. 11, no. 3, pp. 76–83, May 2013.
- [161] M. S. Rahman, F. Rafi, M. J. Hossain, and J. Lu, “Power control and monitoring of the smart grid with EVs,” *Vehicle-to-Grid: Linking Electric Vehicles to the Smart Grid*, p. 107, 2015.
- [162] N. Mahmud and A. Zahedi, “Review of control strategies for voltage regulation of the smart distribution network with high penetration of renewable distributed generation,” *Renew. Sustain. Energy Rev.*, vol. 64, no. Supplement C, pp. 582 – 595, 2016.
- [163] J. M. Guerrero, P. C. Loh, T. L. Lee, and M. Chandorkar, “Advanced control architectures for intelligent microgrids - part II: Power quality, energy storage, and AC/DC microgrids,” *IEEE Trans. Ind. Electron.*, vol. 60, no. 4, pp. 1263–1270, April 2013.
- [164] F. Dorfler, J. W. Simpson-Porco, and F. Bullo, “Breaking the hierarchy: Distributed control and economic optimality in microgrids,” *IEEE Trans. Control Netw. Syst.*, vol. 3, no. 3, pp. 241–253, September 2016.
- [165] V. Nasirian, S. Moayedi, A. Davoudi, and F. L. Lewis, “Distributed cooperative control of DC microgrids,” *IEEE Trans. Power Electron.*, vol. 30, no. 4, pp. 2288–2303, April 2015.
- [166] Q. Shafiee, T. Dragicevic, J. C. Vasquez, and J. M. Guerrero, “Hierarchical control for multiple DC-microgrids clusters,” *IEEE Trans. Energy Convers.*, vol. 29, no. 4, pp. 922–933, December 2014.

-
- [167] S. Moayedi and A. Davoudi, “Distributed tertiary control of DC microgrid clusters,” *IEEE Trans. Power Electron.*, vol. 31, no. 2, pp. 1717–1733, February 2016.
- [168] X. Lu, X. Yu, J. Lai, J. Guerrero, and H. Zhou, “Distributed secondary voltage and frequency control for islanded microgrids with uncertain communication links,” *IEEE Trans. Ind. Informat.*, vol. PP, no. 99, pp. 1–1, 2016.
- [169] W. Liu, W. Gu, W. Sheng, X. Meng, S. Xue, and M. Chen, “Pinning-based distributed cooperative control for autonomous microgrids under uncertain communication topologies,” *IEEE Trans. Power Syst.*, vol. 31, no. 2, pp. 1320–1329, March 2016.
- [170] T. Morstyn, A. Savkin, B. Hredzak, and V. Agelidis, “Multi-agent sliding mode control for state of charge balancing between battery energy storage systems distributed in a DC microgrid,” *IEEE Trans. Smart Grid*, vol. PP, no. 99, pp. 1–1, 2017.
- [171] M. Zeraati, M. E. H. Golshan, and J. Guerrero, “Distributed control of battery energy storage systems for voltage regulation in distribution networks with high pv penetration,” *IEEE Transactions on Smart Grid*, vol. PP, no. 99, pp. 1–1, 2016.
- [172] N. Mahmud, A. Zahedi, and A. Mahmud, “A cooperative operation of novel PV inverter control scheme and storage energy management system based on ANFIS for voltage regulation of grid-tied PV system,” *IEEE Trans. Ind. Informat.*, vol. PP, no. 99, pp. 1–1, 2017.
- [173] M. S. Golsorkhi, Q. Shafiee, D. Lu, and J. M. Guerrero, “A distributed control framework for integrated photovoltaic-battery based islanded microgrids,” *IEEE Trans. Smart Grid*, vol. PP, no. 99, pp. 1–1, 2016.

-
- [174] T. L. Vandoorn, B. Meersman, J. D. M. D. Kooning, and L. Vandeveldde, “Analogy between conventional grid control and islanded microgrid control based on a global DC-link voltage droop,” *IEEE Trans. Power Del.*, vol. 27, no. 3, pp. 1405–1414, July 2012.
- [175] ———, “Transition from islanded to grid-connected mode of microgrids with voltage-based droop control,” *IEEE Trans. Power Syst.*, vol. 28, no. 3, pp. 2545–2553, August 2013.
- [176] M. S. Rahman, M. J. Hossain, F. H. M. Rafi, and J. Lu, “A multi-purpose inter-linking converter control for multiple hybrid AC/DC microgrid operations,” in *2016 IEEE Innovative Smart Grid Technologies - Asia (ISGT-Asia)*, November 2016, pp. 221–226.
- [177] R. Olfati-Saber and R. M. Murray, “Consensus problems in networks of agents with switching topology and time-delays,” *IEEE Trans. Autom. Control*, vol. 49, no. 9, pp. 1520–1533, September 2004.
- [178] C. Li, E. A. A. Coelho, T. Dragicevic, J. M. Guerrero, and J. C. Vasquez, “Multiagent-based distributed state of charge balancing control for distributed energy storage units in ac microgrids,” *IEEE Trans. on Ind. Appl.*, vol. 53, no. 3, pp. 2369–2381, May 2017.
- [179] T. K. Refaat, R. M. Daoud, H. H. Amer, and E. A. Makled, “Wifi implementation of wireless networked control systems,” in *2010 Seventh International Conference on Networked Sensing Systems (INSS)*, June 2010, pp. 145–148.
- [180] D. L. Gerber, V. Vossos, W. Feng, C. Marnay, B. Nordman, and R. Brown, “A simulation-based efficiency comparison of ac and dc power distribution networks in commercial buildings,” *Applied Energy*, vol. 210, pp. 1167 – 1187, 2018.

-
- [181] P. Wang, C. Jin, D. Zhu, Y. Tang, P. C. Loh, and F. H. Choo, “Distributed control for autonomous operation of a three-port ac/dc/ds hybrid microgrid,” *IEEE Transactions on Ind. Electron.*, vol. 62, no. 2, pp. 1279–1290, Feb 2015.
- [182] S. Moayedi and A. Davoudi, “Unifying distributed dynamic optimization and control of islanded dc microgrids,” *IEEE Trans. Power Electron.*, vol. 32, no. 3, pp. 2329–2346, March 2017.
- [183] Z. Wang, F. Liu, Y. Chen, S. H. Low, and S. Mei, “Unified distributed control of stand-alone dc microgrids,” *IEEE Trans. Smart Grid*, vol. PP, no. 99, pp. 1–1, 2017.
- [184] G. Binetti, A. Davoudi, F. L. Lewis, D. Naso, and B. Turchiano, “Distributed consensus-based economic dispatch with transmission losses,” *IEEE Trans. Power Syst.*, vol. 29, no. 4, pp. 1711–1720, July 2014.